CHALMERS

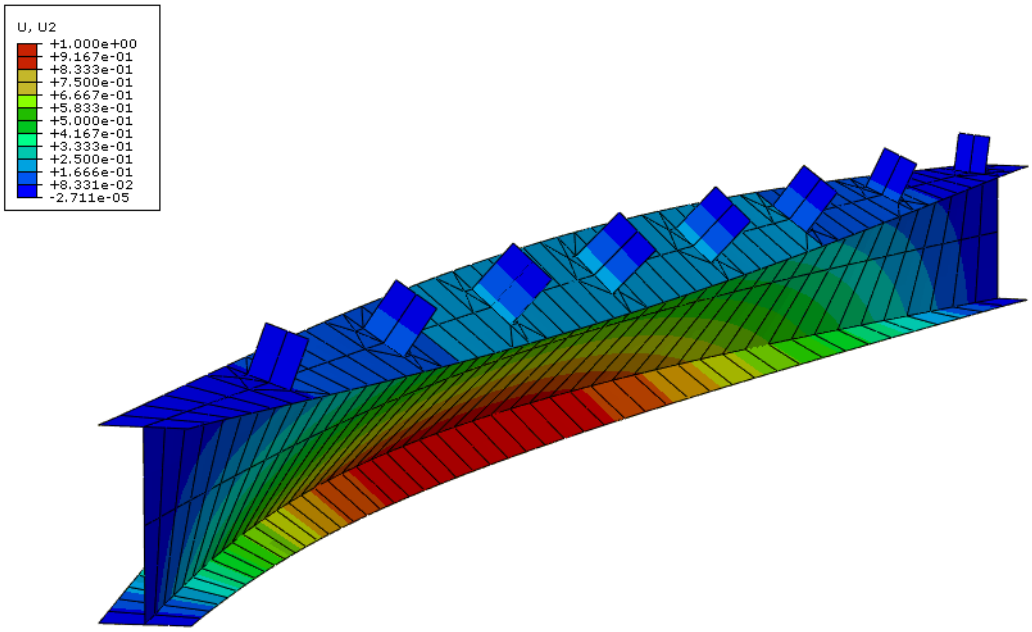

Stable length in steel portal frames

A parametric study of the influence of purlins on lateral-torsional buckling

Master of Science Thesis in the Master's Programme Structural Engineering and Building Technology

MAGNUS HEIDAR BJÖRNSSON

MATHIAS WERNBORG

Department of Civil and Environmental Engineering

Division of Structural Engineering

Steel and Timber Structures

CHALMERS UNIVERSITY OF TECHNOLOGY

Göteborg, Sweden 2013

Master's Thesis 2013:96

MASTER'S THESIS 2013:96

Stable length in steel portal frames

A parametric study of the influence of purlins on lateral-torsional buckling

Master of Science Thesis in the Master's Programme Structural Engineering and Building Technology

MAGNUS HEIDAR BJÖRNSSON

MATHIAS WERNBORG

Department of Civil and Environmental Engineering

Division of Structural Engineering

Steel and Timber Structures

CHALMERS UNIVERSITY OF TECHNOLOGY

Göteborg, Sweden 2013

Stable length in steel portal frames

A parametric study of the influence of purlins on lateral-torsional buckling

Master of Science Thesis in the Master's Programme Structural Engineering and Building Technology

MAGNUS HEIDAR BJÖRNSSON

MATHIAS WERNBORG

Examensarbete / Institutionen för bygg- och miljöteknik,
Chalmers tekniska högskola 2013:96

Department of Civil and Environmental Engineering

Division of Structural Engineering

Steel and Timber Structures

Chalmers University of Technology

SE-412 96 Göteborg

Sweden

Telephone: + 46 (0)31-772 1000

Cover:
Finite element model showing lateral-torsional buckling of a beam from a portal frame.

Chalmers Reproservice / Department of Civil and Environmental Engineering
Göteborg, Sweden 2013

Stable length in steel portal frames

A parametric study of the influence of purlins on lateral-torsional buckling

Master of Science Thesis in the Master's Programme Structural Engineering and Building Technology

MAGNUS HEIDAR BJÖRNSSON

MATHIAS WERNBORG

Department of Civil and Environmental Engineering
Division of Structural Engineering
Steel and Timber Structures
Chalmers University of Technology

ABSTRACT

To date, there exist expressions in Eurocode3 regarding the stable length in portal frames where LT-buckling can be ignored. The expressions provided in Eurocode are semi-empirical and they have been simplified in order to fit for practical application. The steel portal frame industry is interested in utilizing simple expressions, taking into account all influencing parameters. The objective of this thesis is therefore to derive a stable length according to elastic design and study the stabilizing effect of purlins and compare with the existing expressions. The stable lengths will be derived using the buckling curve method in Eurocode3, where second order effects such as geometric imperfections and residual stresses are taken into account. Verification of the derived stable length will be performed with finite element simulation.

The derivation of the stable length for the investigated cross-sections results in relative short lengths when compared to the existing expressions in Eurocode. The short length involves a significant critical buckling moment resulting in LT-buckling of the beam in combination with distortion of the web. Despite distortion, all investigated beams yields in the extreme fibres before occurrence of LT-buckling. It can be concluded that the derived stable length is accurate, according to the results from the finite element analysis.

It is also concluded the plastic stable length as provided in EN 1993-1-1 Annex BB.3 is un-conservative. The expression assumes a greater limit of slenderness for restrained beams compared to recommendations in Eurocode3. According to the non-linear analysis it appears that the greater limit of slenderness is not justified.

The simplified method yields similar result as the derived stable length and corresponds very well with the results from the finite element analysis. Depending on the limit of slenderness assumed in the analytical derivation, it is either more conservative or marginally un-conservative. The approach of the simplified method is considered to be conservative since important parameters have been neglected, which indicates that the method is reliable. However the simplified method has to be used cautiously for beams with large initial imperfection.

Key words: Lateral-torsional buckling, stable length, steel portal frames, purlins, lateral restraints, stability problem, finite element analysis.

Stabila vippningslängden i stålramar

En parametrisk studie av stabiliseringseffekten från takåsar

Examensarbete inom Structural Engineering and Building Technology

MAGNUS HEIDAR BJÖRNSSON, MATHIAS WERNBORG

Institutionen för bygg- och miljöteknik
Avdelningen för konstruktionsteknik
Stål- och träbyggnad
Chalmers tekniska högskola

SAMMANFATTNING

Idag finns det uttryck i Eurocode3 som fastställer den maximala längden mellan vridstag där vippning inte behöver beaktas. Dessa uttryck är namngivna som ”simplified method” samt ”plastic stable length”. Dessa uttryck är kraftigt förenklade och semi-empiriska. Det finns ett intresse inom branschen att bestämma den stabila vippningslängden, genom att beakta samtliga påverkande parametrar, genom enkla beräkningsmetoder. Syftet med rapporten är därför att bestämma ett uttryck för den stabila vippningslängden där den stabiliserande inverkan från takåsar är inkluderad. Vid en jämförelse med de befintliga uttrycken i Eurocode3 kan det sedan fastslås om huruvida den framtagna vippningslängden är tillämpbar i projekteringsskedet. Särskilda antaganden har gjorts vid härledningen av den stabila vippningslängden. Exempelvis finns det i Eurocode3 rekommenderade gränsvärden för slankhet samt bestämda värden för initialkrokighet och initialspänningar. Vidare genomförs finita element-simuleringar för att verifiera uttrycket för vippningslängden.

Den stabila vippningslängden för de undersökta tvärsnitten resulterar i relativt korta längder vilket följaktligen innebär ett betydande kritiskt bucklingsmoment i proportion till slankheten av livet. Detta innebär att tvärsnittet förvrids vilket medför lägre kritiskt bucklingsmoment. Trots förvridning av tvärsnittet uppfylls kriteriet att den elastiska böjkapaciteten uppnås innan balken blir instabil, detta gäller för samtliga undersökta balkar. Slutsatsen utifrån detta är att det härledda uttrycket för den stabila vippningslängden är korrekt.

Utifrån undersökningen kan det fastslås att ”plastic stable length” ger betydande längre stabila vippningslängder i jämförelse, vilket utifrån antaganden i denna rapport ger resultat på den osäkra sidan. I beräkningsuttrycket antas ett högre gränsvärde för slankhet gällande balkar där effekten från takåsar är inkluderat, i jämförelse med rekommendationen i Eurocode3. Utifrån de genomförda icke-linjära analyserna i denna studie är detta inte motiverat.

Metoden ”simplified method” ger liknande resultat som den härledda stabila vippningslängden. Beroende på vilket gränsvärde av slankhet som antas i uttrycket sker instabilitet efter eller samtidigt som den elastiska kapaciteten är uppnådd. Dock anses tillvägagångssättet vid beräkningen av metoden ”simplified method” vara konservativ eftersom viktiga parametrar har försummats vilket visar att metoden är tillförlitlig. Metoden måste dock användas med försiktighet för balkar med betydande initialkrokighet.

Nyckelord: Vippning, kritiska vippningsländen, stålramar, takåsar

Contents

Preface

This Master´s Project has been carried out between January 2013 and June 2013 at the Department of Civil and Environmental Engineering at Chalmers University of Technology, Sweden. The project has been initiated in collaboration with Borga and Chalmers University.

We would like to thank our supervisor and examiner, Mohammad Al-Emrani, for his involvement and many good advices. Furthermore thanks to our supervisor at Borga, Tobias Andersson. We would also thank our families who have been supportive during this time.

Göteborg, June 2013

Magnus Heidar Björnsson

Mathias Wernborg

Notations

Roman upper case letters

A	Cross-sectional area
C	Constant of integration
C_1	Modification factor for a moment gradient
E	Young´s modulus
G	Shear modulus
I_t	Torsion constant
I_w	Warping constant
I_y	Second moment of inertia about the major axis
I_z	Second moment of inertia about the minor axis
K_s	Torsional stiffness of one lateral support
L	Length of the beam
L_c	Stable length according to the simplified method
L_k	Plastic stable length with the tension flange laterally restrained
$L_{k.e}$	Elastic stable length with the tension flange laterally restrained
L_m	Plastic stable length with the tension flange laterally unrestrained
L_{unr}	Derived stable length with the tension flange laterally unrestrained
L_r	Derived stable length with the tension flange laterally restrained
M	Bending moment
M_{cr}	Critical lateral-torsional buckling moment, unrestrained beam
$M_{cr.o}$	Critical lateral-torsional buckling moment, restrained beam
$M_{cr.wo}$	Critical lateral-torsional buckling moment for an unrestrained beam with zero warping stiffness
M_{ref}	Applied reference moment
M_1	Bending moment about the major axis
M_2	Bending moment about the minor axis
N	Applied axial force
P	Concentrated force, axial force in beam-column
P_E	Critical flexural buckling load in between lateral support at the tension flange
$P_{x.cr}$	Critical buckling load for torsional buckling

$P_{y,cr}$ Critical buckling load for major axis buckling

$P_{z,cr}$ Critical buckling load for minor axis buckling

P_{TC} Critical buckling load for overall torsional buckling

W_e Elastic sectional modulus about the major axis

W_{pl} Plastic sectional modulus about the major axis

Roman lower case letters

a Eccentricity of a lateral restraint(purlin)

b Width of the flange

e_0 Equivalent initial bow imperfection

f_y Yielding strength

h Depth of the cross-section

h_x Coordinate of the offset axis of restraint relative to the centroid of a cross-section in the x-direction

h_y Coordinate of the offset axis of restraint relative to the centroid of a cross-section in the x-direction

i Imaginary number

i_s Polar radius of gyration about the restrained longitudinal axis $i_s^2 = i_o^2 + a^2$.

i_z Polar radius of gyration about major axis

i_z Polar radius of gyration about minor axis

i_o Polar radius of gyration about the longitudinal axis through the centroid $i_o^2 = \frac{I_y + I_z}{A}$.

k_x Lateral stiffness of spring support in x-direction

k_y Lateral stiffness of spring support in y-direction

k_φ Equivalent continuous torsional stiffness

n Number of half sinus waves

s Spacing of supports

t_f Thickness of flange

t_w Thickness of web

u Total lateral displacement (y-direction)

u_L Lateral displacement (y-direction) due to bending about minor axis

u_T Lateral displacement (y-direction) due to torsion

v Vertical displacement (z-direction)

Greek lower case letters

ϕ Angle of twist about the longitudinal axis

ϕ_0 Initial imperfection as an angle of twist about the restrained longitudinal axis at the mid-section of a beam

$\bar{\lambda}$ Non-dimensional slenderness

λ Eigenvalue

σ Normal stress

Abbreviations

LT – Lateral-torsional
FE – Finite element
DE – Differential equation
DOF – Degrees of freedom

Definitions

Beam and **beam segment** – Both represent the part extracted from a portal frame in between torsional restraints seen in figure below.

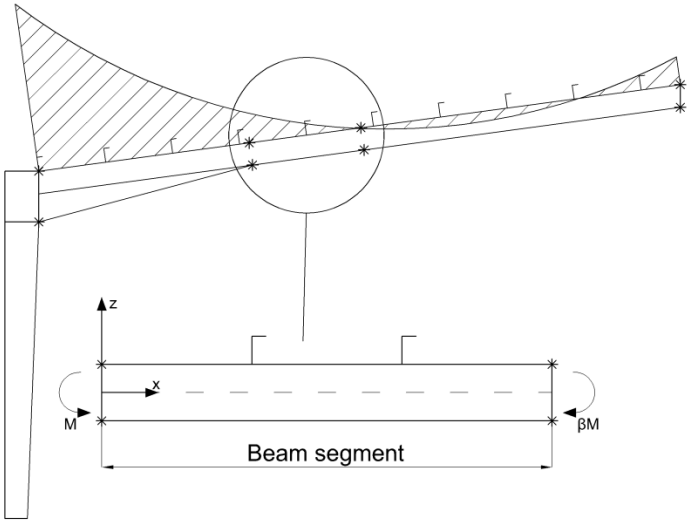

Buckling capacity and **critical buckling moment** – The theoretical critical moment that cause instability in a "perfect" beam; i.e. assuming elastic response and omitting geometrical and mechanical initial imperfections.

Elastic capacity – The moment capacity of a cross sections when yielding occurs in the extreme fibres caused due to constant moment about the major axis. Illustration of elastic capacity is shown in the figure below.

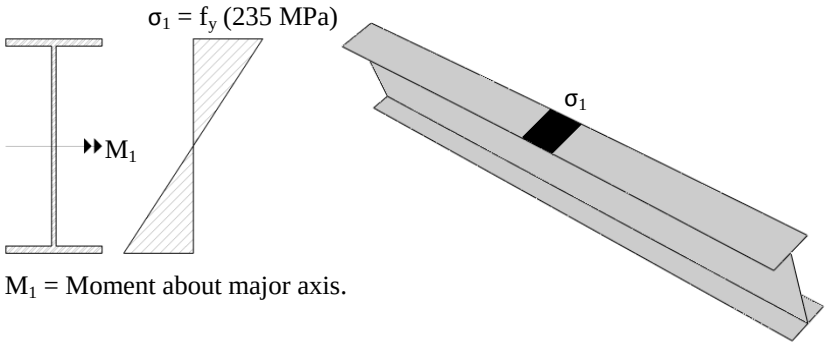

M_1 = Moment about major axis.

Ultimate moment – The maximum moment when considering geometrical imperfections, residual stresses and material plasticity seen in the figure below.

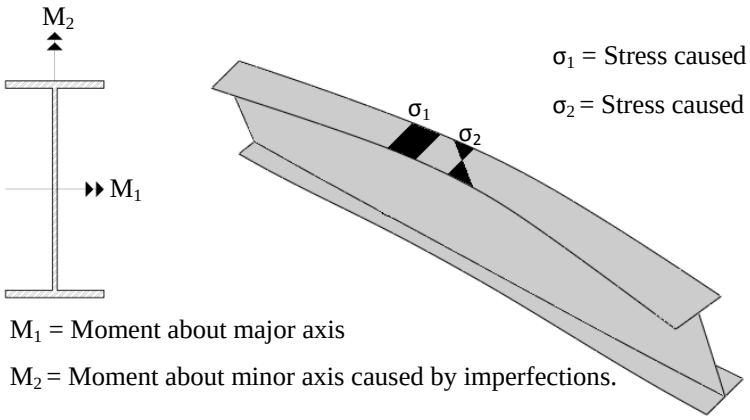

Lateral restraints or **purlins –** Both of these words are used defining lateral restraints on the tension flange.

Linear buckling analysis – Considers only elastic material, no geometrical imperfections or residual stresses.

Non-linear buckling analysis – Considers material plasticity with strain hardening, geometrical imperfections and residual stresses.

Plastic stable length – Stable length assuming the formation of a plastic hinge in accordance with Eurocode3.

Stable length – Length derived in this Master's Project assuming elastic design.

Restrained beams – Beams that are laterally restrained at the tension flange.

Unrestrained beams – Beams that are not laterally restrained at the tension flange.

1 Introduction

1.1 Problem definition

To date, there exist expressions in Eurocode3 regarding the stable length in steel portal frames, where LT-buckling can be ignored and only cross-section checks apply. The stable length comprises the length of a segment in between torsional restraints, which can be either laterally unrestrained or restrained with purlins. EN 1993-1-1 – Annex BB.3 provides several analytical expressions to calculate the stable length in various frame types. These expressions are however simplified and semi-empirical. The industry is interested of utilizing simple expressions which are not time-consuming, taking into account all influencing parameters. Existing expressions might be conservative and possible to simplify. Finding an expression which considers several important parameters like the stabilizing effect from purlins, an extensive investigation must be performed obtaining an overview of the behaviour.

1.2 Aim and objective

The aim of the work performed in this thesis is to investigate the stable length in steel portal frames with respect to lateral-torsional buckling.

The objective is to derive a stable length according to elastic design and study the stabilizing effect of purlins. The new derived stable lengths are verified through plastic 2nd-order analysis and compared to the expressions suggested in Annex BB.3 in EN-1993-1-1.

1.3 Method

A literature review is performed in order to achieve an overview of the most important parameters affecting the phenomenon lateral-torsional buckling in steel portal frames. Furthermore, linear buckling analyses are executed with the finite element software ABAQUS CAE aiding to visualize the behaviour and to verify the models produced. In addition the stable length is derived analytically using the recommendations given in Eurocode3 concerning the limits of slenderness and geometrical imperfections. The stable length is then verified by performing non-linear analyses in ABAQUS CAE.

1.4 Scope and limitations

The scope of this project is to establish an expression for the stable length in a portal frame. However, simplifications have been made to facilitate the analysis. The models studied represent a segment in a portal frame, between torsional restraints. The boundary conditions assumed in the derivation of the analytical expressions utilized in this Master's Project are equivalent to torsional restraints. The same conditions are therefore also assumed for the simulated models. This report will only focus on doubly symmetric cross-sections.

The segments simulated have flat web, uniform geometry and are subjected to constant moment only, i.e. the effect of axial force is neglected. Furthermore the purlins between the torsional restrains are assumed to be laterally rigid but provide no torsional resistance to the beam. The yield strength of the steel is limited to f_y of 235MPa.

Aspects which are not studied but are essential considering portal frames are;

- Haunched and tapered segments.
- Moment gradients both linear and non-linear.
- Axial force.
- Bending stiffness of the purlins.
- Different yield strength of the steel.

1.5 Outline of the Thesis

Below, the content of the following chapters has been described.

Chapter 2 - Comprises the literature review.

Chapter 3 - Covers the method utilized to reach the aim.

Chapter 4 - Explains the procedure of the modelling in ABAQUS.

Chapter 5 - The theory behind lateral-torsional buckling with and without distortion is presented.

Chapter 6 - Results are presented from analytical parametric studies, elastic linear buckling analyses and non-linear studies of the stable length.

Chapter 7 - Conclusions and suggestions for further studies are discussed.

2 Literature review

In this chapter a theoretical background for the following research is established. First, an overview of the phenomena known as lateral-torsional buckling is presented. Secondly the effect of lateral support on the tension flange, both continuous and discrete, for different load cases is studied. Finally, the background of the plastic stable length in Eurocode3 is presented, where the effects of purlins are taken into account.

2.1 Elastic buckling

Structural beams have two equilibrium states; *stable* or *unstable*. A structural element is stable if it returns to its initial position when a small load is applied and then removed. The unstable state is when the loaded element undergoes further increase of deflection. In other words, in the stable state, additional energy is required to produce the deflection, and in the unstable state energy is released. When the unstable state occurs the structure has reached its limit of stability. (Galambos, 1968) The load causing this unstable phenomenon is denoted as the critical load and is obviously of great interest in structural engineering. Furthermore, a structure is a complex system, forces and moments interact, beams are not symmetric etc. which affects the critical load. This report will focus on doubly symmetric cross-sections which simplify the derivations of the equations.

Critical loads or moments can be derived either by equilibrium conditions of differential equations (DE:s) or by energy theorems, taking into account equilibrium between the external load and internal resistance.

The derivations of the critical forces and moments are based on elastic buckling which neglects material non-linearity, geometrical imperfections and residual stresses.

2.1.1 Laterally unrestrained beams

The global buckling mode depends on how the beam is loaded, boundary conditions and the shape of the cross-section. Axial loaded beams will either buckle about minor or major axis as in Figure 1*b* and *c* or pure torsion as in Figure 1*d*. Beams subjected to pure moment will undergo lateral-torsional buckle, a combination of Figure 1*b* and *d.* In this chapter derivation has been executed of different buckling modes for laterally unrestrained beams subjected to either axial compression or pure moment.

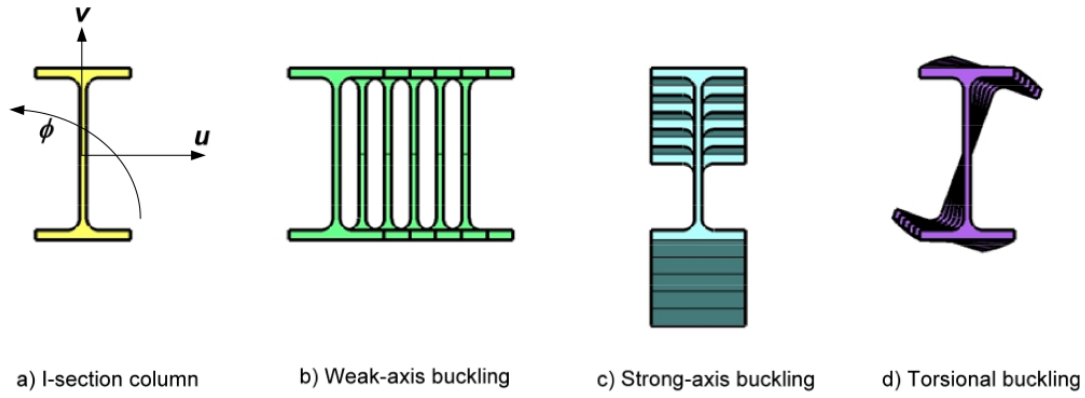

Figure 1 Different buckling modes. (Louw, 2008)

2.1.1.1 Beams subjected to axial compression

Axially loaded beams, when reaching unstable state, have the possibility to buckle in three modes. Three DE:s eqn.(1-3), which can be seen below (representing each buckling mode), can therefore be produced based on equilibrium conditions expressing this unstable phenomenon. The potential buckling modes are lateral displacement about major or minor axis and pure torsional buckling about the longitudinal axis. For a doubly symmetric cross-section there is only one unknown variable (v, u, ϕ) in each expression and the differential equations can be treated separately. Due to the independence of each equation it is necessary to check all three equations to determine the lowest critical load. For asymmetric sections the DE:s contain both twist ϕ and lateral displacement u and the critical load will be found by calculating the determinant of the system equation. (Galambos, 1968)

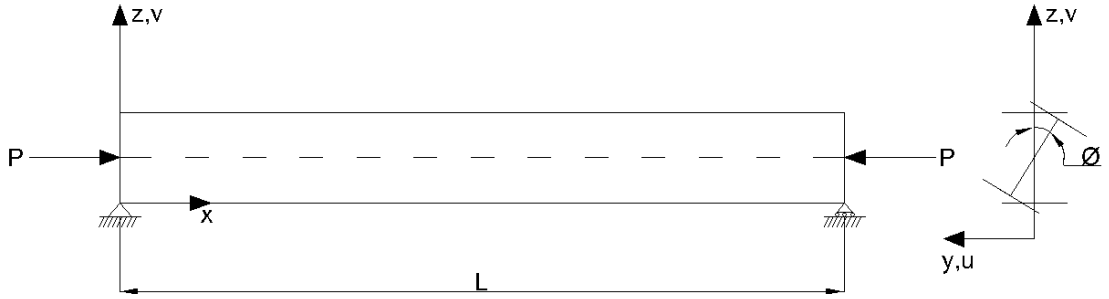

Figure 2 Beam subjected to an axial compression. (Galambos, 1968)

$$EI_y \frac{d^4v}{dx^4} + P\frac{d^2v}{dx^2} = 0 \tag{1}$$

$$EI_z \frac{d^4u}{dx^4} + P\frac{d^2u}{dx^2} = 0 \tag{2}$$

$$EI_w \frac{d^4\phi}{dx^4} + (Pi_o^2 - GI_t)\frac{d^2\phi}{dx^2} = 0 \tag{3}$$

The equations below are obtained by solving the three independent DE:s with respect to the load.

$$P_{y.cr} = \frac{\pi^2 EI_y}{L^2} \tag{4}$$

$$P_{z.cr} = \frac{\pi^2 EI_z}{L^2} \tag{5}$$

$$P_{x.cr} = \frac{1}{i_o^2}\left(\frac{\pi^2 EI_w}{L^2} + GI_t\right) \tag{6}$$

$$where \quad i_o^2 = \frac{I_y + I_z}{A} \tag{7}$$

2.1.1.2 Beams subjected to pure bending

In the same manner as for axially loaded beams, three differential equations are determined from equilibrium conditions for beams subjected to bending. The equations hold for doubly symmetric sections. (Galambos, 1968)

The first equation (8) involves only vertical deflections and is therefore independent of the other two. The latter equations (9&10) are interrelated due to both lateral displacement about minor axis and rotations about the longitudinal axis coexist in the equations. Solving for the lateral displacement in eqn.(9) and insert this into eqn.(10) it is possible to solve for the critical moment when the beam reaches the unstable state and LT-buckling occurs. The procedure can be followed below, (Galambos, 1968).

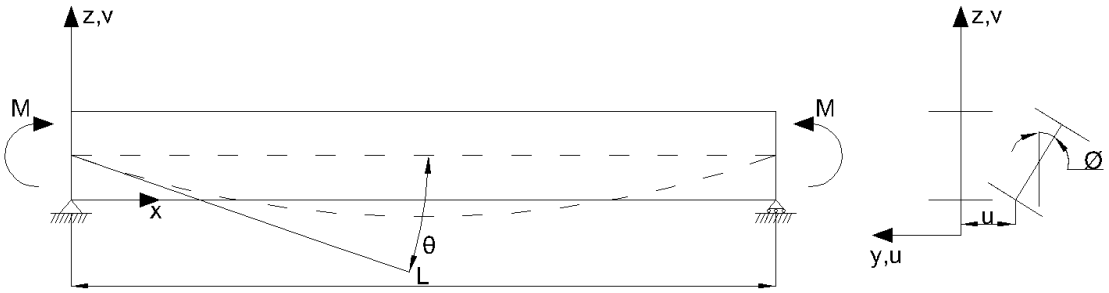

Figure 3 Beam subjected to uniform moment. (Galambos, 1968)

$$EI_y \frac{d^4 v}{dx^4} = 0 \tag{8}$$

$$EI_z \frac{d^4 u}{dx^4} + M \frac{d^2 \phi}{dx^2} = 0 \tag{9}$$

$$EI_w \frac{d^4 \phi}{dx^4} - GI_t \frac{d^2 \phi}{dx^2} - M \frac{d^2 u}{dx^2} = 0 \tag{10}$$

Equation (8) is independent while the latter ones contain both the lateral deflection u and twist ϕ. To be able to solve the system of equations with two unknowns, eqn.(9) is integrated twice, that is,

$$EI_z \frac{d^2 u}{dx^2} + M\phi + C_1 x + C_2 = 0 \tag{11}$$

Where C_1 and C_2 are constants of integration and equal to zero from the boundary conditions (simply supported). If the equation (11) is solved for lateral deflection we get

$$\frac{d^2 u}{dx^2} = -\frac{M\phi}{EI_z} \tag{12}$$

Eqn.(12) is then set into eqn.(10) and the equation obtained when solving for the critical bending can be seen in eqn.(13). The eqn.(13) holds for when the moment distribution is linear and the ratio between the end moments is equal to one.

Furthermore it is assumed that the load is applied in the shear centre of the segment. (NCCI, 2007)

$$M_{cr} = \frac{\pi^2 E I_z}{L^2} \sqrt{\frac{I_w}{I_z} + \frac{L^2 G I_t}{\pi^2 E I_z}} \tag{13}$$

2.1.2 Laterally restrained beams

If lateral supports are added to the tension flange of the beam this has an effect on the differential equations derived previously in eqn.(1-3&8-10). Timoshenko and Gere established and derived the equations for a beam subjected to an axial load with continuous lateral supports. However, lateral supports are often attached at discrete intervals. A study was therefore performed by Dooley considering axially loaded beams with discrete lateral supports. Later Horne and Ajmani determined the critical buckling moment regarding discrete lateral supports. Timoshenko and Gere established the general differential equations assuming the conditions expressed in Figure 4. The point C represents the shear centre of the beam, k_y, k_z, k_ϕ describes the stiffness (produced by the lateral supports) of the beam to deflect and twist. The variables h_y, h_z represent the eccentricity from rotational axis to the shear centre of the beam. (Timoshenko & Gere, 1961)

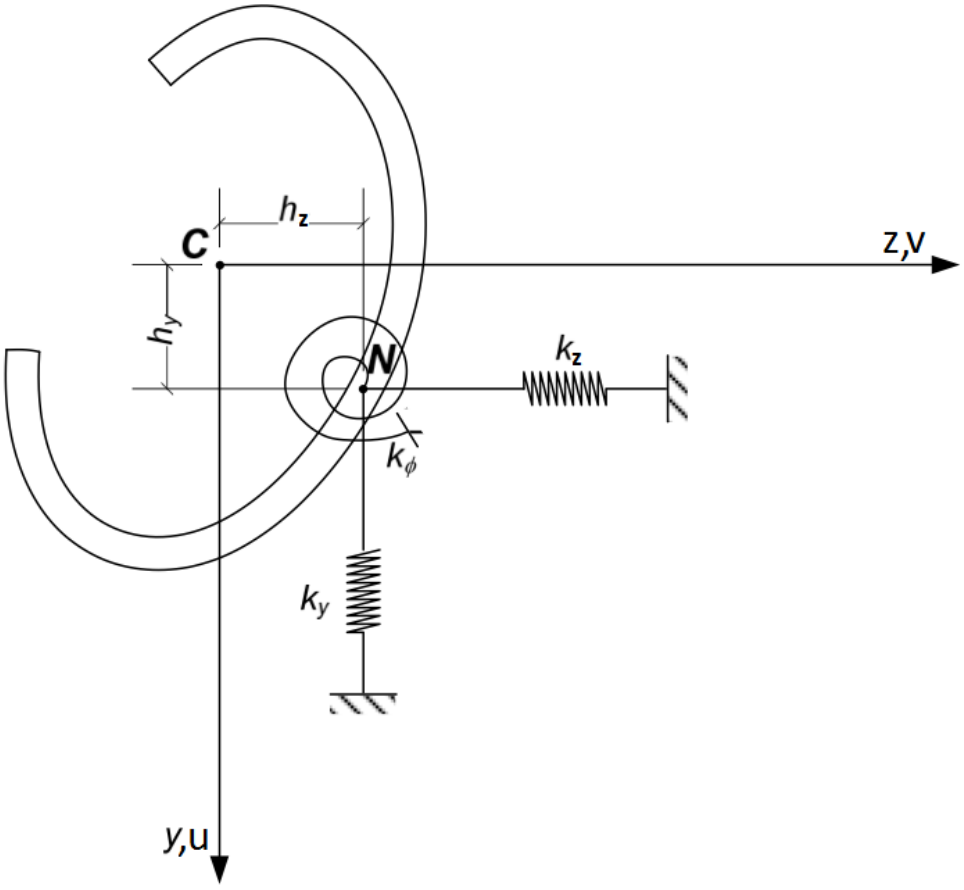

Figure 4 Lateral-torsional buckling of a bar with continuous elastic support. (Timoshenko & Gere, 1961)

2.1.2.1 Beams subjected to axial compression

The differential eqn.(14-16) seen below is the general form for doubly symmetric cross-section subjected to compression load.

$$EI_y \frac{d^4v}{dx^4} + P\frac{d^2v}{dx^2} + k_z[v - h_y\phi] = 0 \tag{14}$$

$$EI_z \frac{d^4u}{dx^4} + P\frac{d^2u}{dx^2} + k_y[u + h_z\phi] = 0 \tag{15}$$

$$\begin{aligned} EI_w \frac{d^4\phi}{dx^4} - (GI_t - Pi_o^2)\frac{d^2\phi}{dx^2} \\ + k_z\big[v - h_y\phi\big](-h_y) - k_y[u + h_z\phi](-h_z) + k_\phi\phi = 0 \end{aligned} \tag{16}$$

Now consider a beam with continuous lateral supports, assuming elastic resistance in the DOF:s seen in eqn.(17-19), attached with a zero eccentricity from the shear centre. When simplifying the DE:s (14-16) the support eccentricity h_y and h_z has evidently been set to zero according to Figure 4. The differential eqn. (14-16) can be solved to determine three respective solutions for the system as following; (Timoshenko & Gere, 1961)

$$P_{y.cr} = \frac{\pi^2 EI_y}{L^2}(n^2 + \frac{L^4 k_z}{n^2\pi^4 EI_y}) \tag{17}$$

$$P_{z.cr} = \frac{\pi^2 EI_z}{L^2}(n^2 + \frac{L^4 k_y}{n^2\pi^4 EI_z}) \tag{18}$$

$$\begin{aligned} P_{x.cr} &= \frac{1}{i_o^2}\left(\frac{\pi^2 n^2 EI_w}{L^2} + GI_t + k_\phi\frac{L^2}{n^2\pi^2}\right) \\ where \quad i_o^2 &= \frac{I_y + I_z}{A} \end{aligned} \tag{19}$$

The first two eqn.(17&18) are the well-known buckling equations about major and minor axis respectively and eqn.(19) represents the critical torsional load. The eqn.(17-19) are considering the lateral and torsional resistance generated by the lateral supports which is the difference compared to the derived expressions in eqn.(4-6). It should be noted that assuming the eccentricity as zero is an optimal case regarding the resistance and will result in a greater critical load.

When considering a beam with continuous lateral restraints(k_y&$k_z = \infty$), prescribed rotation about the longitudinal axis and a non-zero eccentricity h_y from the shear centre the DE:s (14-16) can be solved as following. Eqn.(20&21) will be infinitely great due to that the length between the lateral restraints converges zero.

$$P_{y.cr} = \frac{\pi^2 EI_y}{L^2} = \infty, \qquad when\ L \to 0 \tag{20}$$

$$P_{z.cr} = \frac{\pi^2 E I_z}{L^2} = \infty, \qquad when\ L \to 0 \tag{21}$$

$$P_{x.cr} = \frac{1}{i_s^2}\left(\frac{\pi^2 n^2 E I_z a^2}{L^2} + \frac{\pi^2 n^2 E I_w}{L^2} + G I_t + k_\phi \frac{L^2}{n^2 \pi^2}\right) \tag{22}$$

$$where \quad i_s^2 = i_y^2 + i_z^2 + a^2 \tag{23}$$

Eqn.(22) represents critical torsional load when considering lateral restraints with a certain eccentricity a (h_y has been replaced by a which is the notation in Eurocode3) from the restrained longitudinal axis to the shear centre of the beam. (Louw, 2008)

The major drawback of these equations is the assumption that the lateral restraints acts continuously over the beam. The most common setup of lateral restraints is when they act as purlins on a beam or side-rails on columns which can be seen in Figure 5 below. Dooley studied whether discrete restrains could be regarded as continuous (Dooley, 1966).

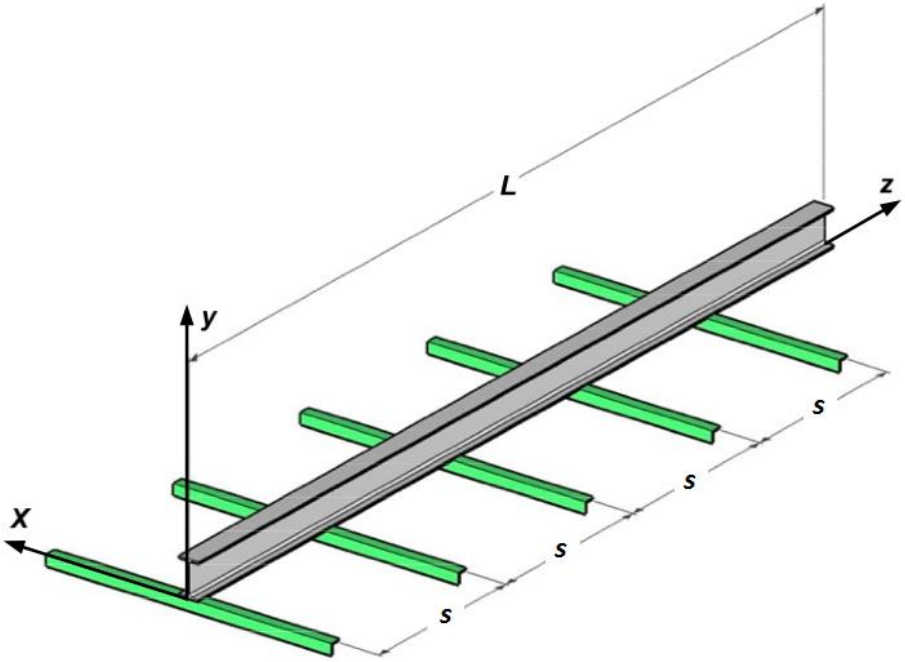

Figure 5 Column with side rails. (Dooley, 1966)

Dooley derived the critical load from the energy theorem considering an axially loaded column with discrete lateral restraints, assuming that the discrete restraints generate an elastic torsional resistance to the beam. From this it was concluded that failure will occur either by flexure buckling in between the lateral restraints (no torsion) or by an overall torsional buckling mode without displacement of the laterally restrained flange. Furthermore, it was concluded for I-sections that if the lateral supports are torsional rigid, flexural buckling will occur before torsional instability in between the lateral restraints.

The equation derived from the energy theorem regarding the overall torsional buckling for axially loaded column is shown below in eqn.(24). It can be noted that it is identical with Timoshenko's eqn.(22) except for the expression considering the torsional spring resistance generated by purlins.

$$P_{x.cr} = \frac{1}{i_s^2}\left(\frac{\pi^2 n^2 E I_z a^2}{L^2} + \frac{\pi^2 n^2 E I_w}{L^2} + G I_t + \frac{2K_s L}{\pi^2 n^2}\sum_{p=1}^{m} sin^2\frac{p\pi n s}{L}\right) \quad (24)$$

$$where \quad \frac{2K_s L}{\pi^2 n^2}\sum_{p=1}^{m} sin^2\frac{p\pi n s}{L} \quad is\ the\ torsional\ spring\ stiffness$$

Further studies made by Dooley (1966) were to compare the difference between the overall torsional instability with discrete and continuous lateral restraints, where he concluded;

"The evident conclusion is that a column attached at discrete intervals to sheeting rails responds as if continuously attached to a foundation of uniform rotational stiffness".

This result is helpful in order to simplify the torsional spring stiffness in eqn.(24) which is complicated to use in practice. It also gives the possibility to use eqn.(22) by Timoshenko and Gere (1961) with an equivalent torsional stiffness for a discrete elastic lateral support shown in the eqn.(25).

$$P_{x.cr} = \frac{1}{i_s^2}\left(\frac{\pi^2 n^2 E I_z a^2}{L^2} + \frac{\pi^2 n^2 E I_w}{L^2} + G I_t + k_\phi \frac{L^2}{n^2\pi^2}\right) \quad (25)$$

$$where \quad k_\phi = K_s/s$$

s is the spacing between purlins.

K_s is the torsional stiffness of an elastic lateral support by taking into account the bending stiffness of the purlins and local stiffness of the beam against distortion.

k_ϕ is the equivalent torsional spring stiffness.

It should be noted that the lowest energy mode n of the torsional buckling load, $P_{x.cr}$, in eqn.(25) must be found by a trial and error method because the term n is both in the nominator and the denominator. If the torsional stiffness is disregarded, as in Eurocode3, then the equation is simplified and the lowest energy mode is with a half sinus curve.

2.1.2.2 Beam subjected to pure bending

In the same manner as Dooley derived the equation for flexural and torsional instability only considering an axial load, Horne determined the instability only allowing for pure moment and discrete lateral supports.

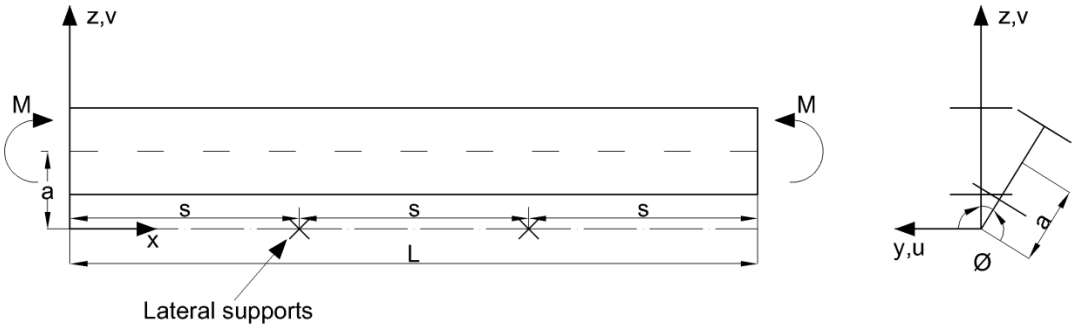

Figure 6 Lateral restrained beam subjected to uniform moment. (Horne & Ajmani, 1969)

Considering the beam presented in Figure 6, it is subjected to pure moment and the lateral supports are assumed totally rigid. At a critical moment LT-instability will occur between lateral restraints or by overall torsion. The lateral displacement is given by,

$$u_1 = u_0 sin\frac{\pi x}{s} \tag{26}$$

However, u_0 is assumed to be zero when the distance in between discrete lateral restraints are sufficiently small, treating the beam as one on continuous supports.

The rotation about the restrained axis is given by,

$$\phi = \phi_n sin\frac{n\pi x}{L} \tag{27}$$

The total lateral displacement u of the centroidal axis is $u_1 + a\phi$ so that

$$u = u_0 sin\frac{\pi x}{s} + a\phi_n sin\frac{n\pi x}{L} \tag{28}$$

The eqn.(29&30) express the energy theorem which is established from equilibrium conditions between total resistance and the added load and moment. The resistance is determined regarding;

- flexural energy
- torsional energy
- warping energy
- rotational energy of elastic supports

The resistance is expressed by the strain energy U and the buckled form is given by

$$U = \frac{1}{2}EI_z\int_0^l (u'')^2 dz + \frac{1}{2}GI_t\int_0^l (\phi')^2 dz + \frac{1}{2}EI_w\int_0^l (\phi'')^2 dz + \frac{1}{2}K_s\sum_v \phi_v^2 \tag{29}$$

The change in potential energy V due to work by axial load P and equal end moments M is given by

$$V = -\frac{1}{2}Pi_0^2\int_0^l (\phi')^2 dz - \frac{1}{2}P\int_0^l (u')^2 dz - 2M\int_0^{l/2} (u'\phi')^2 dz \tag{30}$$

According to equilibrium conditions the strain energy U and potential energy V have to be equal. The next step is to substitute u and ϕ from eqn.(27&28) in eqn.(29&30). To find the location where the stable state converges to unstable a differentiation has to be performed of the sum $U + V$ with respect to both lateral displacement u_0 and twist ϕ_n in eqn. (31&32). This results in a system of two equations. To be able to find the critical moment, the load P has been set to zero and the system of equations is solved for the moment M. (Horne & Ajmani, 1969)

$$\frac{\partial(U+V)}{\partial u_0} = 0 \tag{31}$$

$$\frac{\partial(U+V)}{\partial \phi_n} = 0 \tag{32}$$

When the differentiation is performed and the system of equations is determined, two different situations are regarded. The first case is considered to be general and occurs when the twist is non-zero at lateral supports. The second one is when the twist is zero at lateral supports. The lateral displacement is assumed to be zero at the location of the supports in both cases. (Horne & Ajmani, 1969)

Case 1: $n \neq L/s(twist\ non-zero\ at\ lateral\ supports, overall\ buckling)$

Infinite lateral rigidity and elastic torsional supports is assumed. When solving the system of equations the following result was obtained;

$$M_{cr.0} = \frac{1}{2a}\left(\frac{\pi^2 EI_z n^2 a^2}{L^2} + \frac{\pi^2 EI_w n^2}{L^2} + GI_t + k_\phi \frac{L^2}{n^2\pi^2}\right) \tag{33}$$

Eqn.(33) determines the critical moment when the beam buckles by torsion about the restrained longitudinal axis.

Case 2: $n = L/s(twist\ zero\ at\ lateral\ supports,\ buckling\ in\ between\ support)$

$$M_{cr} = \frac{\pi^2 E I_z}{s^2}\sqrt{\frac{I_w}{I_z} + \frac{s^2 G I_t}{\pi^2 E I_z}} \tag{34}$$

Eqn.(34) is identical to eqn.(13) derived in section 2.1.1.2 and determines the buckling in between lateral supports. However, the critical length has been adjusted from L to s. (Horne & Ajmani, 1969)

Summarizing this chapter the critical moment is governed by three parameters;

- Eccentricity of lateral support a
- Torsional stiffness of lateral support k_ϕ
- Spacing of lateral support s

Depending on these three factors above, the beam will buckle in one of the two following modes;

- Torsion about the laterally restrained longitudinal axis, the critical moment being $M_{cr.0}$ eqn.(33).
- Lateral-torsional buckling in between the lateral supports, with no lateral and torsional displacement at the supported section. The critical moment is then given by M_{cr} eqn.(34). (Horne & Ajmani, 1969)

The governing buckling mode will be the lower of $M_{cr.0}$ and M_{cr}. (Horne & Ajmani, 1969)

2.1.2.3 Beam subjected to bending and axial compression

A similar procedure as in section 2.1.2.2 has to be performed to find the critical combination of P and M. The difference from the previous derivation is that both variables in the energy theorem are taken into account.

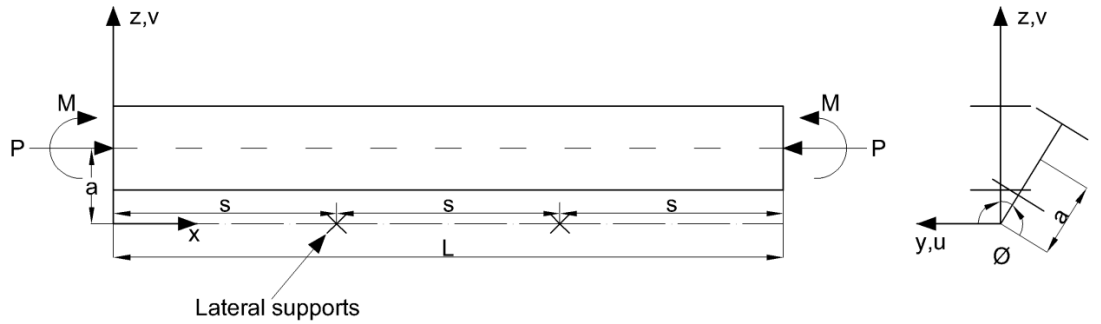

Figure 7 Lateral restrained beam subjected to uniform moment and axial compression. (Horne & Ajmani, 1969)

Case 1: $n \neq L/s$

$$P + \frac{2Ma}{i_s^2} = P_T \tag{35}$$

P_T is the critical load causing overall torsion about the restrained axis.

Case 2: $n = L/s$

$$\left(\frac{M}{M_E}\right) - \left(1 - \frac{P}{P_E}\right)\left(1 - \frac{P}{P_{TC}}\right) = 0 \tag{36}$$

Eqn.(36) is an interaction formula where;

M_E expresses the lateral-torsional buckling moment in between the supports.

P_E is the flexural buckling load in between the supports.

P_{TC} is the axial load producing torsional buckling in an unsupported beam of length s.

The eqn. can be seen below (40-42).

$$M_E = M_{cr} = \frac{\pi^2 E I_z}{s^2}\sqrt{\frac{I_w}{I_y} + \frac{s^2 G I_t}{\pi^2 E I_z}} \tag{37}$$

$$P_E = P_z = \frac{\pi^2 E I_z}{s^2} \tag{38}$$

$$P_{TC} = \frac{M_E^2}{P_E i_o^2} \tag{39}$$

If **Case1** gives the lowest P, buckling is by torsion about the restrained axis, otherwise lateral-torsional buckling occurs in between the lateral restraints. (Horne & Ajmani, 1969)

2.2 Stable length in Eurocode3

In En 1993-1-1, Annex BB.3 there exists a method for calculating thestable length regarding lateral-torsional stability taking into account the effect of purlins. Studies by Horne et al. (1964, 1971, 1979) constitute the theoretical background of the method.

The stable length gives the limiting length of a segment in a portal frame, between torsional restraint at a plastic hinge and the adjacent torsional restraint for which lateral torsional buckling may be ignored. The method is only appropriate for plastic design and where the spacing of the purlins is sufficiently small for the section between the purlins to be stable against LT-buckling. (King, 2002)

2.2.1 Plastic stable length-Tension flange unrestrained

To be able to conclude that no LT-buckling occurs in between the purlins on the tension flange, a check of the maximum length L_m has to be performed. This procedure ensures that an overall torsional instability is the critical one. The stable length L_m for combined axial compression and moment is shown below; (King, 2002)

$$L_m = \frac{38 i_z}{\sqrt{\frac{1}{57{,}4}\left(\frac{N}{A}\right) + \frac{1}{756 C_1^2}\left(\frac{W_{pl}^2}{A I_t}\right)\left(\frac{f_y}{235}\right)^2}} \tag{40}$$

C_1 takes into account the shape of bending moment diagram.

N is the applied axial force.

A is the cross-sectional area.

W_{pl} is the plastic sectional modulus.

I_t is the torsional constant.

f_y is the steel yield strength.

The stable length is based on the work by Horne et al. (1964) where the authors found the limit of slenderness L_m/i_z in which an unrestrained beam segment in a portal frame with a uniform moment can be regarded as stable against LT- buckling when the cross-section reaches its plastic moment resistance.

Horne concluded that if a beam segment is subjected to a near uniform moment it is impossible for the section to reach complete plasticity due to the loss of stiffness about the minor axis. However the requirement that the cross-section of the segment reaches complete plasticity was determined not to be the essential criteria when considering a segment within a continuous structure, where re-distribution of stresses occurs.

The criteria for plastic design were (Horne, 1964)

1) *The curve of the applied moment versus end rotation is sufficiently flat-topped*
2) *The peak of the moment-rotation curve is not more than a few percentages below the theoretical full plastic moment.*

This limit of slenderness L_m/i_z proved difficult to obtain theoretically and therefore it was established with experiments on full scale I-sections using the previous criteria. It was detected that the sections subjected to uniform moment were stable as long as the length L_m was smaller than 0.6 L, where the length L is the unrestrained length when the elastic capacity is equal to critical buckling moment M_{crW0} with zero warping stiffness.

The derivation of the stable length for a uniform moment is shown below. (King, 2002)

Stable length under uniform moment is $L_m = 0.6L$

$$W_e f_y = M_{crW0} = \sqrt{\frac{\pi^2 E I_z G I_t}{L^2}}$$

This is rearranged to find L

$$L = \sqrt{\frac{\pi^2 E I_z G I_t}{\left(W_e f_y\right)^2}}$$

Then inserting $L = L_m / 0.6$ gives the stable length for a uniform moment.

$$L_m = 0.6 \sqrt{\frac{\pi^2 E I_z G I_t}{\left(W_e f_y\right)^2}} \tag{41}$$

2.2.2 Plastic stable length–Tension flange restrained

The plastic stable length L_k is the only method in Eurocode3 where the beneficial effect of the purlins on the tension flange is taken into account. It is still quite conservative since the bending stiffness of the purlins is ignored. This is done because of the difficulty to consider the torsional resistance produced by the purlins. The properties of the purlins are case specific (different types of connections). In addition it was mentioned in section 2.1.2.1, that the lowest energy buckling mode is difficult to determine due to the number of half sinus curves *n* present both in the numerator and denominator of the analytical expressions. In order to apply this in practice it was necessary to ignore this effect.

The beneficial effect of the purlins acting as only lateral restraints is still significant. The derivation of the elastic stable length without imperfection and the plastic stable length with imperfection are shown next section.

2.2.2.1 The elastic stable length L_{ke} - Tension flange restrained

Although the elastic stable length is not used in Eurocode3 it is convenient to examine it in order to understand the more complicated plastic stable length.

The stable length L_{ke} is derived from the critical moment eqn.(42) by solving for L when the critical bucking moment is equal to the yield moment. The purlins are assumed to have no torsional resistance.

$$M_{cr.0} = \frac{1}{2a}\left(\frac{\pi^2 EI_z a^2}{L^2} + \frac{\pi^2 EI_w}{L^2} + GI_t\right) \tag{42}$$

By inserting the expression of the warping constant in eqn.(42), eqn.(43) is obtained.

$$M_{cr.0} = \frac{1}{2a}\left[\frac{\pi^2 EI_z}{L}\left(a^2 + \frac{(h-t_f)^2}{4}\right) + GI_t\right] \tag{43}$$

This is rearranged to find L.

$$\begin{aligned} L^2 &= \frac{\pi^2 EI_z\left(a^2 + \frac{(h-t_f)^2}{4}\right)}{2aM_{cr} - GI_t} = \frac{\frac{\pi^2 EI_z}{GI_t}\left(a^2 + \frac{(h-t_f)^2}{4}\right)}{\frac{2aM_{cr}}{GI_t} - 1} \\ &= \frac{\frac{\pi^2 EI_z}{GI_t}\left(a^2 + \frac{(h-t_f)^2}{4}\right)}{\frac{2a}{GI_t}\left[\frac{\sigma_{cr} I_y}{\frac{h}{2}}\right] - 1} = \frac{\frac{\pi^2 EI_z}{GI_t}\left(a^2 + \frac{(h-t_f)^2}{4}\right) i_z^2}{\frac{4a}{h}\left(\frac{\sigma_{cr}}{G}\right)\left(\frac{I_y}{I_t}\right) - 1} \\ &= \frac{\left[2(1+v)\pi^2\left(\frac{a^2}{h^2} + \frac{(h-t_f)^2}{4h^2}\right)\right]\left(\frac{Ah^2}{I_t}\right) i_z^2}{\left[8(1+v\frac{a}{h}\right]\left(\frac{\sigma_{cr}}{E}\right)\left(\frac{I_y}{I_t}\right) - 1} \end{aligned} \tag{44}$$

The equation was limited to a hot rolled I-section with the eccentricity a equal to $0.75h$. In addition, sectional dimensions and material constants are approximated for an I-section in order to present the equation with fewer parameters. The approximations are $G/E = 0{,}4$, $d/b = 2{,}5$ and $t_w/t_f = 0{,}6$ (King, 2002).

By expressing normal stress σ_{cr} as yield strength f_y, the length L_{ke} is the limit where the section yields before it buckles.

$$L_{ke} = i_z 3{,}27 \left(\frac{\left[1 + 0{,}75\left(1 - t_f/d\right)\left(1 + {t_f}/{d}\right)\right]}{\left(f_y/E\right)\left[1 + 0{,}25\left(1 - {t_f}/{d}\right)^3\right] - 0{,}226\left({t_f}/{d}\right)^2\left(1 + {t_f}/{d}\right)} \right)^{0{,}5} \quad (45)$$

The equation above is difficult to use in practice and therefore a more simple empirical expression was established that gives results that are in close agreement.

$$L_{ke} = \frac{\left(8{,}0 + \frac{150 f_y}{E}\right)\left(\frac{h}{t_f}\right) i_z}{\sqrt{4{,}4\left(\frac{f_y}{E}\right)\left(\frac{h}{t_f}\right)^2 - 1}} \quad (46)$$

h is the depth cross-section.

t_f is the thickness of the flanges.

f_y is the yield strength.

E is the Young´s modulus.

i_z is the polar radius about the minor axis

2.2.2.2 The plastic stable length-Tension flange restrained

The plastic stable length L_k is based on the work by Horne et al. (1964, 1971, 1979) where they found the limiting slenderness L_k/i_z, in which a plastic collapse mechanism is formed before LT-buckling. The work took the form of theoretical and parametric studies, which was supported by test work.

In the research by Horne the most severe loading condition, constant moment about the major axis, was assumed. Furthermore, elastic-plastic material and imperfections as an initial twist about the restrained axis were assumed. The fillets were neglected which is a conservative approach giving lower torsional stiffness. In addition, the spacing of the lateral restraints were sufficiently close (1,5m) producing an overall torsional buckling of the beam. Also the eccentricity a was fixed to 75% of the depth of the beam.

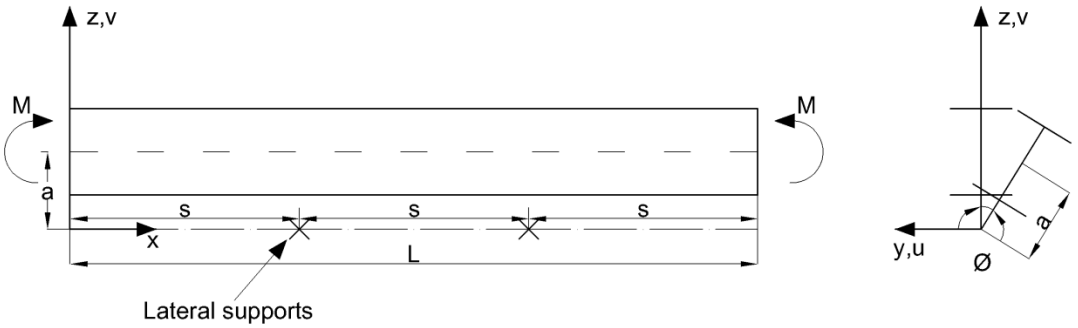

Figure 8 Laterally restrained beam subjected to uniform moment. (Horne & Ajmani, 1969)

As mentioned in section 2.1.1 it was concluded that for an unrestrained beam with a uniform moment, complete plasticity was impossible to reach before a loss in stability. This also applies for a restrained beam and the criteria for the plastic design was: (Horne, 1964)

1) *The curve of the applied moment versus end rotation is sufficiently flat-topped*
2) *The peak of the moment-rotation curve is not more than a few per cent below theoretical full plastic moment.*

As for an unrestrained beam it was difficult to get a pure theoretical expression for the limit of slenderness. Therefore a theoretical expression combined with criterion that was established from tests on full scale I-sections was used to find the limit of slenderness.

In order to explain the work, it is best to reflect on the graph in Figure 9 that shows the relation between the applied moment and the angle of twist in the middle of the beam.

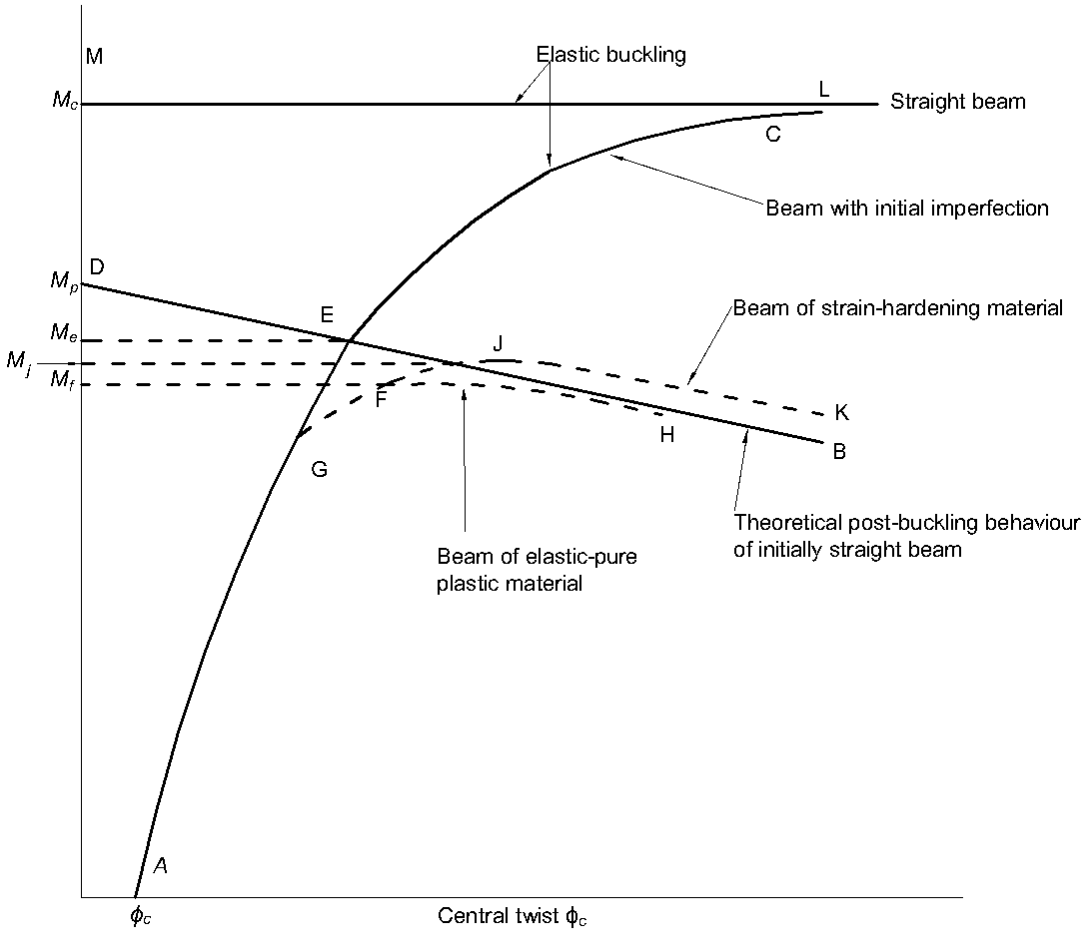

Figure 9 Out-of-plane behaviour of restrained I-beam under uniform moment. (Horne, Shakir-Khalil & Akhtar, 1979)

The curve AGC is the elastic response of the beam with an initial imperfection and DB is the plastic mechanism line. These curves are convenient to obtain theoretically, while the curve AGFH (plastic response with imperfection) and curve AGJK (plastic response with imperfection and strain hardening) are on the other hand difficult to obtain. In order to extend the work for plastic response it was necessary to use a criterion that was found by a full-scale test of I-sections. Test results have shown that the point E, where the elastic response and the plastic mechanism line intersect is closely related to the plastic response. It has been shown that if the moment M_E at intersection point E is not less than 96% of M_P then the curve of the applied moment versus the rotation is reasonably flat topped, satisfying the stated requirement. With this criterion established it was possible to find the limit of slenderness by using the more easily obtained curve AGC (the elastic response).

The elastic response curve AGC in Figure 9 is derived by assuming an initial twist Φ about the restrained axis, at the middle of the column.

$$\Phi_0 = 0.003 \frac{Li_z}{ba} \tag{47}$$

The maximum twist at the middle of the beam, with a uniform moment has been shown by Horne to be:

$$\Phi = \frac{GI_t + \frac{\pi^2 EI_z}{L}\left(a^2 + \frac{d^2}{4}\right)}{GI_t + \frac{\pi^2 EI_z}{L}\left(a^2 + \frac{d^2}{4}\right) - 2M_{Ed}a}\Phi_0 \qquad (48)$$

In order to present the eqn.(48) with fewer parameters sectional dimensions and material constants are approximated for standard I-sections, $G/E = 0,4$, $d/b = 2,5$ and $t_w/t_f = 0,6$. The general equation is expressed in the parameters of h/t_f and f_y/E. The equation is extensive and can be seen in the article; *The post-buckling behaviour of laterally restrained column* by Horne and Ajmani.

The general expression was used to determine the limit of slenderness with trial and error method. The procedure was to try different lengths in the general equation simplified from eqn.(48). The limit of slenderness was obtained by trying different lengths until the curve AGC (elastic response with initial imperfections) intersects the mechanism line at a moment equal to $0,96M_P$.

The graph of the critical slenderness limits L_k/i_z obtained is reproduced and shown in Figure 10.

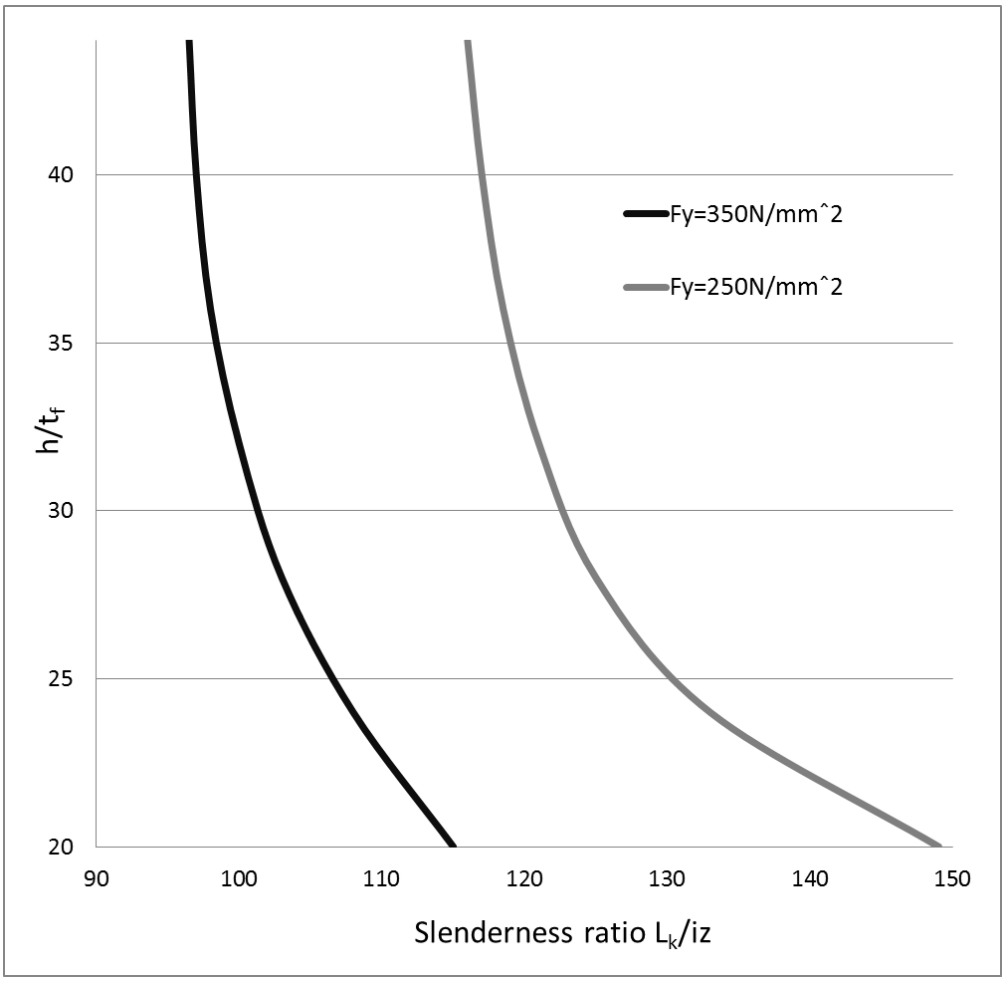

Figure 10 Critical slenderness ratios of restrained I-sections.(Horne, Shakir-Khalil & Akhtar, 1979)

An empirical expression for the plastic stable length L_k was found using the curves for the limiting slenderness in the Figure 10.

$$L_k = \frac{\left(5{,}4 + \frac{600 f_y}{E}\right)\left(\frac{h}{t_f}\right) i_z}{\sqrt{5{,}4\left(\frac{f_y}{E}\right)\left(\frac{h}{t_f}\right)^2 - 1}} \tag{49}$$

h is the depth cross-section.

t_f is the thickness of the flanges.

f_y is the yield strength.

E is the Young´s modulus.

i_z is the polar radius about the minor axis.

Horne concluded that the limit of slenderness given in eqn.(50) is significantly greater for a restrained beam than for an unrestrained beam. The limit of slenderness for a restrained beam was found to vary from 0,63 to 0,71 while for the unrestrained beam it varies from 0,38 to 0,46.

$$\bar{\lambda} = \frac{Plastic, with\ imperfection}{Elastic, without\ imperfection} = \frac{\frac{L_k}{i_z}}{\frac{L_{k.e}}{i_z}} \tag{50}$$

It should be noted that Horne did not mention the effect of the residual stresses in his work, however by using test results on full-scale I-sections, it can be reasoned that the effect is taken into account. In addition the initial imperfection used in Horne's research is significantly smaller than the imperfection according to the buckling curve method in Eurocode3.

3 Method

The objective is to derive a stable length in steel portal frames according to elastic design and study the stabilizing effect of purlins. Furthermore compare the length with existing expressions in Eurocode3. The stable lengths will be derived using the buckling curve method in Eurocode3 where second order effects such as geometric imperfections and residual stresses are taken into account. Verification of the derived stable length will be performed with finite element simulation.

3.1 Analytical parametric study

To date, there exist analytical expressions for the critical buckling moment regarding unrestrained and restrained I-sections with flat web. To be able to gain an understanding of these expressions an analytical parametric study is performed in order to examine the influence from purlins. The analytical equations are then verified with numerical studies assuming first order analysis.

In the equations for the critical buckling moment the following parameters are studied;

- influence of the eccentricity *a* of the lateral restraint on the tension flange
- different types of cross-sections (standard and customized cross-sections)
- different lengths combined with having restraints at two different eccentricities of *a*

3.2 Stable length between torsional restraints

As mentioned previously the aim the thesis is to find an analytical expression for the stable length between torsional restraints. The beam segment which is investigated is extracted from the portal frame shown in Figure 11. The beam is assumed to be subjected to a constant moment, which results in the most severe condition and consequently will give the shortest length between torsional restraints. Furthermore it is assumed that the beam is free to warp at the edges, which is considered to be conservative. The beam segments with its notations can be seen in Figure 11 below.

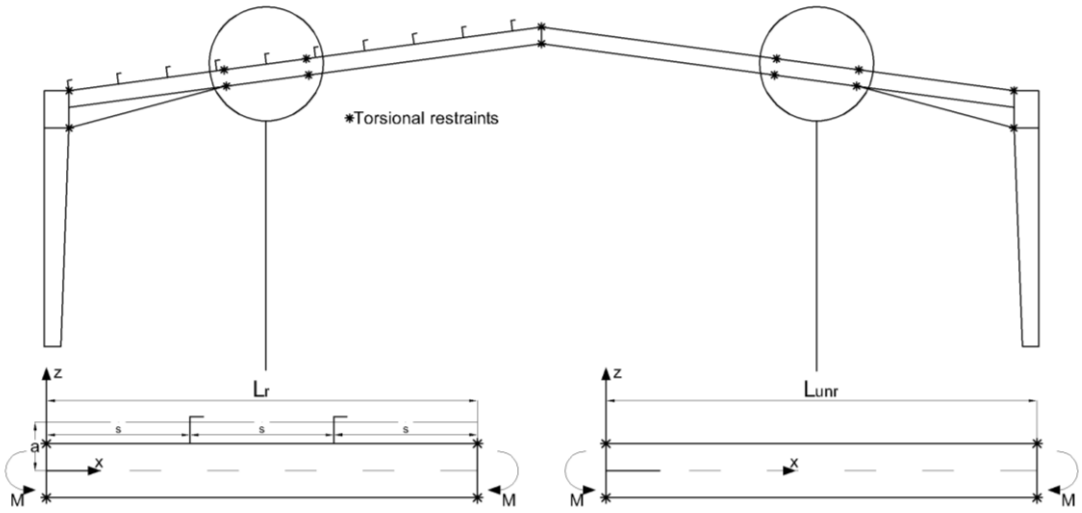

Figure 11 Beam segments, laterally restrained to the left and laterally unrestrained to the right.

Attacking this problem analytically, reasonable assumptions have to be made. For example the non-dimensional slenderness of the beam that defines the limit where buckling effects may be ignored and only cross-sectional checks apply. The equation for the non-dimensional slenderness is seen in eqn.(51).

$$\bar{\lambda} = \sqrt{\frac{w_e * f_y}{M_{cr} \; or \; M_{cr0}}} \tag{51}$$

$$where \qquad M_{cr} = \frac{\pi^2 E I_z}{{L_{unr}}^2} \sqrt{\frac{I_w}{I_z} + \frac{{L_{unr}}^2 G I_t}{\pi^2 E I_y}} \tag{52}$$

$$M_{cr.0} = \frac{1}{2a}\left(\frac{\pi^2 E I_z a^2}{{L_r}^2} + \frac{\pi^2 E I_w}{{L_r}^2} + G I_t \right) \tag{53}$$

In theory LT-buckling effects can be ignored if the limit of slenderness $\bar{\lambda}$ is equal or greater than one. However in reality the beam is not completely straight, creating additional bending moment about the minor axis. Furthermore residual stresses generated in the manufacturing of the beams influence the ultimate capacity significantly. According to Eurocode3 imperfections and residual stresses are considered with the buckling curve method.

Each buckling curve represents different imperfection factors depending on the cross-section. There is a limit where the buckling curves converge despite different imperfection factors.

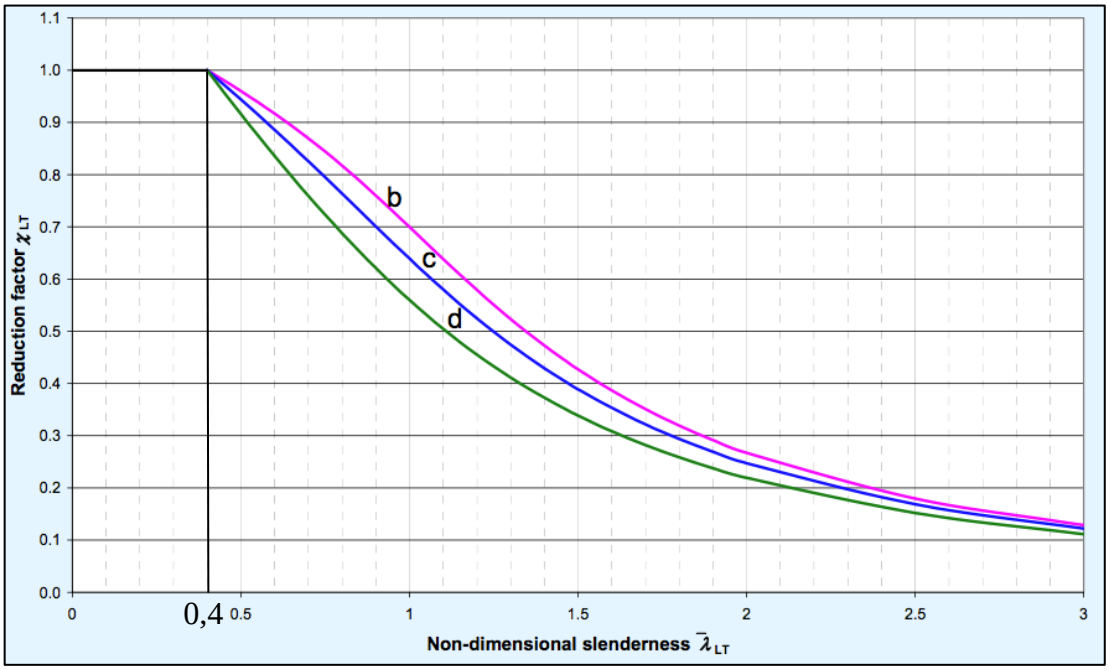

Figure 12 Buckling curve according to Eurocode3. (M E Brettle, 2009)

In Eurocode3 for unrestrained beams the slenderness limit $\bar{\lambda}$ is recommended to be equal to 0,4 where the capacity of the cross-section is reached before the occurrence of LT-buckling. By assuming the limit presented and solving for the length L_{unr} in eqn.(54) a reasonable stable length for an unrestrained beam is found.

$$0{,}4 = \sqrt{\frac{w_e * f_y}{\frac{\pi^2 E I_z}{{L_{unr}}^2}\sqrt{\frac{I_w}{I_z} + \frac{{L_{unr}}^2 G I_t}{\pi^2 E I_y}}}} \tag{54}$$

Unfortunately it is not possible to find an expression for the unrestrained stable length when solving for L_{unr} in eqn.(54), the result can be seen in eqn.(55) which includes an imaginary number. This occurs because the length of the beam is both in the nominator and in the denominator. However, the length is still found by iteration and compared to the restrained stable length L_r.

$$L_{unr} = i\sqrt{\frac{\pi^2 E I_w}{G I_t}} \tag{55}$$

When restraining the beam on tension flange is it reasonable to utilize the same limit of 0,4? According to previous research there is a greater limit for restrained beams and this is something that has to be studied.

Solving for L_r in eqn.(56) when using M_{cr0}, assuming the already stated slenderness limit 0,4 and elastic capacity of the cross-section, the restrained stable length is established in eqn.(57). The results from a non-linear finite element simulation will determine whether the restraint has an impact and if a different slenderness limit should be utilized for laterally restrained beams.

$$0{,}4 = \sqrt{\frac{w_e * f_y}{\frac{1}{2a}\left(\frac{\pi^2 E I_z a^2}{{L_r}^2} + \frac{\pi^2 E I_w}{{L_r}^2} + G I_t\right)}} \tag{56}$$

$$L_r = \sqrt{\frac{\pi^2 E (I_z a^2 + I_w)}{\frac{2aW_y f_y}{0{,}4^2} - G I_t}} \tag{57}$$

The critical buckling moment for laterally restrained beams includes the variable a which is the distance from the shear centre of the beam to the shear centre of the lateral restraint which is seen in Figure 13.

In this investigation the parameter "a" is limited to the following two values; 50% and 75% of the depth of the beam (0,5*h* and 0,75*h*). The distance 0,5*h* is chosen of theoretical interest since it is the same as having the flange restrained without having any volume of the restraint. Restraint at 0,75*h* is chosen for two reasons. In Eurocode3 there exists a semi-empirical expression for the plastic restrained stable length. When investigating the derivation of that equation it has been assumed that the distance is 0,75*h* to simplify the equation. By using the same eccentricity in the derived analytical equation for the stable length a more accurate comparison to the Eurocode3 equations can be performed. The second reason is to have a distance which is in proportion with the depth of the beam.

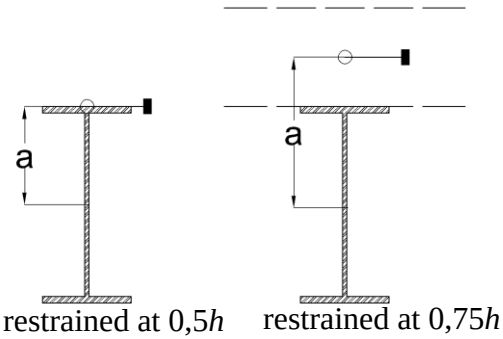

Figure 13 Illustrating the level of the restraints.

3.3 Finite element analysis

The investigation is performed with finite element analysis (FE-analysis) and the software executing the calculations is ABAQUS CAE. The models are constructed to represent analytical assumptions considering boundary conditions and loads. The numerical results are then verified by comparing with existing analytical equations.

The first verification is to perform an elastic static analysis and then continue with a linear buckling analysis of the models created. Similar or equal results between analytical and numerical solutions will consequently verify the models. Additionally the elastic linear buckling analysis is performed to obtain a greater understanding of the LT-stability. By investigating the buckling modes it is possible to determine what conditions affect the flexural- and torsional displacement. Furthermore the LT-buckling shape is recorded and used in the non-linear analysis. By assuming a geometrical imperfection shape as the LT-shape the worst case scenario is obtained.

A non-linear analysis is carried out in order to get closer to the real behaviour of the studied beam. The non-linear analysis considers geometrical imperfections, residual stresses and elastic-plastic material. The analyses are limited to a yield strength of f_y=235N/mm^2. Comparing the results for beams, with different cross-sections, different lengths, unrestrained and restrained at two eccentricities the stabilizing effect from purlins can be seen. Performing the non-linear analysis verifies if the non-dimensional slenderness $\bar{\lambda}$ equal to 0,4 is a satisfactory limit when deriving the restrained stable length.

The boundary conditions assumed in the analytical eqn.(52&53) are equivalent to fork- support at the edges. In order to enable a verification of the models produced in the FE-simulation the boundary conditions have to be the same as in the analytical equations.

As mentioned previously the aim is that this Master´s project can be applied on portal frames. Instead of modelling the whole frame, simplified models are produced. The assumption made is to consider segments in between torsional restraints in the portal frame. By assuming fork-supports as the torsional restraints in the portal frame it will represent the reality sufficiently well. The assumption will be on the safe side since the model is free to warp which in reality is not true and the critical buckling moment will be increased.

3.4 Investigated beams

When performing a parametric study there has to be a discussion of how to make the survey as reliable as possible. The results obtained have to be comprehensive thus the overall picture can be seen. Achieving this aim several cross-sections have to be checked. The aim is also to apply this survey to portal frames therefore only cross-sections often used in frames are considered. In the analytical parametric study both standard (hot-rolled) and customized (welded) cross-sections are studied and the dimensions are seen in Table 1.

Table 1 Dimensions of cross-sections studied in the investigation.

Cross-section	h [mm]	b [mm]	t_f [mm]	t_w [mm]	Buckling curve	Cross-section class
IPE200	200	100	8,5	5,6	b	1
IPE400	400	180	13,5	8,6	c	1
IPE600	600	220	19	12	c	1
200	200	200	10	6	c	2
400	400	200	10	6	c	2
600	600	200	10	6	d	3

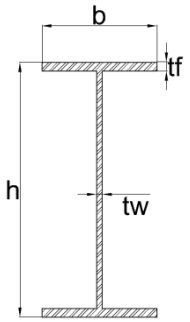

Studying both standard- and customized sections different buckling curves apply in the non-linear analyses making the investigation more extensive. In the survey an initial aim is to check several cross-section classes. However, when studying slender customized cross-sections with a short length local buckling occurs despite that the cross-section is not in class four. To get around this problem in the linear and non-linear analyses standard cross-sections in class one are utilized and geometrical imperfection is applied assuming it is welded. This procedure will therefore still cover both welded and standard cross-sections and all buckling curves.

4 Modelling

The numerical results are obtained with finite elements analysis using the commercial software package ABAQUS CAE version 6.12-1. The investigated beams will be simulated without welds.

The modelling is performed in the following steps

- Linear buckling analysis
- Non-linear buckling analysis

4.1 Linear buckling analysis

The first step is performing a linear buckling analysis where the critical buckling moment is obtained and verified with the analytical results. The buckling shape is also recorded and used in the non-linear buckling analysis in chapter 4.2. For the linear buckling analysis the material response is elastic with a Young modulus E of 210GPa and Poisson's ratio ν of 0,3. This analysis records the eigenvalue λ required to reach the LT-buckling mode. The critical buckling moment is then obtained by multiplying the eigenvalue with the applied reference moment.

$$M_{cr} = \lambda M_{ref} \tag{58}$$

All analyses are performed with eight node shell elements with quadratic base function and reduced integration. The elements have five integration points over its thickness and Simpson integration rule is utilized. For the linear buckling analysis a fine mesh of 25mm is used. This is a much finer mesh than needed according to the convergence study in chapter 4.3 but since the analysis is not time consuming and in order to get as accurate results as possible a fine mesh is chosen.

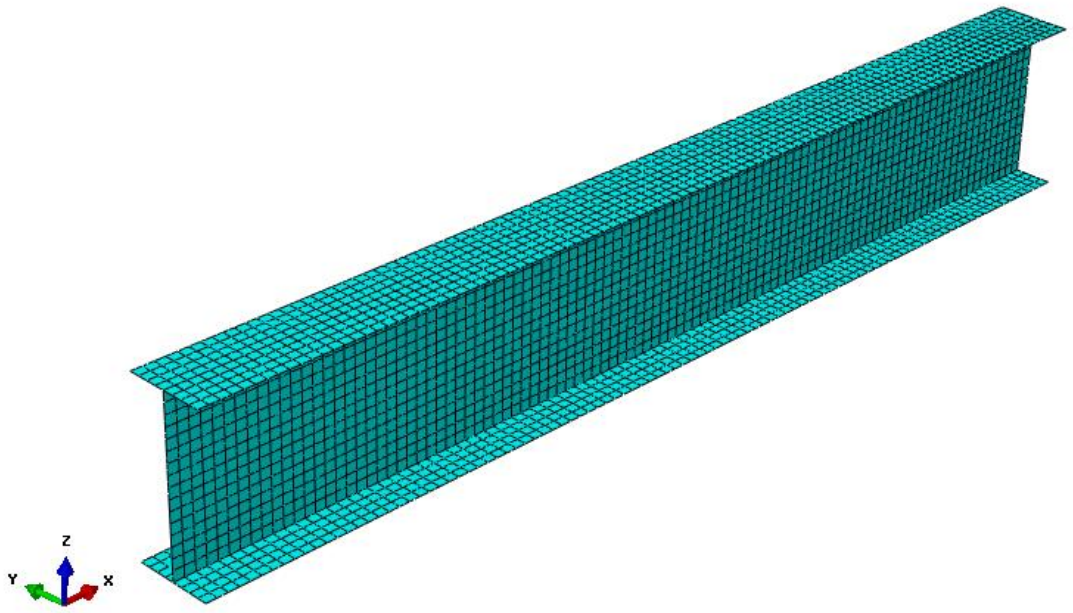

Figure 14 Fine mesh of 25mm.

The investigated models are all subjected to a constant reference moment of 100kNm. According to the ABAQUS manual only a concentrated load or a pressure load can be used in following analyses (buckle and static risk). In order to simulate a constant moment, an evenly distributed load is applied on the flanges (shell edge loading), creating a force couple at each end corresponding to 100kNm. The top flange is subjected to tension and the bottom flange to compression. The load follows the rotation of the section and is defined to act on the un-deformed area of the flanges. The load conditions can be seen in Figure 15 below.

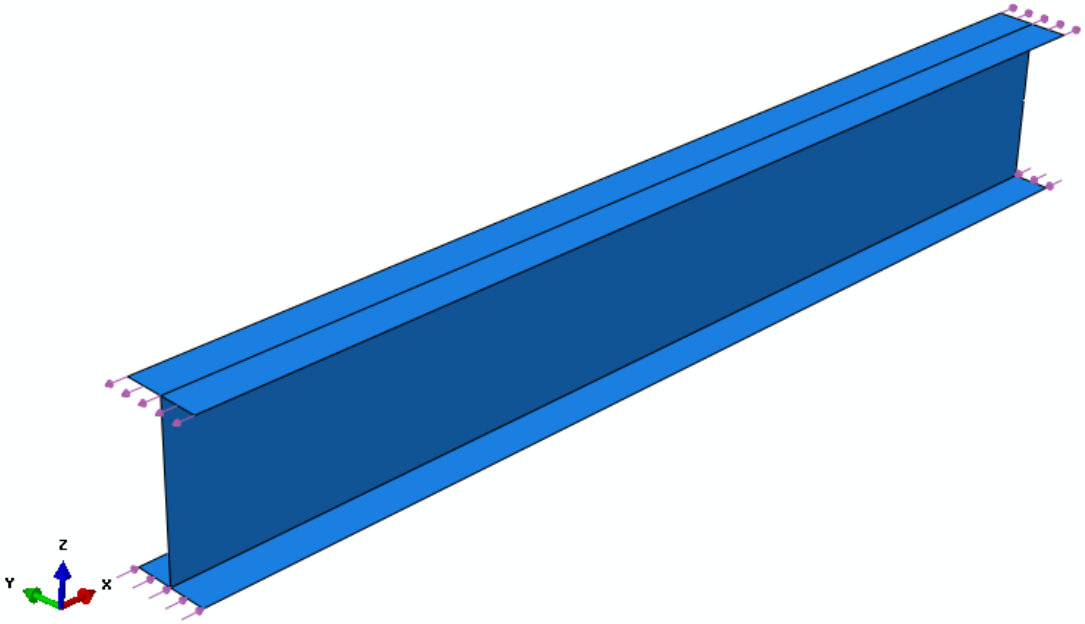

Figure 15 The applied load.

In this study there are three types of boundary conditions (see Figure 16) and in the following text will be termed as follows;

- Unrestrained; Fork supports at the ends.
- Restrained at 0,5*h*; Fork supports at the ends and a continuous lateral restraint at the top of the tension flange.
- Restrained at 0,75*h*; Fork support at the ends and a discrete lateral restraint above the tension flange at the eccentricity of 0,75*h* from the shear centre of the web.

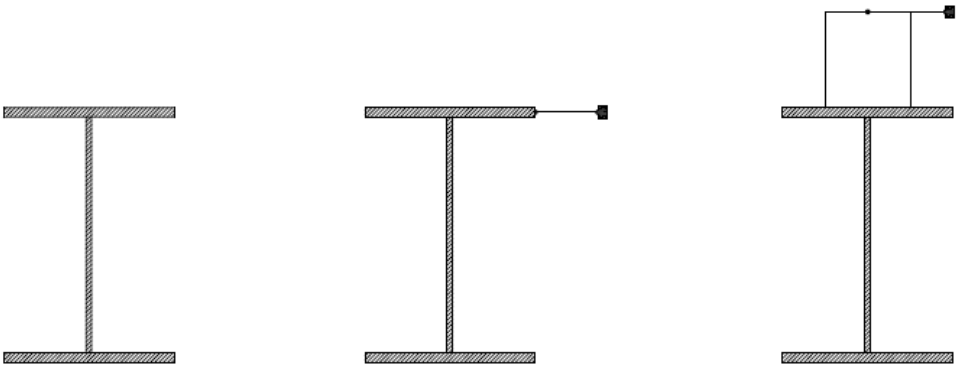

(a) unrestrained (b) restrained at 0,5*h* (c) restrained at 0,75*h*

Figure 16 Types of lateral restraints considered in analysis.

Unrestrained

The boundary conditions for the lateral unrestrained beam (see Figure 17) are equivalent to fork supports at the ends and are simulated as follow;

- Point a is restrained in all directions (x, y and z) and to rotate about the longitudinal axis (x).
- Point b is restrained from translating in vertical (z) and lateral (y) direction. It is also restrained to rotate about the longitudinal axis (x).
- Line A is restrained with a feature in ABAQUS called coupling constraint, were all the nodes on Line A are coupled to displace the same amount in the lateral (y) direction as the reference point a.
- Line B is coupled to point b to displace the same amount in the lateral (y) direction.

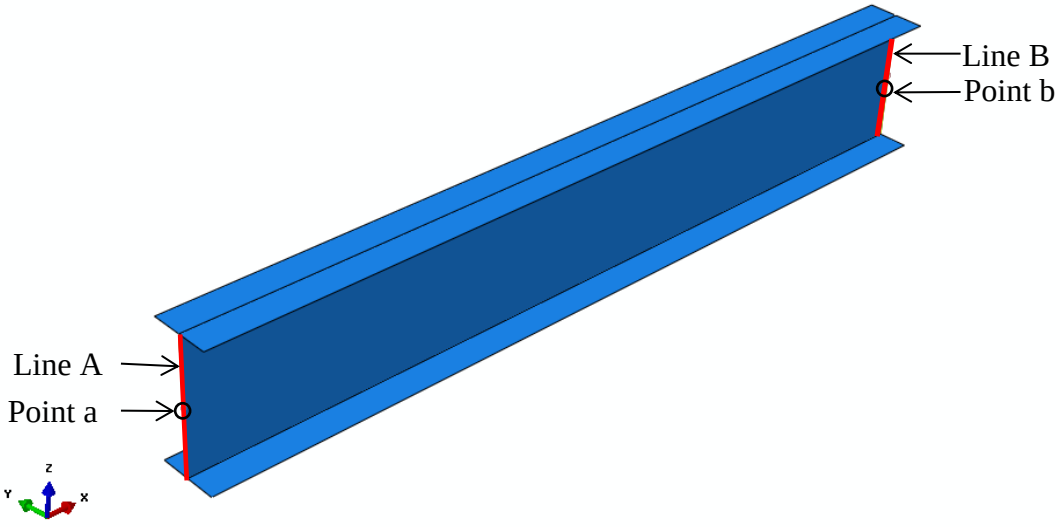

Figure 17 Illustration of how the fork supports at the ends are simulated.

Restrained at 0,5h

The boundary conditions at the ends are the same as for the laterally unrestrained beam. In addition a continuous restraint is applied at top of the tension flange, preventing it to displace laterally (y). The continuous lateral restraint is shown in Figure 18 below.

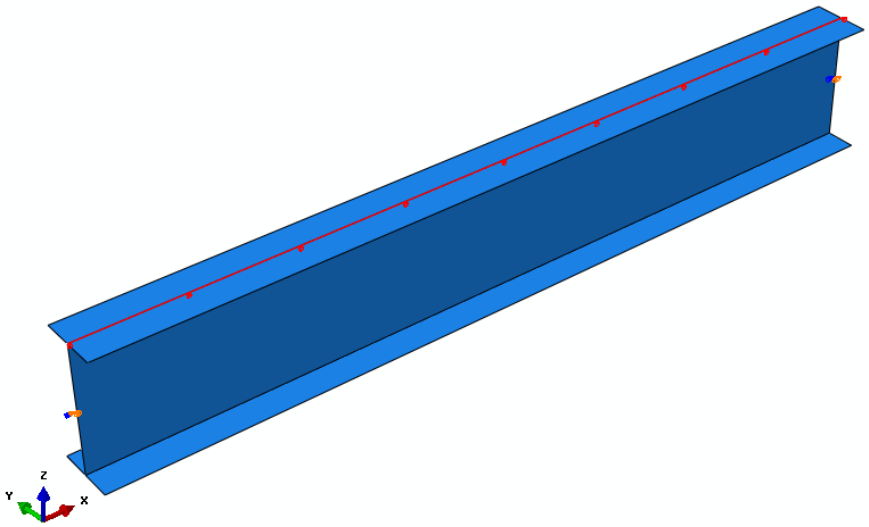

Figure 18 Boundary condition of the laterally restrained beam at the tension flange.

Restrained at 0,75h

The boundary conditions at the ends are the same as for the laterally unrestrained beam. In addition, discrete lateral restraints are applied above the tension flange. The distance from the shear centre of the web to the discrete restraint is 75% of the total depth of the cross-section. This is simulated by adding plates on the top of the tension flange with a spacing of 1,2m. The plate is half the width of the corresponding flange and the thickness is the same as the web. A spacing of 1,2m is sufficient to assume it acts like a continuous restraint. For short beams as in Figure 19 a restraint is added in the mid span.

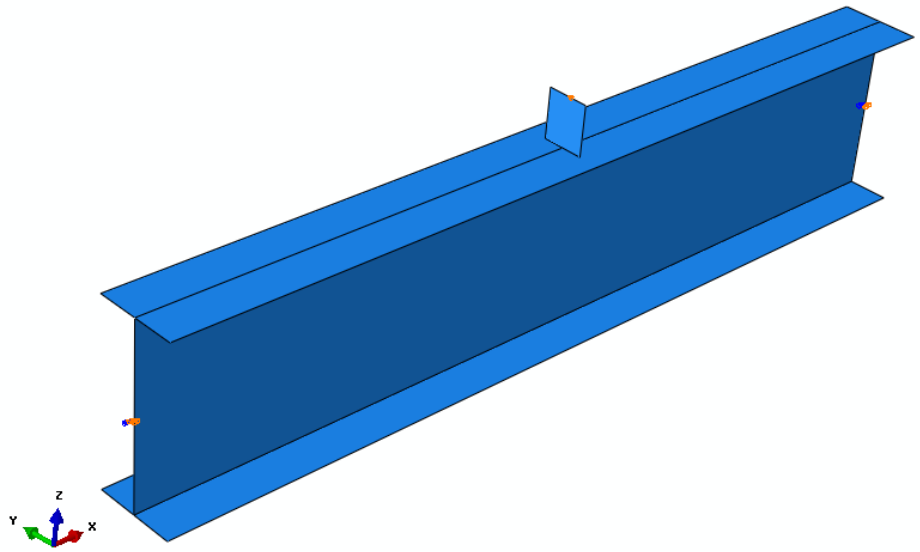

Figure 19 Boundary condition of the beam laterally restrained above the tension flange.

4.2 Non-linear buckling analysis

The second step is performing a non-linear buckling analysis where imperfection, residual stresses and material plasticity are taken into account. In this analysis the ultimate moment is obtained, where the relation between load and displacement gives a zero stiffness (unstable). In ABAQUS a step module ‘’Static Risk’’ is used to simulate the non-linear behaviour. The number of increments used is 100 when generating the moment-displacement curve.

In the “Static Risk” step the buckling shape obtained in the linear buckling analysis is used as a reference shape, which is multiplied by the equivalent initial bow imperfection, recommended in Eurocode3, where both geometrical imperfection and residual stresses are taken into account. The magnitude of the bow imperfection is found in table 5.1 in Eurocode3 and depends on the length of the beam and the buckling curve of the cross-section.

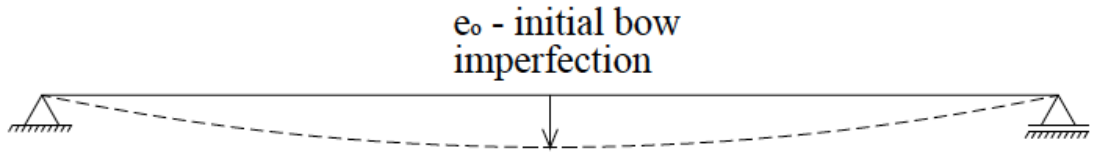

Figure 20 Initial bow imperfection. (Sabat, 2009)

The initial imperfection in table 5.1 in Eurocode3 only applies for columns subjected to compression. In order to take into account the lateral torsional buckling of a beam in bending, Eurocode3 suggest multiplying the initial bow imperfection by a factor *k*. By using this procedure no additional torsional imperfection needs to be considered. The value of *k* is taken as 0,5.

$$e_0 = k * e_{0.k} \tag{59}$$

The moment and the boundary conditions are the same as in the linear buckling analysis in chapter 4.1. Furthermore the elements are the same except the size. In this analysis it was necessary to use a larger mesh of 250mm, which is sufficient according to the convergence study in chapter 4.3. A non-linear buckling analysis is time consuming and in order to make the work more efficient a coarser mesh is chosen. In addition it proved difficult to obtain the descending shape of the moment-displacement curve when a fine mesh is used.

The stress and strain relation is considered to follow an elastic-plastic path with strain hardening assuming mild steel with a yield strength f_y of 235MPa. The plastic material model can be seen in Figure 21.

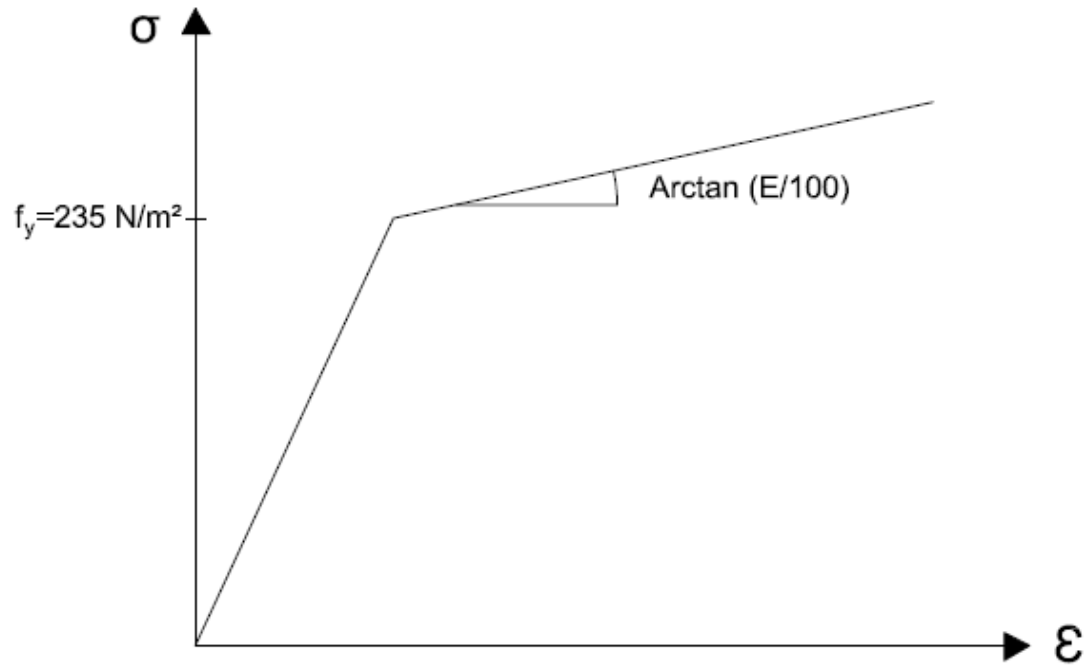

Figure 21 Stress-strain curve.

4.3 Convergence study

Results from FE-analyses are more accurate as the mesh gets finer. However, using a fine mesh also increases the computation time. In order to find a satisfactory balance between accurate results and computation time, a convergence study is performed.

The convergence study is based on results from a linear buckling analysis and is performed for all the cross-sections. The critical buckling moment versus element size is plotted and the point of convergence is found. For all the cross sections, a mesh with an element size of 250mm is sufficient. The results from the convergence study can be seen in Figure 22-24.

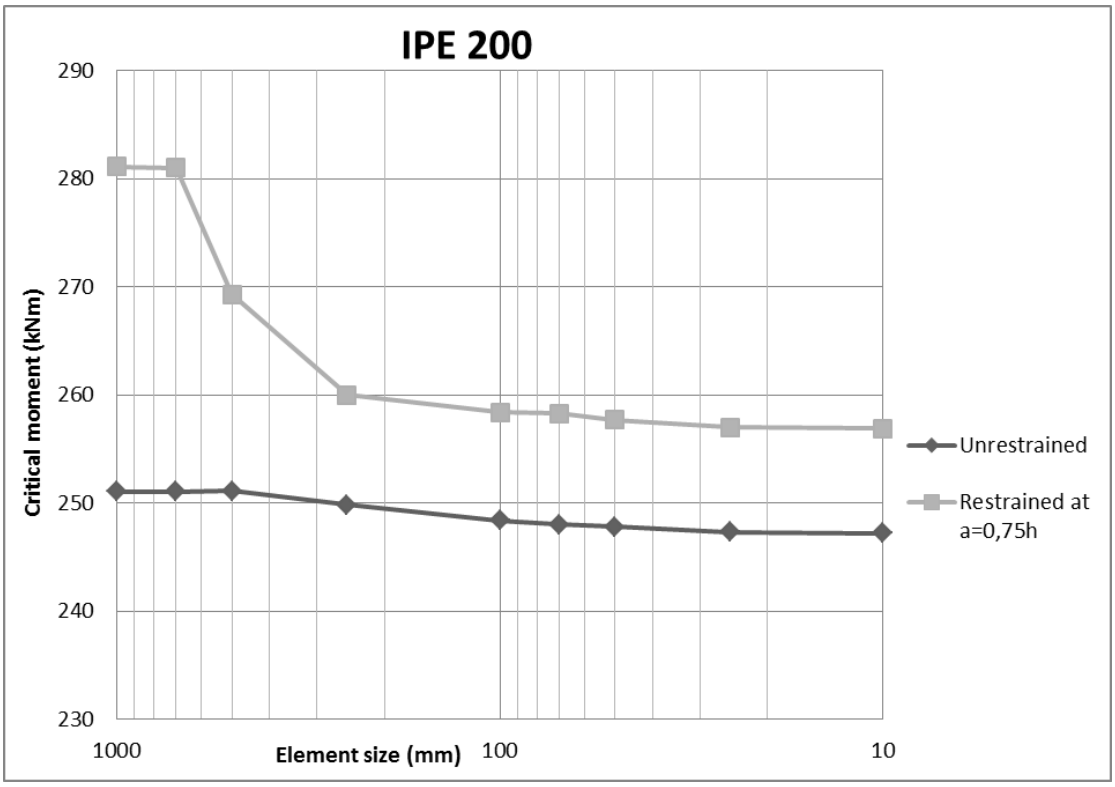

Figure 22 Convergence study of an IPE 200, with the tension flange unrestrained and restrained.

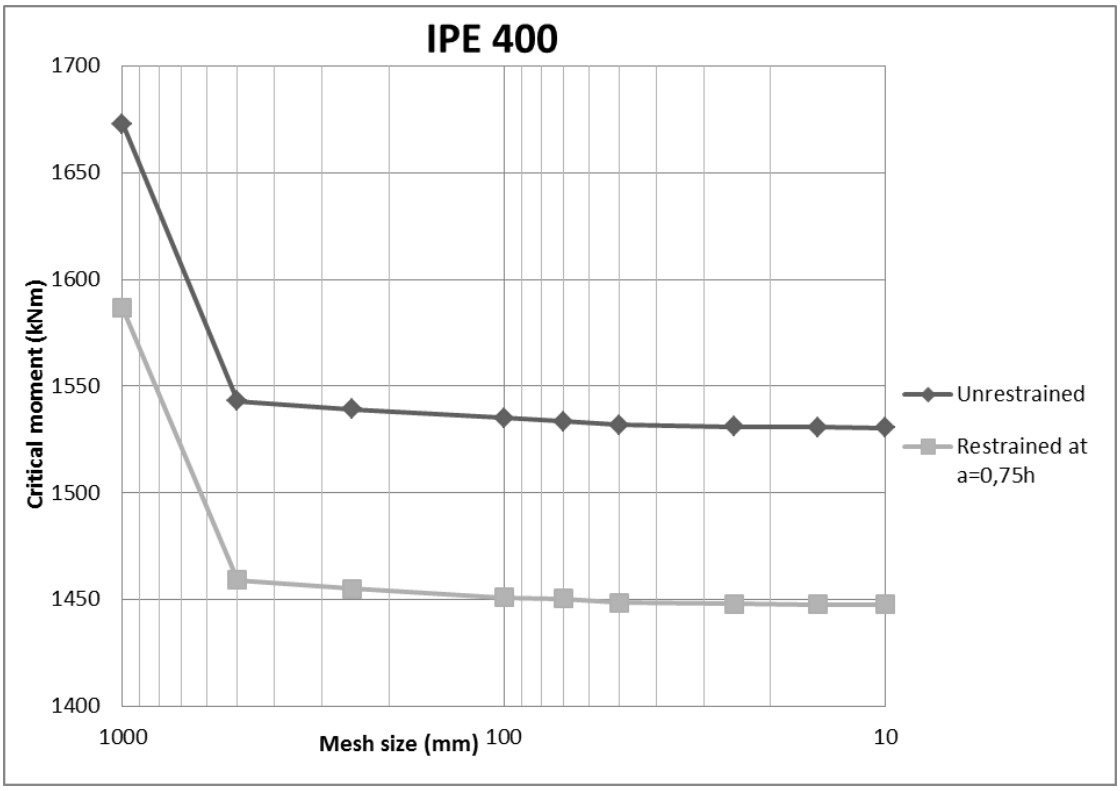

Figure 23 Convergence study of an IPE400, with the tension flange unrestrained and restrained.

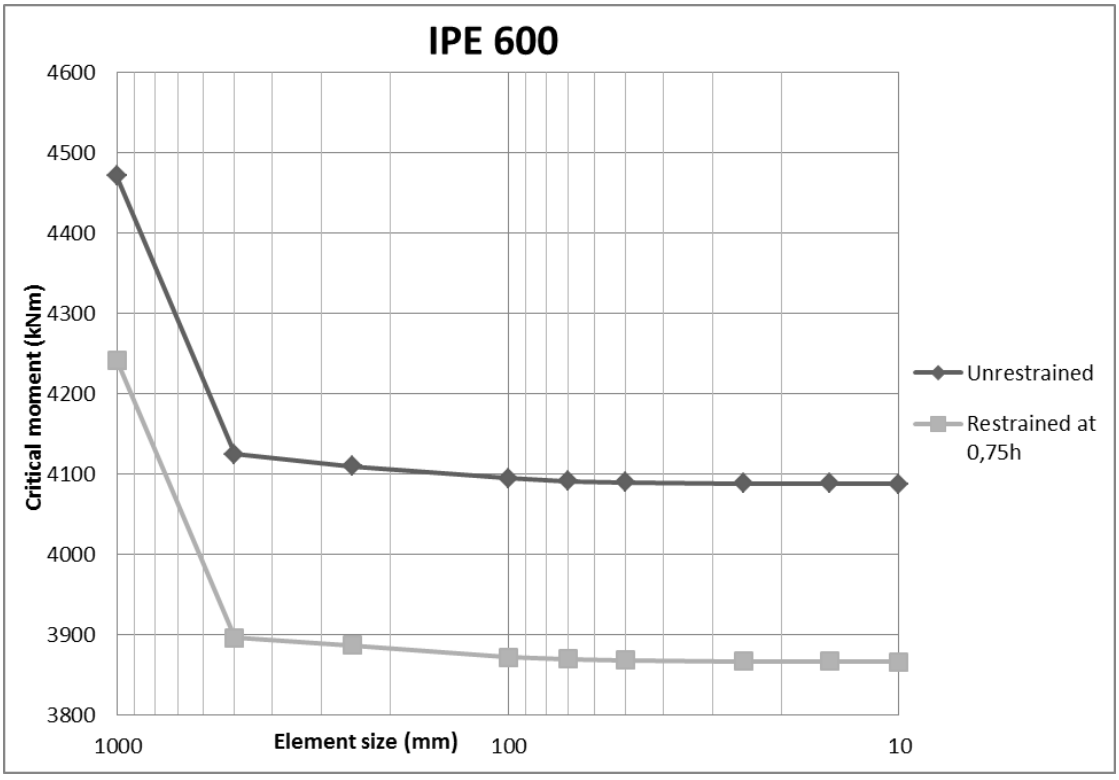

Figure 24 Convergence study of an IPE600, with the tension flange unrestrained and restrained.

5 Theory

The phenomena studied in this Master's project, are lateral-torsional buckling and distortion. This chapter is intended to be an introduction, explaining the behaviour that occurs and thereby providing the reader with an explanation of the results obtained.

5.1 Lateral-torsional buckling

In chapter 2.1 the differential equations for a laterally unrestrained beam is established giving a critical moment when the beam becomes unstable and laterally displace and twist. The total lateral displacement is divided into two parts provided by; flexure buckling about minor axis u_L and torsional buckling u_T. The proportions of each displacement are of interest since it determines the location of the free rotational axis illustrated in Figure 25.

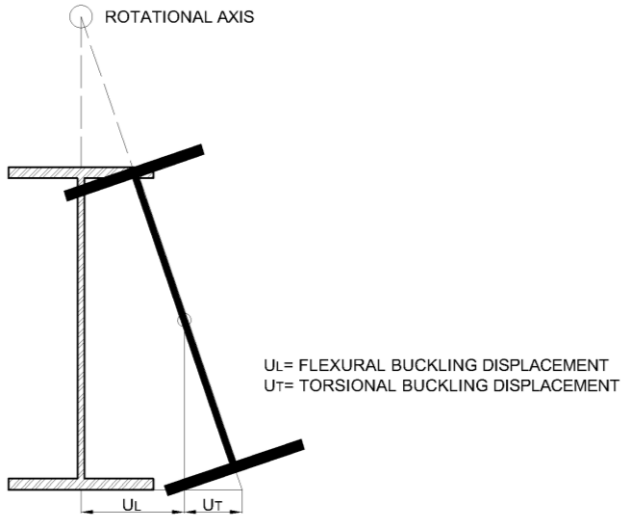

Figure 25 Lateral- torsional buckling of a beam unrestraint laterally on the tension flange.

The distance from the shear centre to the rotational axis differs between cross-sections and is not in proportion with the depth of the section. This effect causes some cross-sections to flexural buckle about minor axis more than others and correspondingly affects the efficiency of lateral restraints. When the beam is laterally restrained at the tension flange the shear centre is displaced to the location of the lateral restraint giving rotation about the tension flange. This results in an increase of the rotational angle corresponding to an increasing buckling capacity. Having the beams laterally restrained at a height which is above the tension flange, with an eccentricity of 0,75h from the shear centre of the beam, will also have positive influence on the buckling capacity. However, it is distinguished differently depending on the cross-section. For shallow beams the lateral restraints above its tension flange has a significant impact but for deep beams the buckling shape coincides with the unrestrained shape. This is illustrated in Figure 26.

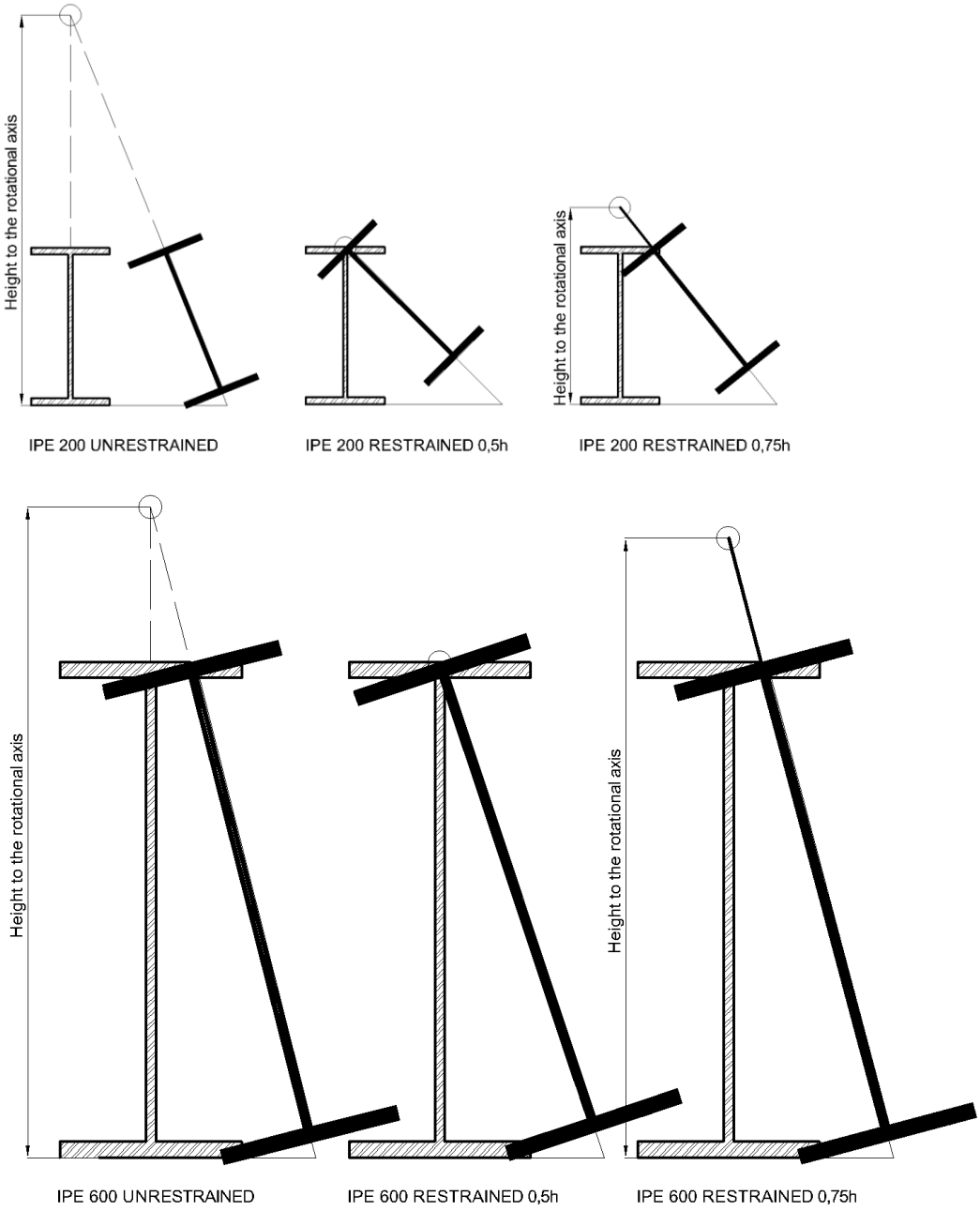

Figure 26 Buckling modes IPE200 and IPE600, unrestrained, restrained at 0,5h and 0,75h.

The previous reasoning is true for long lengths (about 6m and longer) for the cross-sections, with corresponding slenderness, studied in this report. For laterally unrestrained beams with short lengths the flexural buckling displacement are significantly decreased, resulting in no or almost negligible lateral displacement of the tension flange. The rotational axis is then very close to the tension flange. The buckling shape will therefore significantly consist of lateral displacement caused by torsion which is almost identical to the buckling shape when having lateral restraints at the tension flange. The conclusion is that lateral restraints at 0,5*h* for short lengths have no influence. However, lateral restraints above the tension flange will increase the buckling capacity for short lengths. Restraining the beam above the tension flange with an eccentricity of 0,75*h* will evidently force the rotational axis to act above its

initial unrestrained location which correspondingly increases the buckling capacity as more energy is required. The buckling shapes for a short beam are seen in Figure 27.

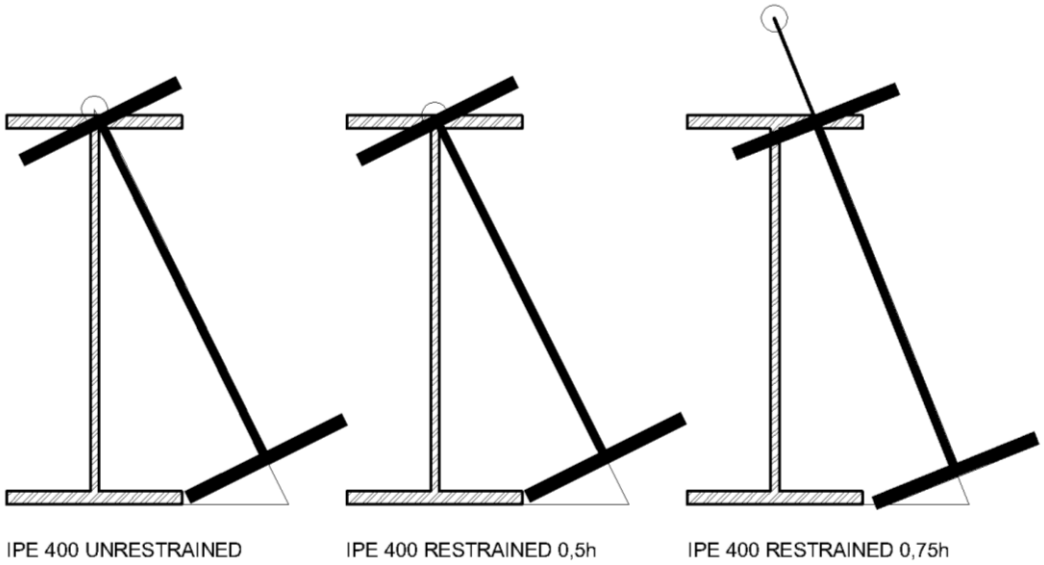

Figure 27 Buckling modes IPE400 with length 1,85m, unrestrained, restrained at 0,5h and 0,75h.

5.2 Lateral-torsional buckling with distortion

The analytical expressions eqn.(52&53) determine the critical buckling moment considering LT-buckling assuming that the section remain plane. However, these equations do not apply for all cases because of local buckling of the web called distortion (see Figure 28). Since the web is slender it will locally deform in combination with LT-buckling. This effect significantly reduces the buckling capacity of the beam.

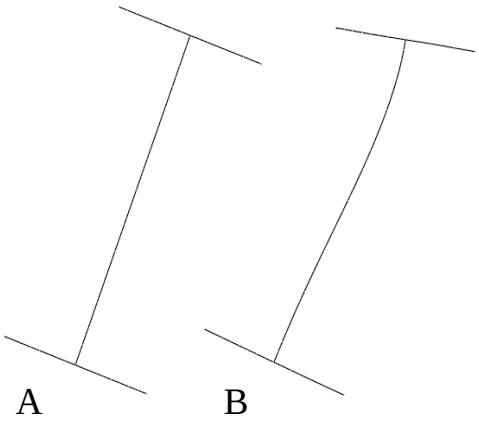

Figure 28 The buckling shape of IPE sections; A is without distortion and B is with distortion

In the following investigation, distortion is detected but only for beams with short length. When the length of the beam is decreased the corresponding buckling load capacity increases until a certain point where the web is unable to withstand the load without buckling locally. The behaviour is more pronounced for beams laterally restrained above the tension flange since the rotational axis is further from the tension flange. This phenomenon can be seen in section 6.3.1.

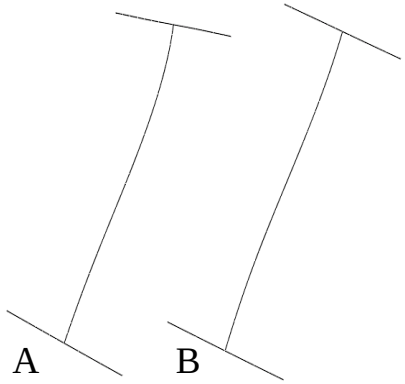

Figure 29 The distortion of IPE sections; A is beam laterally restrained above the tension flange and B is a beam not restrained laterally at the tension flange.

6 Results and Discussion

This chapter consists of an analytical parametric study, establishing an understanding to the critical buckling moment equations. Furthermore the stable lengths are presented for each cross-section and compared with FE-simulations using linear analyses. The last section presents non-linear analyses of the stable length confirming the assumptions made in the method chapter.

6.1 Analytical parametric study

According to the analytical expressions it is obvious that the dimensions of the cross-section as well as the length of the beam have a significant impact on the critical buckling moment. However, other parameters also affect the end result. In the equation for the lateral restrained critical buckling moment eqn.(61), there exists a variable a that has a significant impact. The variable a is the distance between shear centres of the beam and the lateral restraint. In the following results the critical buckling moment equations will be compared.

The critical buckling moment for a laterally unrestrained beam:

$$M_{cr} = \frac{\pi^2 E I_z}{L^2}\sqrt{\frac{I_w}{I_z} + \frac{L^2 G I_t}{\pi^2 E I_z}} \tag{60}$$

The critical buckling moment for a laterally restrained beam:

$$M_{cr.0} = \frac{1}{2a}\left(\frac{\pi^2 E I_z a^2}{L^2} + \frac{\pi^2 E I_w}{L^2} + G I_t\right) \tag{61}$$

6.1.1 Influence of eccentricity *a*

The influence of the eccentricity a is observed analytically by examining the critical buckling moment applying a as a variable. Several cross-sections are studied assuming a long length of 10m and a short length of 2m. In the figures below it can be seen how a influences the critical buckling moment for standard and customized cross-sections. In the Figure 30 to Figure 33, the y-axis represents the ratio of critical buckling moment between lateral restrained $M_{cr.0}$ - and unrestrained M_{cr}. It should be noted that the y-axis is in logarithmic scale. The x-axis denotes a ratio of the eccentricity a and the depth of the beam h. The grey area in the graphs represents a realistic value of the eccentricity a ($0{,}5h$ to $0{,}75h$).

Standard cross-sections

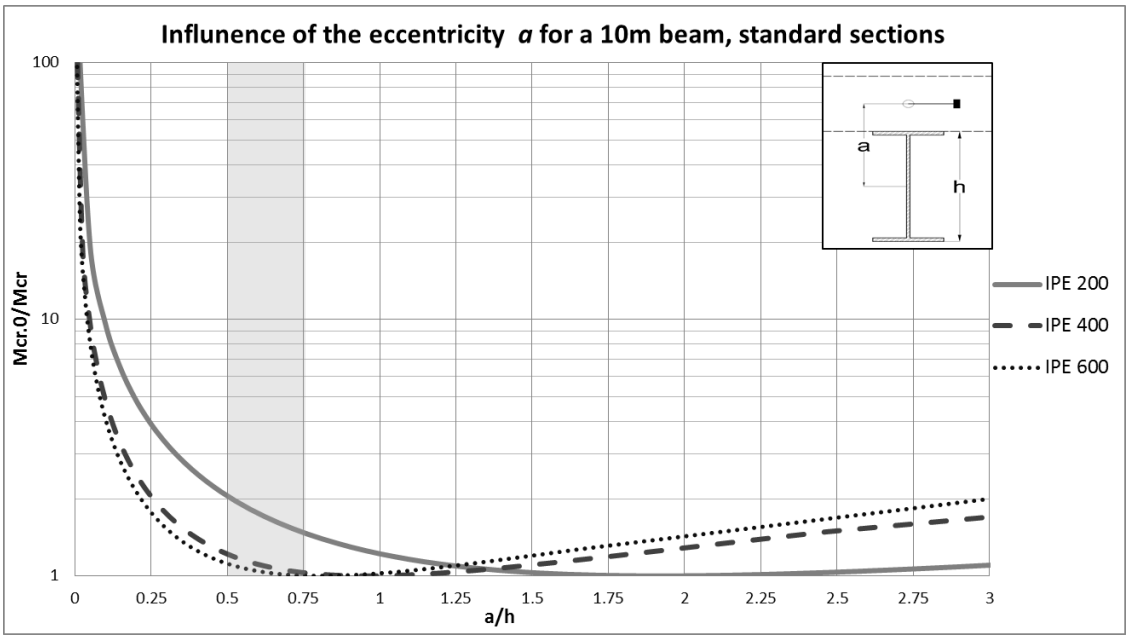

Figure 30 Ten meter beam illustrating the impact of restraints at different eccentricities for three standard cross-sections.

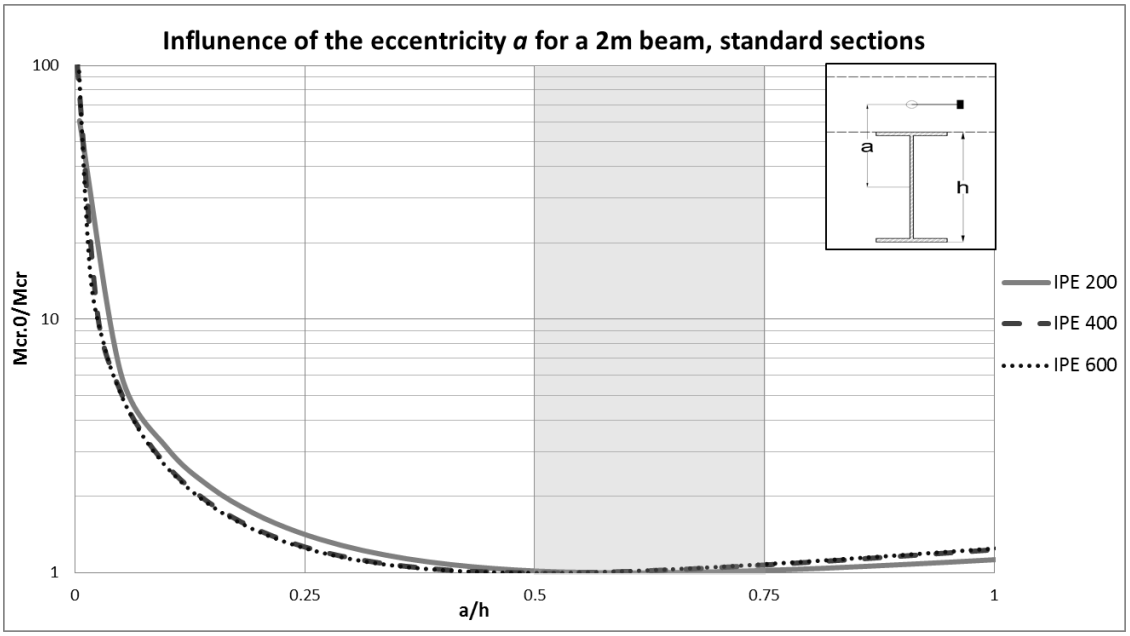

Figure 31 Two meter beam illustrating the impact of restraints at different eccentricities for three standard cross-sections.

Welded cross-sections

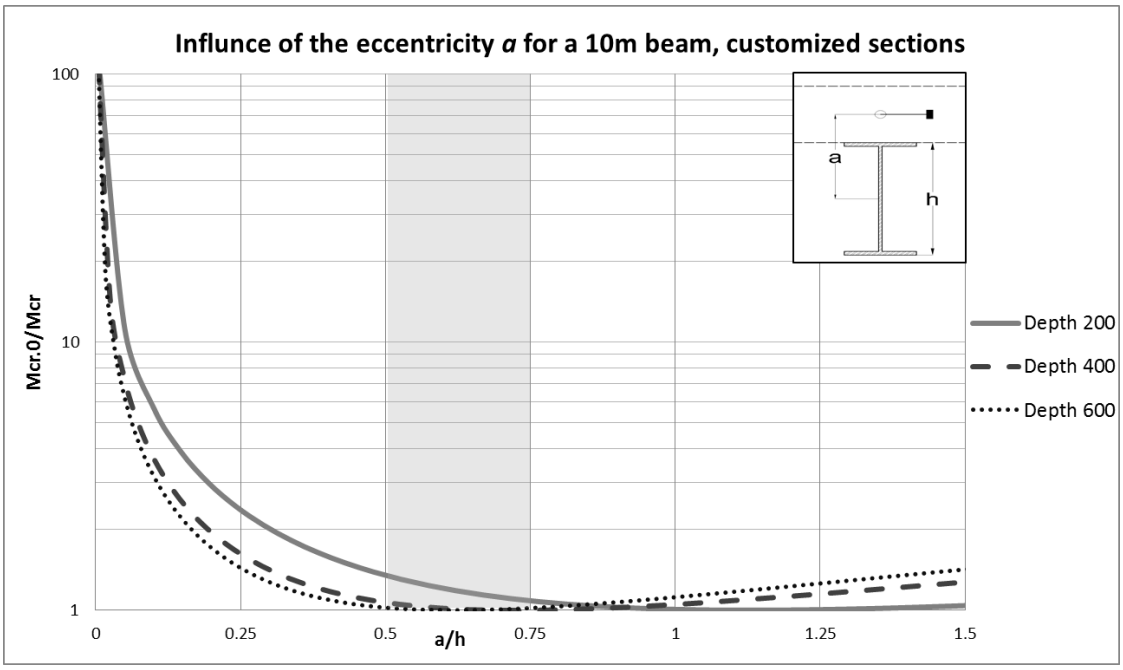

Figure 32 Ten meter beam illustrating the impact of restraints at different eccentricities for three customized cross-sections.

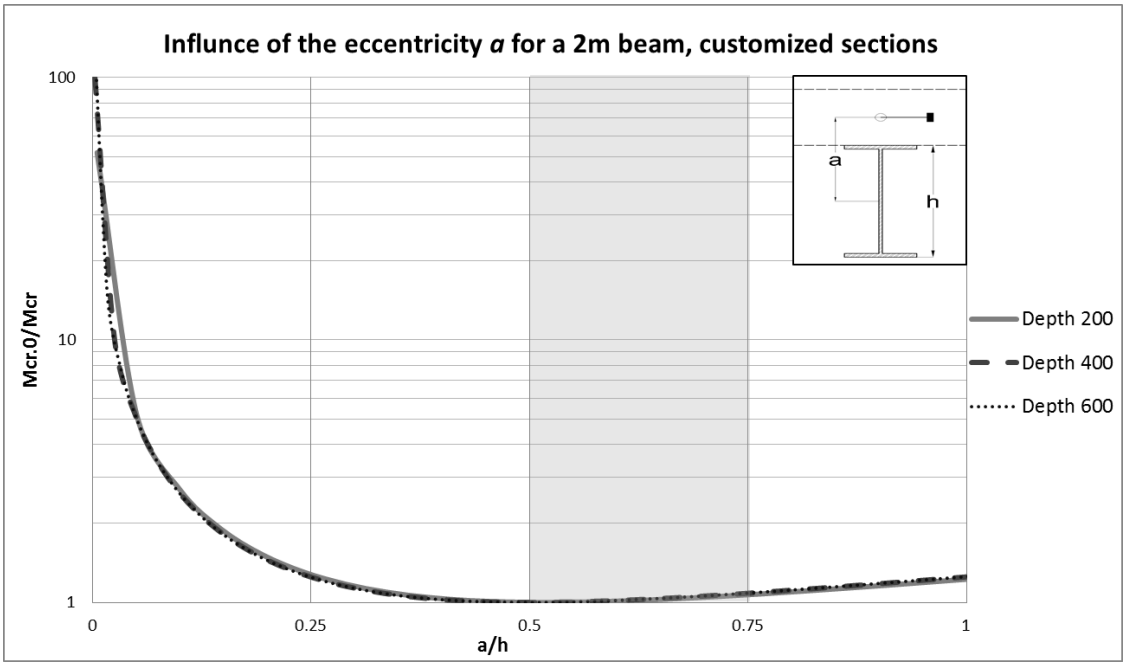

Figure 33 Two meter beam illustrating the impact of restraints at different eccentricities for three customized cross-sections.

For both long and short beams, lateral restraints close to the shear centre of the beam increase the critical buckling moment significantly and result in that only torsion about the longitudinal axis in the shear centre of the beam occurs. Due to the significant critical buckling moment the instability phenomenon can be ignored.

When the lateral restraint is located further from the shear centre the ratio reduces until it reaches a turning point where there is no benefit of the lateral restraint. The turning point occurs when the buckling shape of the unrestrained and restrained beam coincides corresponding to similar location of the rotational axis. When the rotational axis is forced to act above the initial unrestrained location, the lateral restraint once again has a beneficial effect. This phenomenon is illustrated in the Figure 34.

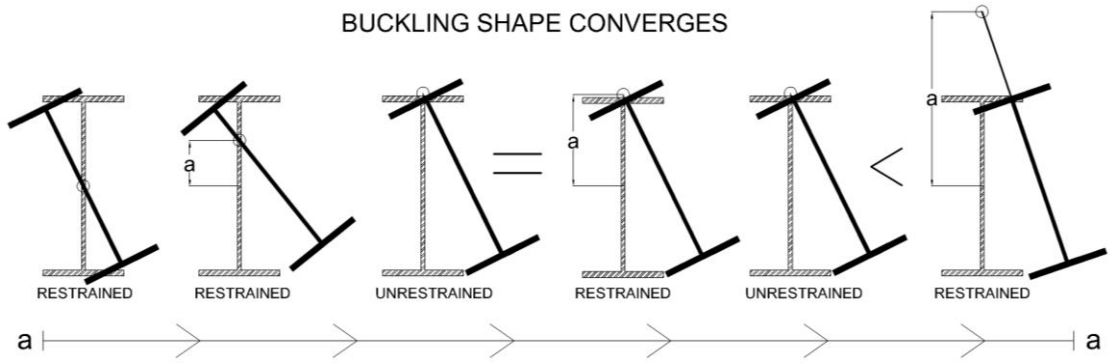

Figure 34 Illustration of the influence of the variable a on the critical buckling moment for 2m beam.

It is noted that the influence of lateral restraints differs significantly between short and long lengths for both standard- and customized sections. For long beams the turning point, where there is no benefit of lateral restraint, occurs for greater eccentricity of a. In addition the location of the turning point differs between cross-sections. This is because the distance to the rotational axis differs between sections. For shallow cross-sections the rotational axis acts further from the shear centre of the beam in proportion to its depth resulting in greater ratio of a/h to converge to the unrestrained buckling shape. However, great eccentricities of a is not of importance due to its improbability to be present in reality. The proportions in size between the beam and the restraint have to be realistic. A realistic eccentricity a is between $0{,}5h$ to $0{,}75h$ (grey area in the graphs) which have significant beneficial effect for cross-sections with shallow depth. For deeper beams the effect is not as pronounced.

For all cross-sections with short length the position of the turning point, where there is no benefit of lateral restraint are similar, about $0{,}5h$. This result implies that for short beams laterally restrained at the top of the tension flange ($0{,}5h$) result in a similar buckling shape as for unrestrained beams. Lateral restraints above $0{,}5h$ have a positive influence. As mentioned previously the positive effect is due to forcing the rotational axis to act above the unrestrained location.

For the customized cross-section the contours are similar as for a standard cross-section. The variance is not as pronounced as for a standard cross-section.

6.1.1.1 Summary

Adding lateral restraints increases the critical buckling moment except at the so-called turning point, where the buckling shapes of the unrestrained- and restrained beam coincide.

For realistic eccentricity of *a*, the increase in the critical buckling moment is either caused by forcing the rotational axis to act above or below the initial unrestrained rotational axis. Depending on the length of the beam one of these actions occurs. For long beams lateral restraints force the rotational axis to act below the initial unrestrained location and the positive effect is more pronounced for shallow sections. For short beams the opposite applies. Restraints acting above the tension flange force the rotational axis above its unrestrained location. This action increases the critical buckling capacity and occurs for all cross-sections despite depth.

6.1.2 Influence of beam length

To be able to see what effects the restrains have on different cross-sections with variable lengths, plots have been produced to visualize the behaviour. Two different eccentricities of lateral restraints are studied 0,5*h* and 0,75*h* (Figure 35). In the following Figure 36 to Figure 41 the y-axis represents the ratio of critical buckling moment between lateral restrained $M_{cr.0}$ - and unrestrained M_{cr} while the x-axis denotes the length.

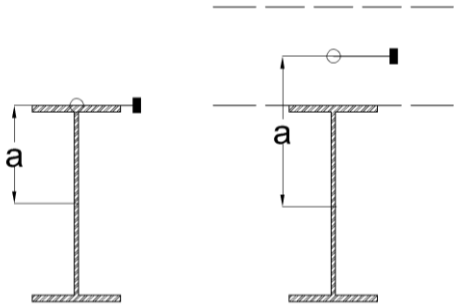

Figure 35 The investigated eccentricities of a.

Standard cross-sections

It can be seen in Figure 36 that for the IPE200 the restraint has a significant impact on longer lengths which was mentioned in the previous chapter. The increase in critical buckling moment for a 10m beam unrestrained compared to one restrained at 0,5*h* is about 100%. The difference having the beam restrained at 0,75*h* is about 50%. Furthermore for a 1m beam restraining it at 0,75*h* has a positive effect of approximately 7%. For short beams restraint at 0,5*h* is negligible.

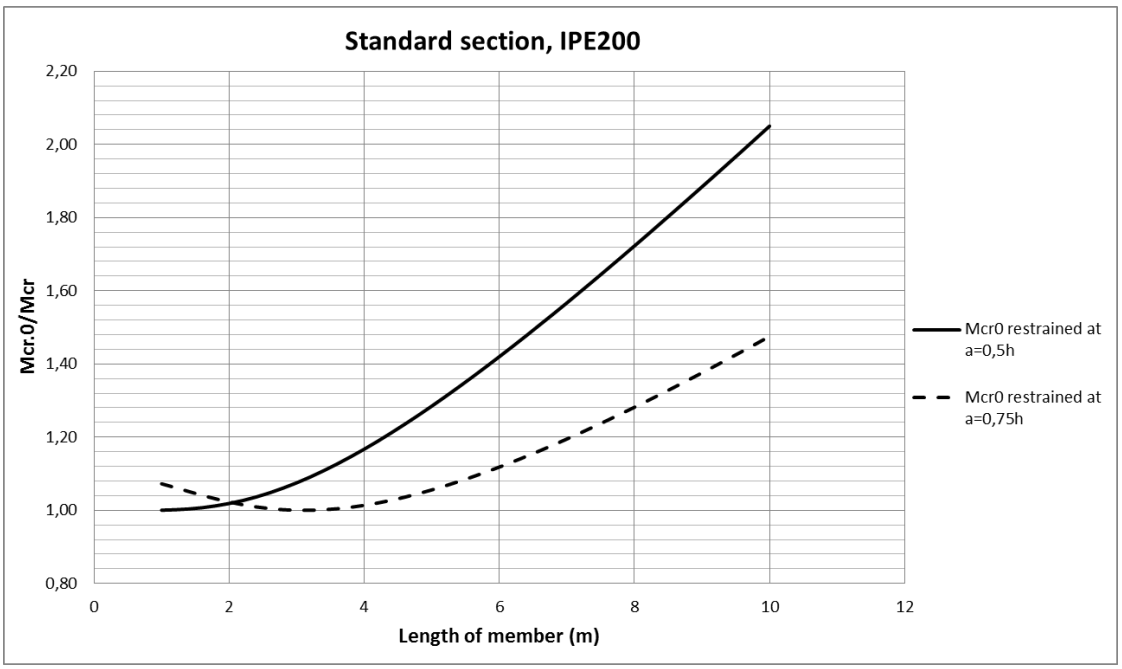

Figure 36 Ratio of critical buckling moment with length as a variable for a IPE200.

Considering an IPE400 in Figure 37, the impact of restraints for longer lengths has less impact compared to IPE200. For a 10m beam the increase in critical buckling moment is about 3% compared to 48% for IPE200. However, restraints at 0,5*h* are still about 20% better for a 10m beam. As for the IPE200 the 0,75*h* restraints has a positive effect for shorter lengths with a magnitude of about 9%. It is seen in the figure below, at length 7m for the restrained beam at 0,75*h*, the ratio starts to increase again. For shorter lengths than 7m the restraint at 0,75*h* forces the rotational axis to act above its unrestrained location. For longer lengths than about 7m the rotational axis is forced to act below corresponding to an increase of the buckling capacity.

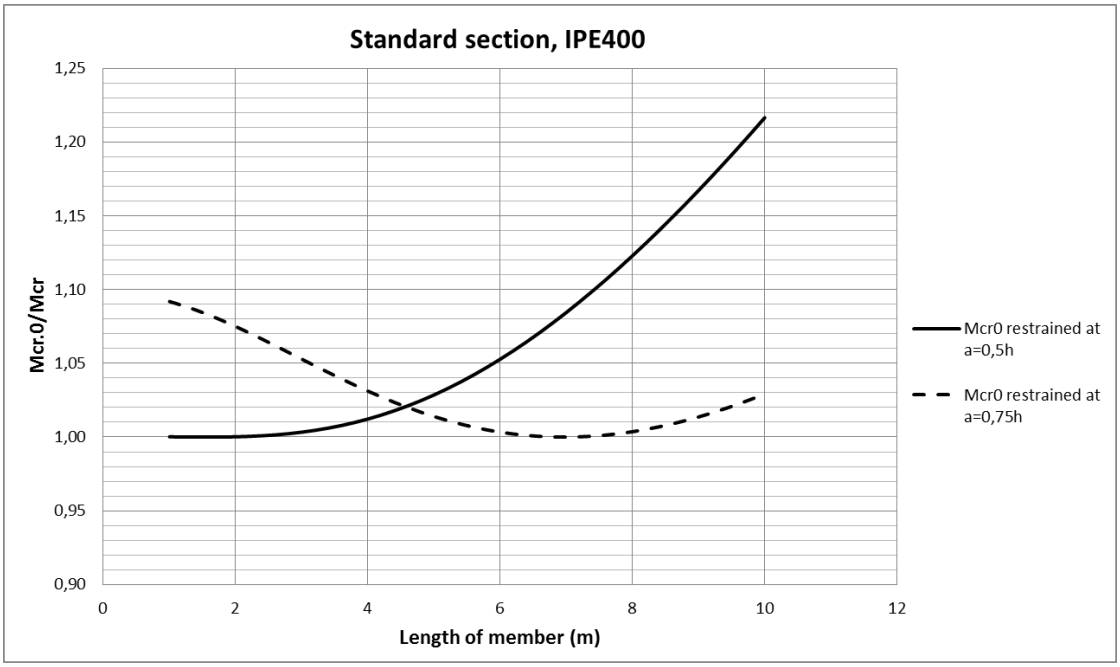

Figure 37 Ratio of critical buckling moment with length as a variable for a IPE400.

The IPE600 is seen in Figure 38. The difference between unrestrained and restrained at 0,75h is for a 1m beam about 9%. At six meters the difference is less than 2%. For the IPE600 the point where the rotational axis acts below its initial unrestrained location appears at about 9m.

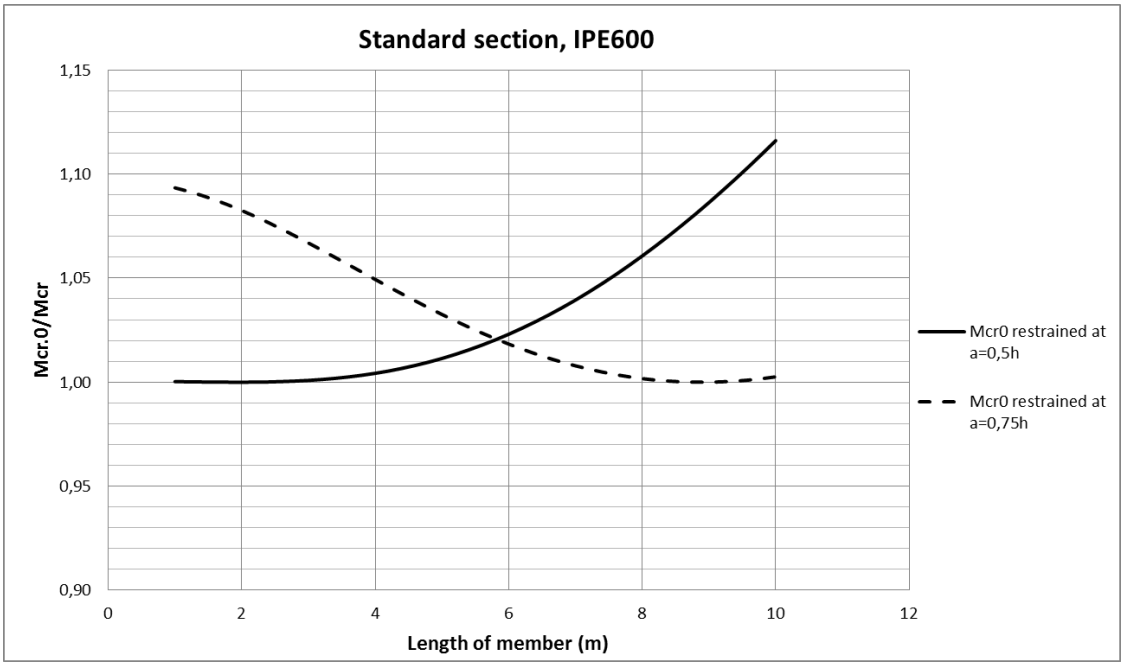

Figure 38 Ratio of critical buckling moment with length as a variable for a IPE600.

Customized cross-sections

The customized cross-section with depth 200mm seen in Figure 39 follows the same pattern as the standard sections. In a comparison between standard and customized 200mm cross-sections, it can be noted that restraints for longer customized lengths have less impact on the buckling capacity. The customized cross-section has more than twice as large flanges than the standard which obviously influences the behaviour. A possible reason for this is that the stiffness about the minor axis is significantly greater in proportion to the torsional stiffness causing less lateral displacement of the tension flange consequently decreasing the impact of lateral restraints.

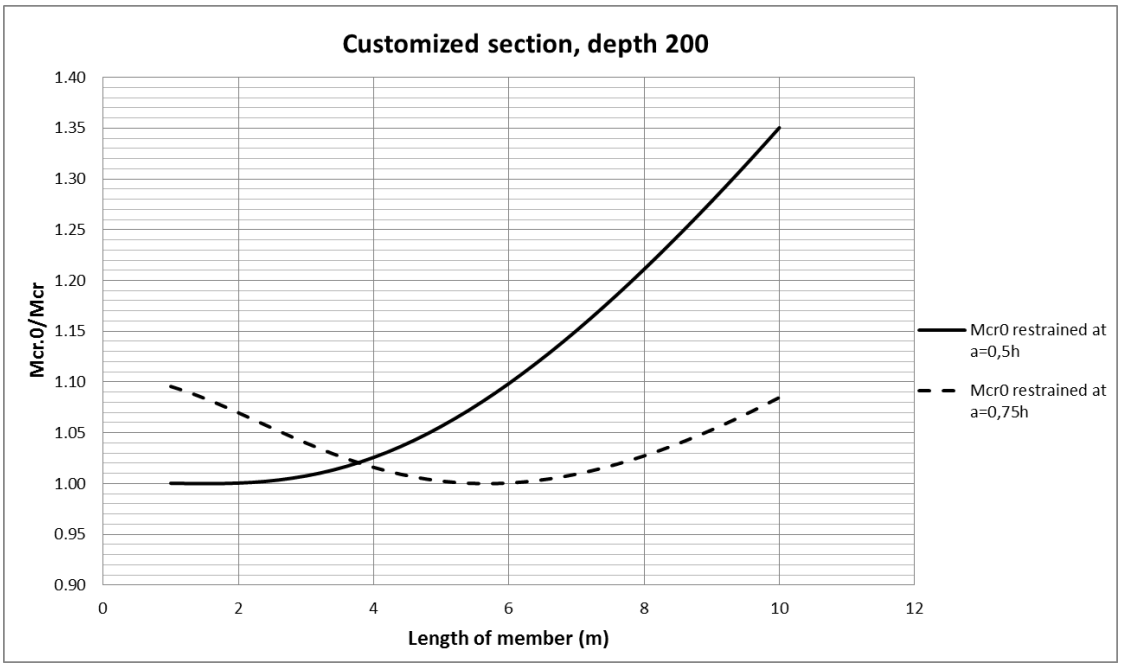

Figure 39 Ratio of critical buckling moment with length as a variable for a customized beam with depth 200mm.

The customized cross-section with depth 400mm in Figure 40 restrained at 0,75*h* has about 9% higher critical moment for 1m beam compared to having it unrestrained or restrained at 0,5*h*. As for previous cross-sections the critical moment declines when the length is increased. For the previous cross-sections the ratio of the critical moment between unrestrained and restrained beam declines until a certain length and then the ratio starts to increase again due to the location of the rotational axis. Although for the customized 400mm cross-sections this increase is not seen within 10 meters.

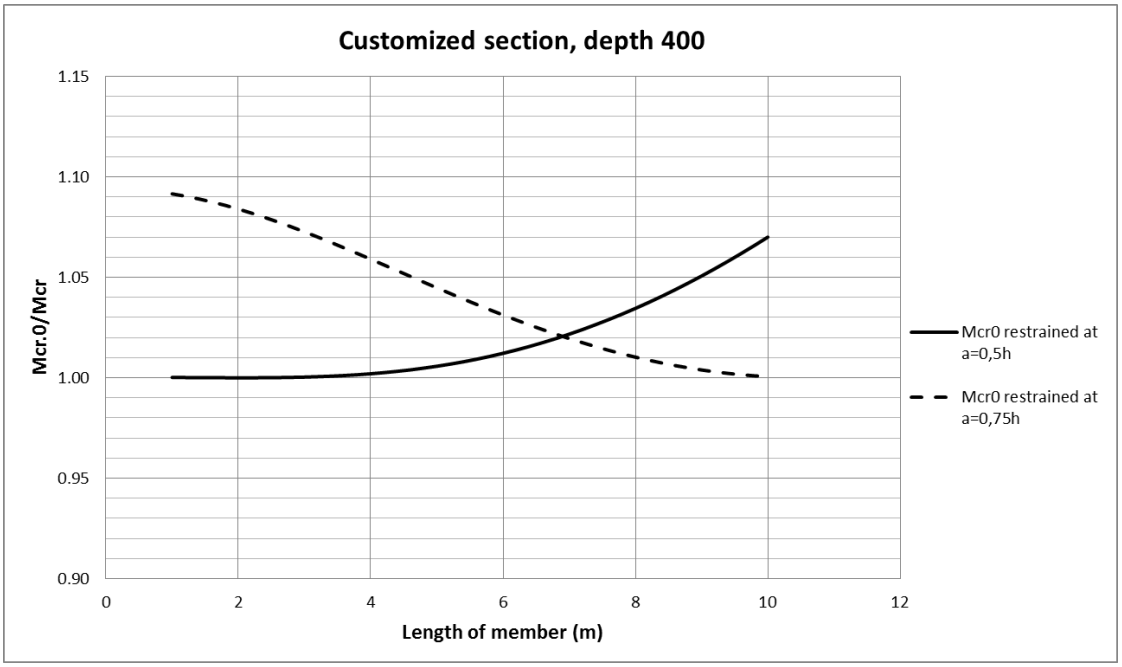

Figure 40 Ratio of critical buckling moment with length as a variable for a customized beam with depth 400mm.

For the customized beam, with depth 600mm in Figure 41, it can be noted that there is almost no difference between unrestrained and restrained at both 0,5*h* and 0,75*h* when considering a 10m beam.

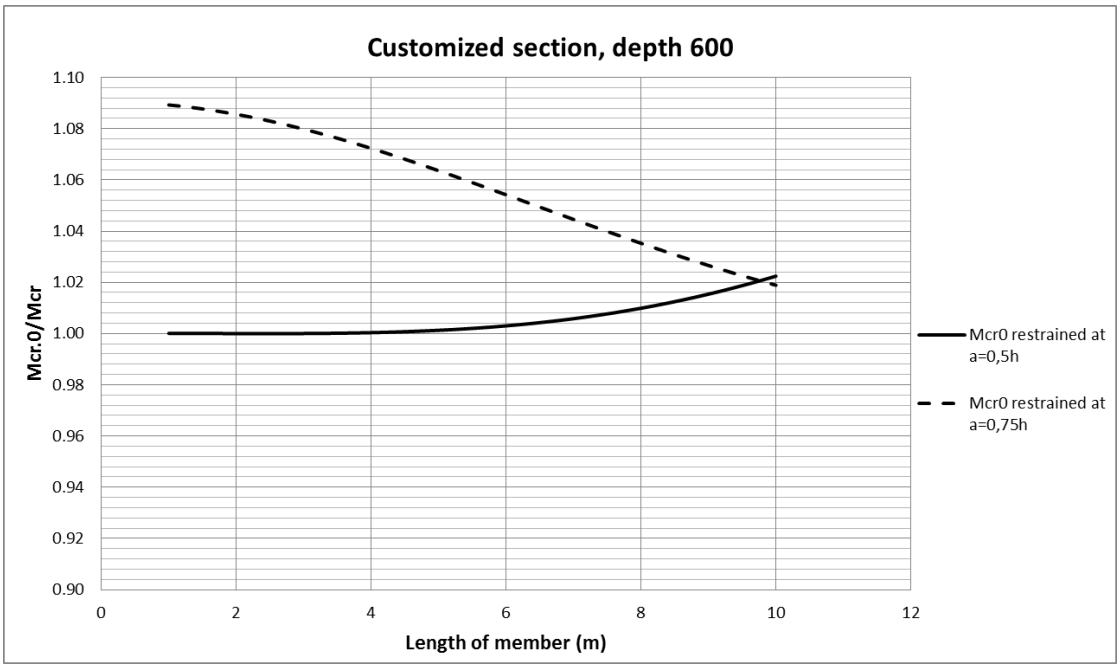

Figure 41 Ratio of critical buckling moment with length as a variable for a customized beam with depth 600mm.

6.1.2.1 Summary

For all cross-sections with short lengths the magnitudes of the critical buckling moment are similar between unrestrained and restrained beams at the level of the tension flange (0,5*h*). However, when the length is increased the effect of restraints at 0,5*h* will improve the buckling capacity. Restraints at 0,75*h* will for all cross-sections provide greater buckling capacity for short lengths. However, the positive influence will decline until a certain length where the restraint has no impact. Thereafter the influence of restraints will once again have a positive effect on the buckling capacity due to forcing the rotational axis to act below the unrestrained location. The critical length where the restraints at 0,75*h* have no effect differs between cross-sections. For shallow sections with low stiffness about the minor axis in proportion to the torsional stiffness the critical point will occur at shorter lengths.

6.2 Stable length

In order to find the stable length where no LT-buckling occurs before yielding due to bending in the major axis some assumptions have to be determined. Using 0,4 as limit of slenderness, assuming constant moment and elastic capacity of the cross-section, the following results are obtained. The stable length for both unrestrained and restrained at two different eccentricities is presented in Table 2 and Table 3 for standard and customized-sections.

Table 2 Stable length for standard cross-sections

Cross-section	Unrestrained L_{unr}	Restrained at 0,5h $L_{r.0,5h}$	Restrained at 0,75h $L_{r,0,75h}$
IPE200	1,060m	1,060m	1,098m
IPE400	1,854m	1,854m	1,927m
IPE600	2,215m	2,215m	2,304m

Table 3 Stable length for customized cross-sections.

Cross-section	Unrestrained L_{unr}	Restrained at 0,5h $L_{r.0,5h}$	Restrained at 0,75h $L_{r,0,75h}$
Depth 200	2,257m	2,258m	2,330m
Depth 400	2,047m	2,047m	2,132m
Depth 600	1,944m	1,944m	2,027m

Assuming a constant moment is conservative and results in a short length in between torsional restraints. It is noted that there is no difference in the stable length between unrestrained and restrained beams at 0,5h. As can be seen in section 6.1.2, for a short length the critical buckling moment is almost unchanged between unrestrained and restrained at 0,5h. However, having the beams restrained at 0,75h, a small improvement of the stable length is obtained. For standard cross-sections the length is increased for greater cross-sections. In addition it is noted that the stable length decreases for deeper customized cross-sections. The customized cross-sections have similar stiffness about minor axis but the elastic capacity of the shallower beams is significantly smaller, corresponding to larger stable lengths according to the eqn.(57) in section 3.2.

6.2.1 Comparison with Eurocode3

In Annex BB.3 in Eurocode3 there are expressions for the plastic stable lengths where LT-buckling effects may be ignored. The length denoted as L_m considers the unrestrained plastic stable length in between torsional restrains assuming one plastic hinge. Furthermore there is an expression determining the plastic stable length L_k assuming the same conditions as for L_m, provided that there are one or more discrete lateral restraints between the torsional restraints at a sufficiently small spacing. It is interesting to compare these lengths analytically with the derived stable length (L_{unr} & $L_{r0,75h}$). In the derivation of the Eurocode3 plastic stable length L_k, a lateral restraint at a location of 0,75h is assumed. Therefore the comparable lengths are; L_m with the unrestrained stable length L_{unr} and L_k with the restrained stable length at 0,75h $L_{r0,75h}$. Following results were obtained for standard and customized cross-sections seen in Table 4 and Table 5.

Table 4 Comparison of stable length with Eurocode3 for standard cross-sections.

Cross-section	Unrestrained L_{unr}/L_m	Restrained at 0,75h $L_{r0,75h}/L_k$
IPE200	0,80	0,52
IPE400	1,00	0,55
IPE600	1,08	0,57

The results for the standard cross-section can be seen in Table 4 above. For the unrestrained beams, Eurocode3 gives shorter or equal lengths with the exception of the IPE200. In Eurocode3 the section is assumed to plasticise and it is reasonable to assume that the length should be shorter than the derived stable length. Therefore the longer length of the IPE200 is unanticipated. For a restrained beam the difference is more pronounced and Eurocode3 gives significantly longer lengths. It can be noted that the difference declines for greater cross-section from ratio of 0,52 to 0,57 but it is still substantial. The longer length of the plastic stable length raises the questions if the derived stable length is too conservative or if the expressions in Eurocode3 are not accurate. In the derivation of the stable length the same limit of slenderness is assumed for both unrestrained and restrained beams and the initial imperfections are based on the buckling curve method. A comparison of the derivation of the two stable lengths concludes that Eurocode3 assumes a smaller initial imperfection and a greater limit of slenderness for restrained beams. In order to verify the stable length a non-linear buckling analysis is performed in section 6.3.2.

Table 5 Comparison of stable length with Eurocode3 for customized cross-sections.

Cross-section	Unrestrained L_{unr}/L_m	Restrained at 0,75h $L_{r0,75h}/L_k$
Depth 200	0,67	0,45
Depth 400	1,35	0,56
Depth 600	2,07	0,60

The results comparing customized cross-sections are seen in Table 5. For the unrestrained beams the length in Eurocode3 is shorter except for the cross-section with the depth of 200mm. Furthermore the difference is more pronounced for the customized cross-sections. For the restrained beams the plastic stable length in Eurocode3 is significantly longer. It should be noted that a comparison of the stable length for customized cross-sections is questionable due to the derivation of the partly empirical expressions in Eurocode3. The derivation is based on standard cross-sections, where certain proportions of web and flanges are accounted for. However for customized cross-sections these proportions are not taken into account and a comparison may not be as relevant.

In Eurocode3 there also exists a simplified method, finding the stable length L_c. The simplification considers only the compression flange and one third of the compressed web. The parts of the beam that are in tension are neglected which includes the influence from the purlins. In the simplified method it is recommended to assume a limit of slenderness of 0,5 for cross-sections in class 1 and 2. It is of interest to compare the stable length derived from the simplified method assuming both 0,4 and 0,5 as limit of slenderness with the stable length derived in this Master's project assuming lateral restraints both at 0,5*h* and 0,75*h*. The comparison can be seen in Table 6.

Table 6 Comparison of stable length with simplified method for standard cross-sections.

Cross-section	Simplified method($\bar{\lambda} = \mathbf{0,4}$) $L_{r0,75h}/L_c$	Simplified method($\bar{\lambda} = \mathbf{0,5}$) $L_{r0,75h}/L_c$
IPE200	1,12	0,89
IPE400	1,09	0,87
IPE600	1,08	0,87

Table 7 Comparison of stable length with simplified method for customized cross-sections.

Cross-section	Simplified method($\bar{\lambda} = \mathbf{0,4}$) $L_{r0,75h}/L_c$	Simplified method($\bar{\lambda} = \mathbf{0,5}$) $L_{r0,75h}/L_c$
Depth 200	1,12	0,90
Depth 400	1,07	0,87
Depth 600	1,06	0,85

It is noticed that when assuming a limit of slenderness of 0,4 in the simplified method, the derived stable length $L_{r0,75h}$ is between 6% and 12% greater for both standard and customized cross-section. However, when assuming a limit of slenderness of 0,5 the length determined from the simplified method is greater for all sections. The difference is not as significant as for the plastic stable length.

Performing a non-linear analysis using the stable length derived from the simplified method, assuming the worst initial imperfection, will conclude whether it is more efficient to utilize the simplified method or the stable length derived in this thesis.

6.2.1.1 Summary

The derived stable length is conservative compared to expressions in Eurocode3. Furthermore the difference is more pronounced for beams laterally restrained at the tension flange. It is observed that the simplified method, when assuming a limit of slenderness of 0,5, will give slightly greater lengths than the derived stable length.

6.2.2 Sensitivity of different slenderness limits

According to Eurocode3 the non-dimensional slenderness $\bar{\lambda}$ equal to 0,4 is the maximum limit where LT-buckling may be ignored and only cross-section checks apply. In this report the limit of slenderness is set to 0,4 but it is of interest to understand analytically how a different slenderness limit affects the stable length for unrestrained and restrained at two levels. The results are presented in Figure 42 and Figure 43. The y-axis represents the ratio of the stable length for a non-dimensional slenderness of 0,4 versus 0,3 and 0,5. It is evident that changing the slenderness affects the stable length significantly (about 28%) which concludes that the length is sensitive to the change. The effect is similar between cross-sections.

Figure 42 The stable length for unrestrained and restrained beam at 0,5h, assuming different non-dimensional limit of slenderness

Figure 43 The stable length for a restrained beam at 0,75h, assuming different non-dimensional limit of slenderness.

6.2.2.1 Summary

The derived stable length is sensitive to a change of the non-dimensional slenderness.

6.3 Finite element analyses

The finite element analyses (FE-analyses or FE-simulations) are performed by the software ABAQUS CAE. By FE-simulations several analyses can be obtained. Elastic linear buckling analysis executes numerical calculations determining the critical buckling modes for the produced models. Furthermore a non-linear buckling analysis is performed taking into account geometrical imperfections, residual stresses and plasticity. In the FE-simulations only standard cross-sections are investigated. The reason for this is to ensure that no local buckling occurs. However, in the non-linear buckling analysis different initial imperfections are utilized for the same cross-section representing both hot-rolled and welded.

6.3.1 Linear buckling analysis

Linear analyses determine the critical load when buckling occurs. The buckling mode considered is LT-instability. The analysis does not consider initial imperfections or plasticity in the material which is a condition verifying the analytical equations. The verification of the produced models is done by comparing the numerical results with the analytical, which is presented in the tables below for different cross-sections and lengths, unrestrained and restrained at 0,5*h* and 0,75*h*. The linear buckling analyses also contribute to an understanding to the analytical parametric study. By simulating models with different parameters, the buckling shapes are obtained and compared to the analytical results. In Table 8, unrestrained 10m beams are compared between analytical- and numerical results and in Table 9 for the stable lengths.

Laterally unrestrained beams

Table 8 Analytical and numerical results for unrestrained 10m beams.

Cross-section	Length [m]	Analytical [kNm]	Numerical [kNm]	Ratio [%]
IPE200	10	11,3	11,1	98,3
IPE400	10	104,0	101,5	97,6
IPE600	10	338,7	329,9	97,4

Table 9 Analytical and numerical results for unrestrained beams regarding stable lengths.

Cross-section	Length [m]	Analytical [kNm]	Numerical [kNm]	Ratio [%]
IPE200	1,060	271,1	257,0	94,8
IPE400	1,854	1606,0	1531,0	95,3
IPE600	2,215	4324,0	4088,2	94,5

For 10m beams the models are considered verified due to a maximum difference of only 2,6%. However, when shorter lengths are studied, the ratio between analytical and numerical results declines. The cause of this occurrence, for short beams, is due to distortion which is something the analytical equations do not account for. The distortion is observed in the software and the models can be confirmed to represent the reality closer.

The analytical results are therefore for short beams on the unsafe side. The buckling deformation of the cross-section IPE400, both 10m and 1,85m, is presented in Figure 44 showing the distortion for the short beam.

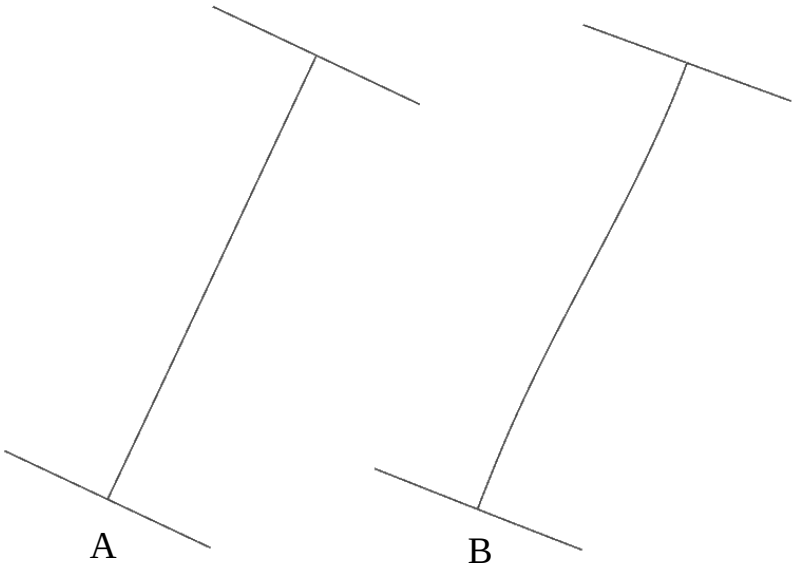

Figure 44 IPE400 unrestrained for the following lengths; A=10m, B= 1,85m.

Laterally restrained beams at 0,5*h*

When restraint is added to the tension flange the following results are obtained. Table 10 and Table 11 present the results when assuming continuous restraint at an eccentricity of 0,5*h*.

Table 10 Analytical and numerical results for a 10m beam restrained at 0,5h.

Cross-section	Length [m]	Analytical [kNm]	Numerical [kNm]	Ratio [%]
IPE200	10	24,1	23,3	96,8
IPE400	10	129,1	124,4	96,3
IPE600	10	383,7	369,5	96,3

Table 11 Analytical and numerical results regarding stable lengths for a beam restrained at 0,5h.

Cross-section	Length [m]	Analytical [kNm]	Numerical [kNm]	Ratio [%]
IPE200	1,060	271,9	257,4	94,8
IPE400	1,854	1606,0	1531,8	95,4
IPE600	2,215	4324,0	4090,0	94,5

The ratios between numerical and analytical results for 10m beams restrained at 0,5*h* are within a satisfactory limit, seen in Table 10.

Similarly as for unrestrained beams distortion occurs for the stable lengths, in Table 11. An IPE400 cross-section with length 10m and 1,85m restrained at 0,5*h* is presented in Figure 45.

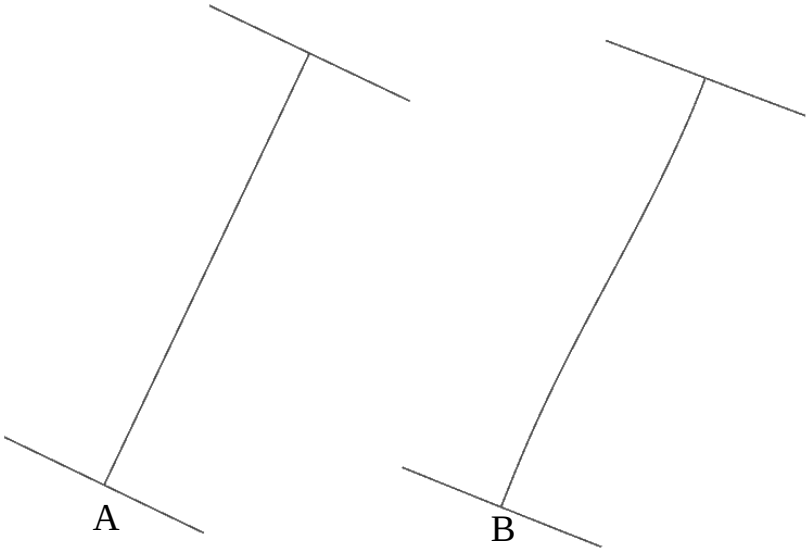

Figure 45 IPE400 restrained at 0,5h for the following lengths; A=10m, B=1,85m.

Laterally restrained beams at 0,75*h*

An elastic linear analysis is also performed for models restrained at 0,75*h*. The lateral restraints are applied every 1,2m for the 10m beams and in the midspan for the stable lengths. Both stable- and 10m lengths are verified and presented in Table 12 and Table 13.

Table 12 Analytical and numerical results for a 10m beam restrained at 0,75h.

Cross-section	Length [m]	Analytical [kNm]	Numerical [kNm]	Ratio [%]
IPE200	10	16,7	16,2	97,2
IPE400	10	107,1	104,1	97,2
IPE600	10	339,6	330,6	97,4

Table 13 Analytical and numerical results regarding stable lengths for a beam restrained at 0,75h.

Cross-section	Length [m]	Analytical [kNm]	Numerical [kNm]	Ratio [%]
IPE200	1,098	271,1	247,3	91,2
IPE400	1,927	1606,0	1447,9	90,2
IPE600	2,304	4323,0	3867,0	89,5

The ratio in Table 12 between analytical and numerical results for the 10m beams are satisfactory, however for the stable length in Table 13 the ratio is decreased compared to unrestrained and restrained at 0,5*h*. It can be concluded that greater distortion occurs for beams restrained at 0,75*h* which is presented in Figure 46.

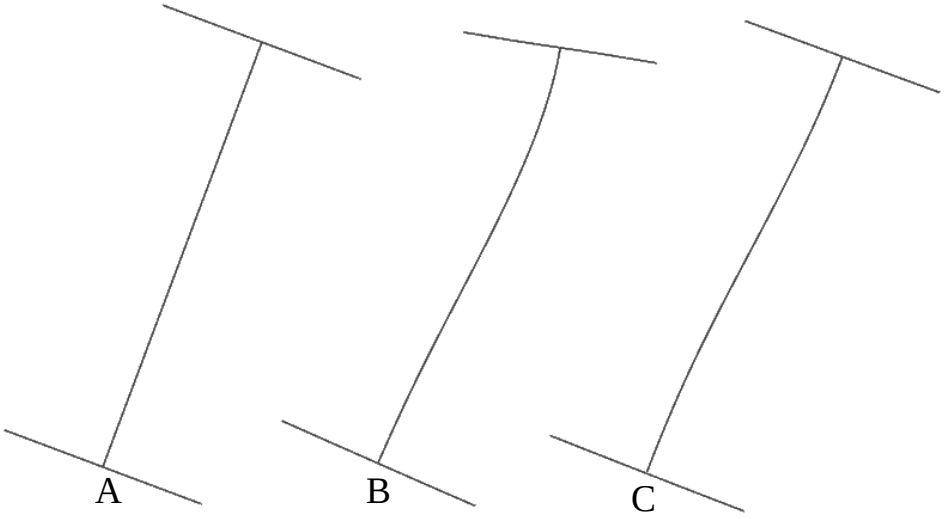

Figure 46 IPE400 restrained at 0,75h for following lengths; A=10m, B=1,927m. Cross-section C is showing unrestrained IPE400 with length C=1,85m.

Figure 44 to Figure 46 show that small or almost negligible distortion occurs for the 10m beams unrestrained or restrained. The greatest distortion occurs for the 1,927m beam restrained at 0,75*h*, which reflects the previous results in Table 12 and Table 13.

6.3.1.1 Summary

The derivation of the stable length for the investigated cross-sections results in relative short lengths. This corresponds to a significant critical buckling moment in proportion to its slenderness resulting in distortion of the web. The magnitude of the distortion is increased when the rotational axis acts further away from the shear centre of the beam. It can be concluded that the analytical expressions are not as reliable for short lengths as for long.

6.3.2 Non-linear buckling analysis

In this chapter the derived stable lengths are verified with non-linear buckling analyses. By comparing the ultimate moment (unstable) obtained from the analysis with the elastic capacity of the section, conclusion can be made if the derived length is stable regarding LT-buckling, when considering non-linear effects and distortion. As in the previous chapter, the investigated models are unrestrained ($L_{.unr}$), restrained above ($L_{r.0,75h}$) and at the tension flange ($L_{r.0,5h}$).

In the analysis, geometric non-linarites and residual stresses are taken into account by applying an equivalent initial bow imperfection as recommended in Eurocode3. Furthermore a plastic material model shown in Figure 47 is assumed.

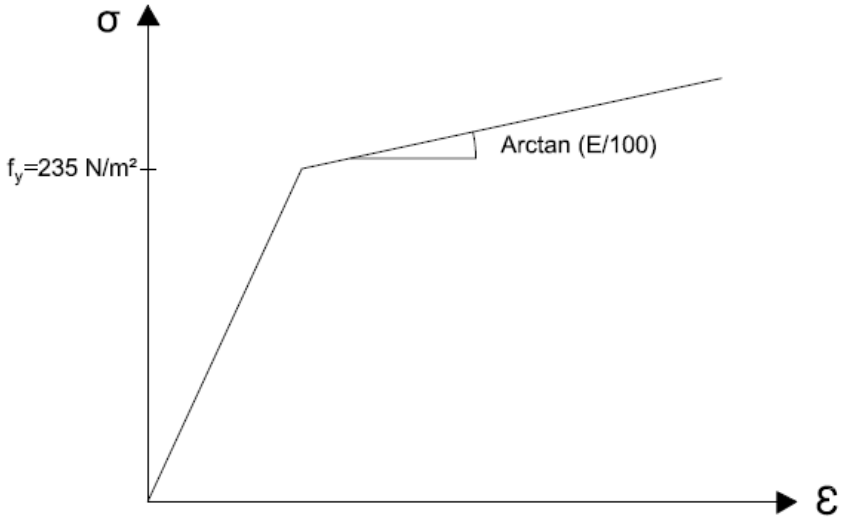

Figure 47 Stress-strain curve.

The shape of the imperfection (see Figure 48) is acquired from the previous linear buckling analysis in section 6.3.1.

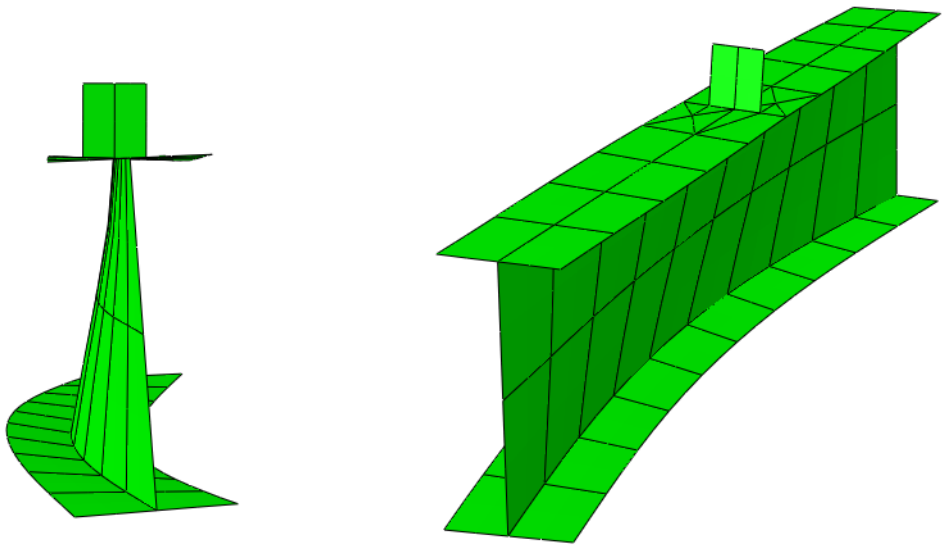

Figure 48 Shape of the imperfection for: IPE400 with stable length $L_{r.0,75h}$= 1.93m.

The magnitude of the initial bow imperfection in Eurocode3, depends on the buckling curve related to the cross-section. In this analysis only beams with standard cross-section dimension are checked because of the risk of local buckling.

In order to represent both standard and welded cross-sections, analyses are performed with two initial imperfections: one according to the dimensions of the cross-section and another with imperfection, representing an equivalent welded cross-section. The buckling curve category for the standard and an equivalent welded cross-section are shown in Table 14 below.

Table 14 The buckling curve for a standard and equivalent welded cross-sections.

Cross-section	Standard cross-section Buckling curve	Eq. Welded cross-section Buckling curve
IPE200	b	d
IPE400	c	d
IPE600	c	d

The results from the non-linear buckling analyses can be seen in Figure 49 to Figure 54 where the y-axis represents the applied moment and the x-axis denotes the maximum lateral displacement of the compression flange. It should be noted that the x-axis is in logarithmic scale. In the graphs, the maximum applied moment before it reaches unstable state (plateau) will be regarded as the ultimate moment of the beam. If the plateau is formed above the elastic capacity of the cross-section no LT-buckling will occur before yielding in the extreme fibre, caused by a moment about the major axis.

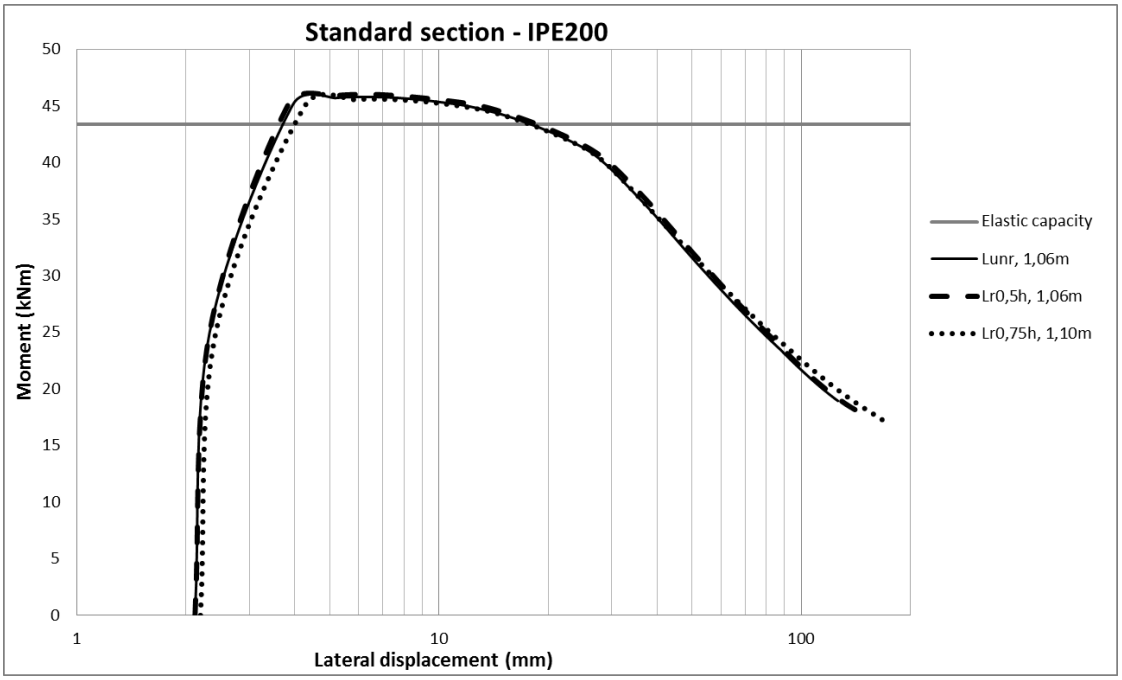

Figure 49 A non-linear buckling analysis of the stable lengths for a standard section IPE200: $L_{.unr}$ = unrestrained at the tension flange, $L_{r.0,5h}$ = restrained at the tension flange, $L_{r.0,75h}$ = restrained above the tension flange.

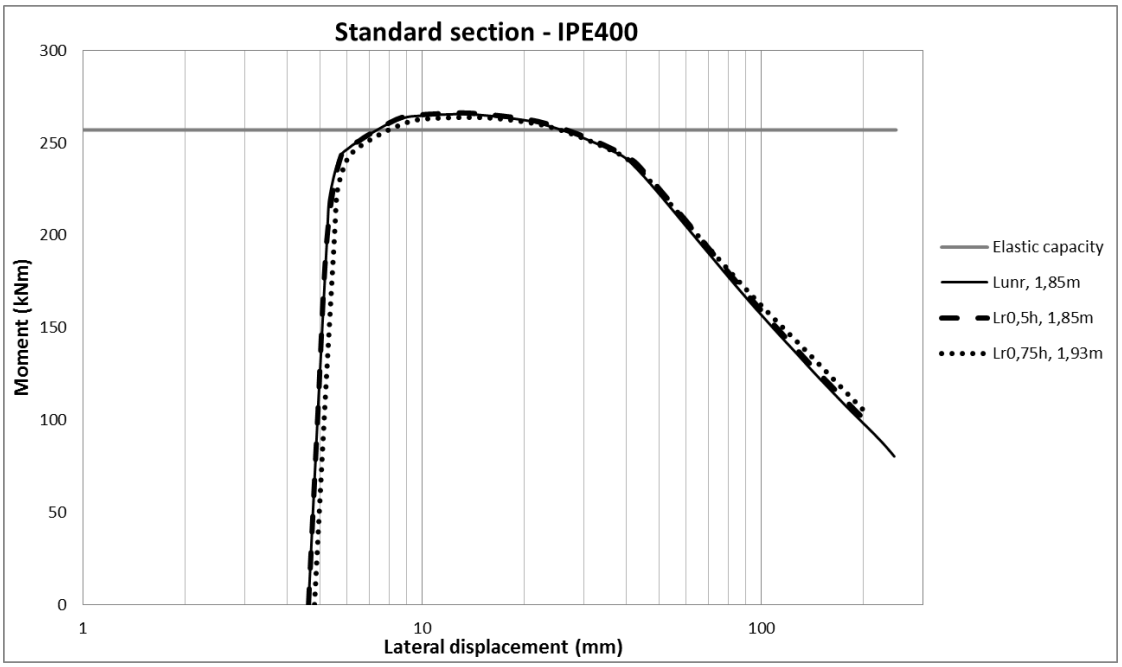

Figure 50 A non-linear buckling analysis of the stable lengths for a standard section IPE400: $L_{.unr}$ = unrestrained at the tension flange, $L_{r.0,5h}$ = restrained at the tension flange, $L_{r.0,75h}$ = restrained above the tension flange.

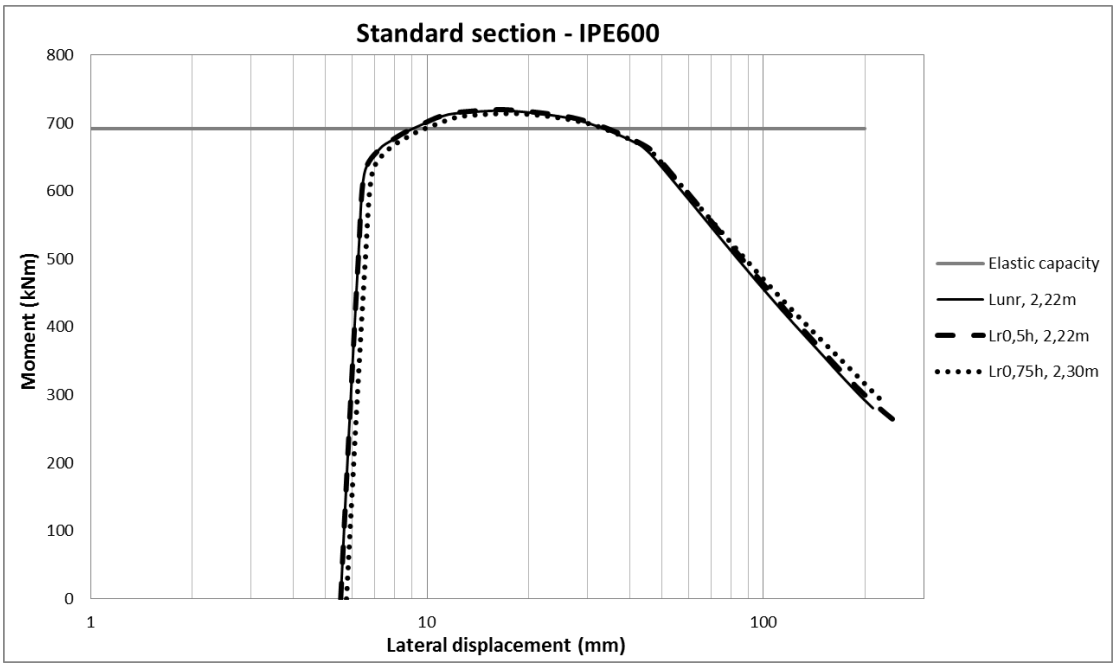

Figure 51 A non-linear buckling analysis of the stable lengths for a standard section IPE600: $L_{.unr}$ = unrestrained at the tension flange, $L_{r.0,5h}$ = restrained at the tension flange, $L_{r.0,75h}$ = restrained above the tension flange.

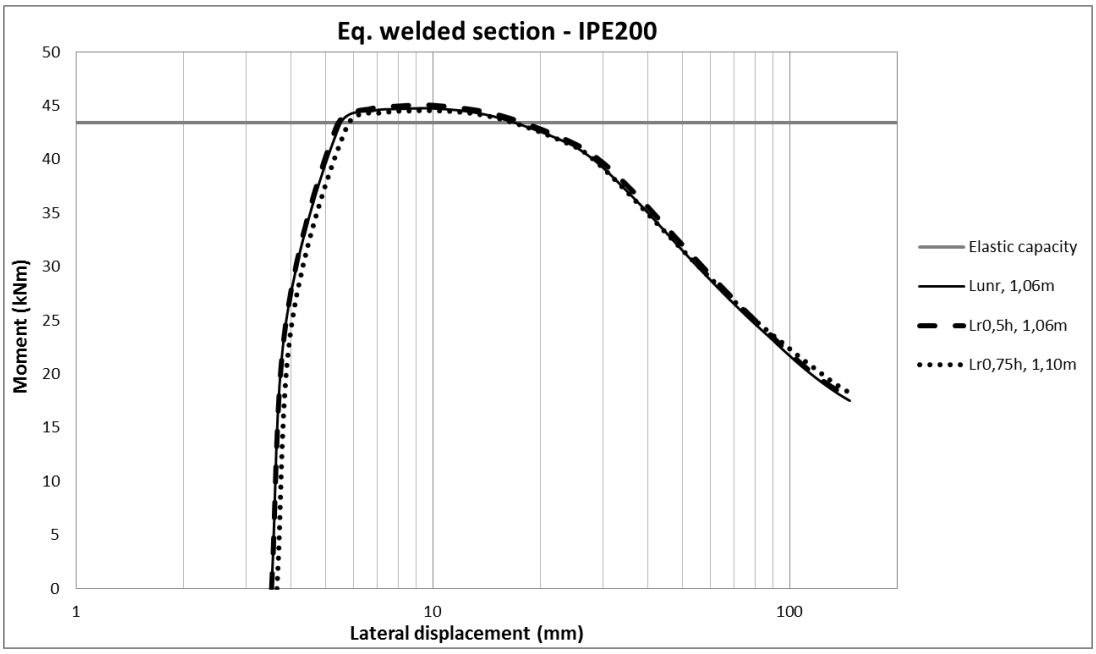

Figure 52 A non-linear buckling analysis of the stable lengths for an equivalent welded section IPE200: $L_{.unr}$ = unrestrained at the tension flange, $L_{r.0,5h}$ = restrained at the tension flange, $L_{r.0,75h}$ = restrained above the tension flange.

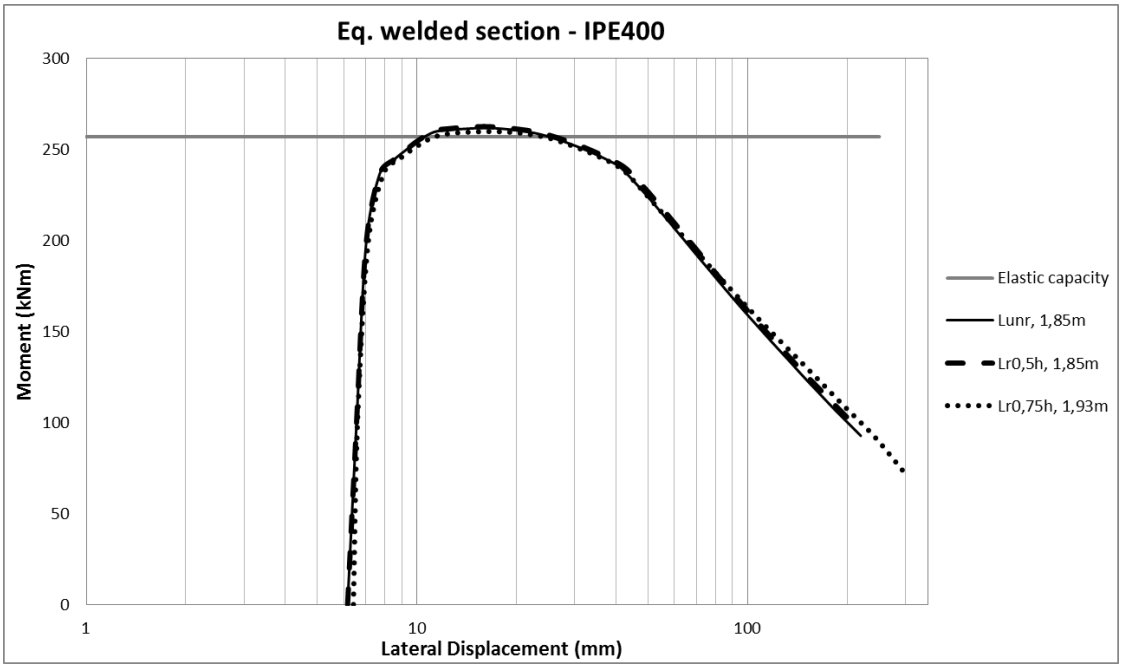

Figure 53 A non-linear buckling analysis of the stable lengths for an equivalent welded section IP400: $L_{.unr}$ = unrestrained at the tension flange, $L_{r.0,5h}$ = restrained at the tension flange, $L_{r.0,75h}$ = restrained above the tension flange.

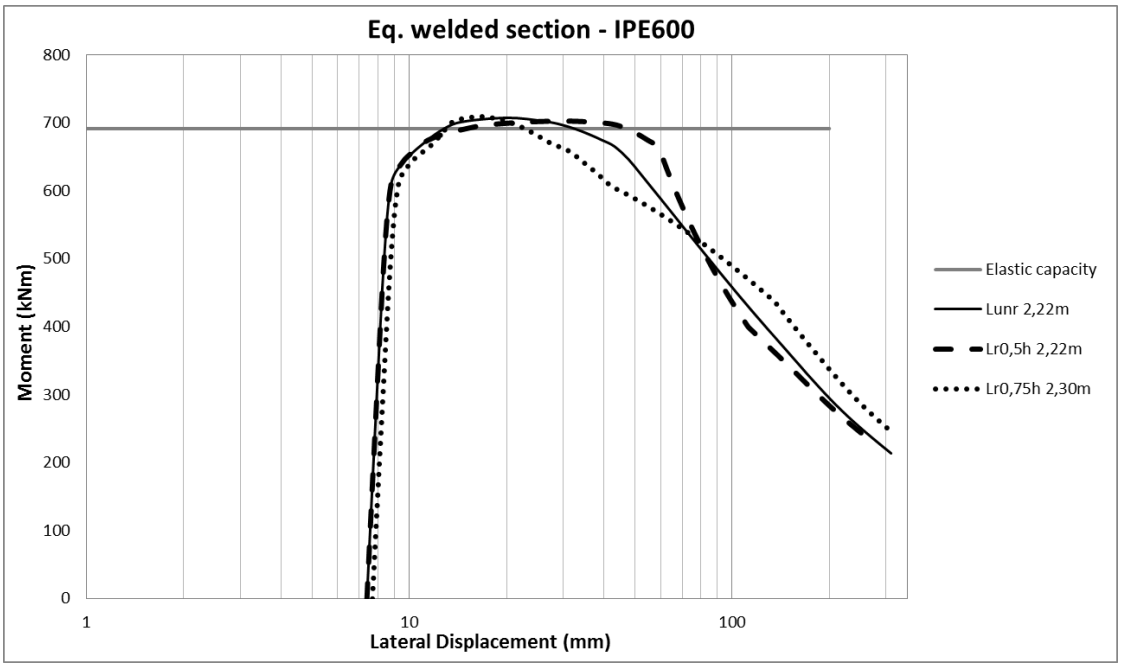

Figure 54 A non-linear buckling analysis of the stable lengths for an equivalent welded section IP600: $L_{.unr}$ = unrestrained at the tension flange, $L_{r.0,5h}$ = restrained at the tension flange, $L_{r.0,75h}$ = restrained above the tension flange.

For all the beams both standard and equivalent welded cross-sections the stable lengths are fairly accurate and give an ultimate moment that is about 2-5% greater than the elastic capacity of the sections. This concludes that the non-dimensional slenderness assumed in the derivation of the stable length is appropriate for both lateral restrained and unrestrained beams. Furthermore it appears that although the beams distort, the limit of slenderness gives accurate results. The ratio between the ultimate moment and the elastic capacity can be seen in the Appendix A.

It is of interest comparing the derived stable length to the already existing expressions in Eurocode3, both the simplified method and the plastic stable length. In section 6.2, it is concluded that the plastic stable lengths (L_k and L_m) are significantly longer and according to the result in this section it is obvious that they are un-conservative. On the other hand the lengths (L_c) from the simplified method in Eurocode3 are closer to the stable length and are relevant to investigate. In order to represent the worst case possible, an analysis is performed with the largest initial imperfection assuming the recommended limit of slenderness of 0,5 for an unrestrained beam. The result from a non-linear buckling analysis for the simplified method length is presented in Figure 55.

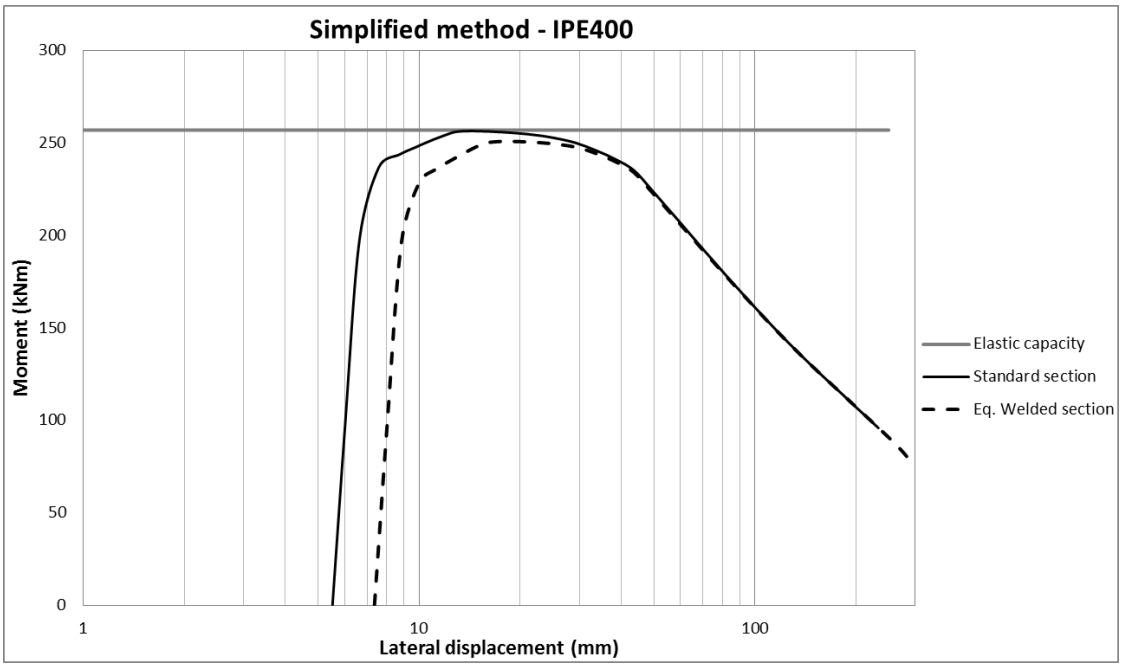

Figure 55 The ultimate moment when assuming length according to the simplified method in Eurocode3 and buckling curve d.

As can be observed form the figure above, the simplified method length gives an ultimate moment that is 2,4% lower than the elastic capacity of the cross-section when assuming the worst imperfection. When an initial imperfection according to the dimensions of the cross-section is applied the length is very accurate.

7 Conclusions

The critical buckling moment (or capacity) is increased by forcing the rotational axis either to act above or below its initial unrestrained rotational axis. One of these actions occurs when lateral restraints at the tension flange are added. However, there are conditions where the location of the restrained- and unrestrained rotational axis coincide resulting in similar buckling shape and capacity.

Lateral restraints at the level of the tension flange (0.5h) has no or negligible effect for short beams. However, when the length is increased, the influence of lateral restraints at 0,5h will considerably improve the buckling capacity. This occurs for all the investigated beams, although more noticeable for shallow sections with low ratio between stiffness's about the minor axis I_z and torsion I_t.

Lateral restraints, with its shear centre located above the tension flange, will increase the buckling capacity for short beams where almost no lateral displacement of the tension flange is taking place. However, when increasing the length, the restrained buckling shape approaches the shape of the unrestrained beam, resulting in similar capacity. The length where no impact of lateral restraints occurs depends on the properties of the cross-section.

The derivation of the stable length for the investigated cross-sections results in relative short lengths. This corresponds to a significant critical buckling moment in proportion to the slenderness of the web resulting in distortion. The magnitude of the distortion is increased when the rotational axis acts further away from the shear centre of the beam. Since analytical expressions do not account for this phenomenon, it indicates that they are not as reliable for short lengths as for long. Although distortion occurs, the limit of slenderness of 0,4 assumed in the derivation appears to take this phenomenon into account. For all investigated beams yielding in the extreme fibres occurs before LT-buckling. It can be concluded that the derived stable length is accurate although the ultimate moment is overestimated with about 2-5% compared to the elastic capacity of the cross-sections.

There are two expressions in Eurocode3 that are comparable to the derived stable length; the plastic stable length and the simplified method.

The plastic stable length is un-conservative. Furthermore the difference is more pronounced for laterally restrained beams at the tension flange. The expression assumes a smaller initial imperfection and a greater limit of slenderness for restrained beams of a 0,63 to 0,72. According to the non-linear analysis it appears that the greater limit of slenderness is not justified.

The simplified method yields similar result as the derived stable length. Depending on the limit of slenderness assumed in the expression (0,4 or 0,5) it is either more conservative or marginally un-conservative for the maximum imperfection. Since the bending stiffness of the purlins, generating torsional resistance to the beam, are not accounted for in the simplified method it indicates that the method is reliable. However the simplified method has to be used cautiously for beams with large initial imperfection.

7.1 Suggestions for further studies

To make this Master's Project broader and more applicable to portal frames further studies have to be performed considering the points below.

- Non-uniform moment
- Haunched and tapered models
- Axial force

Further studies are to consider the modification factor for the moment gradients, both linear and non-linear, which will result in greater critical buckling moment corresponding to longer lengths in between torsional restraints. Furthermore it is of interest to investigate how haunched and tapered beams will influence the stable length. Additionally when considering portal frames the rafters are commonly inclined and an axial force will be present.

Other interesting parameters to study can be seen in the points below.

- Corrugated web
- Bending stiffness of the purlins

From this study it can be concluded that the depth of the cross-section and the ratio between the stiffness about the minor axis and the torsional stiffness determines the efficiency of laterally restraining a beam. By establishing a reliable ratio of the mentioned stiffness's for a corrugated web it can be concluded if the influence of purlins differs compared to beams with flat web. In addition it is of interest to see if the corrugated web distorts less which results in longer stable lengths.

Furthermore the bending stiffness of the purlin (added as a torsional spring on the simulated beam segment) has a significant impact on the buckling capacity. This is something which is neglected in Eurocode3 due to its complexity resulting in a conservative approach. If there were a simplified method including the bending stiffness to the existing analytical expressions a lot would be gained.

8 References

Dooley, J. F. (1966). On the Torsional Buckling of Columns of I-Section Restrained at Finite Intervals. *International Journal of Mechanical Sciences, Volume 9*, pp.1-9.

European Committee for Standardization. (2003). *Eurocode 3: Design of steel structures - Part 1-1: general rules for building.* Brussels.

Galambos, T. V. (1968). *Structural Members and Frames.* Englewood Cliffs N.J.: Prentice-Hall, Inc.

Horne, M. R. (1964). Safe loads on I-section columns in structure designed by plastic theory. *Proceeding of the Institution of Civil Engineers, Volume 29*, p. 137-150.

Horne, M. R., & Ajmani, J. L. (1969). Stability of Columns Supported Laterally by Side-Rails. *International Journal of Mechanical Sciences, Volume 11*, pp.159-174.

Horne, M. R., & Ajmani, J. L. (1971). The post-buckling behaviour of laterally restrained columns. *The Structural Engineer*, Volume 49.

Horne, M. R., Shakir-Khalil, H., & Akhtar, S. (1979). The stability of tapered and haunched member. *Proceedings of the Institution of Civil Engineers, Vol.67*, p.677-694.

King, C. M. (2002). *Origins of the Stable Length Formulae in prEN1993-1-1.* The Steel Construction Institute.

Louw, G. S. (2008). *Lateral support of axially columns in portal frame structures provided by sheeting rails.* Stellenbosch.

M E Brettle, D. G. (2009). *Steel Building Design:Concise Eurocodes.* Berkshire: The Steel Construction Institute .

NCCI. (2007). *Elastic critical moment for lateral torsional buckling, SN003a-EN-EU.* Access Steel.

Sabat, A. K. (2009). *Lateral-torsional buckling analysis of steel frames with corrugated wbs.* Göteborg.

(u.d.). *Single-Storey Steel Buildings Part4: Detailed Design of Portal Frames.*

Timoshenko, S. P., & Gere, J. M. (1961). *Theory of Elastic Stability* (Andra uppl.). McGraw-Hill Book Company, Inc.

Appendix A

The results from the non-linear buckling analysis

Unrestrained

Table 15 The ratio of the ultimate moment and the elastic capacity for the derived stable lengths, standard sections.

Cross-section	Derived length L_{unr}	Ratio M_{ult}/M_{el}
IPE200	1,060m	1,06
IPE400	1,854m	1,03
IPE600	2,215m	1,04

Table 16 The ratio of the ultimate moment and the elastic capacity for the derived stable length, Eq. welded sections.

Cross-section	Derived length L_{unr}	Ratio M_{ult}/M_{el}
Eq. welded 200	1,060m	1,03
Eq. welded 400	1,854m	1,02
Eq. welded 600	2,215m	1,02

Table 17 The ratio of the ultimate moment and the elastic capacity for the length according to the simplified method.

Cross-section	Simplified method L_c	Ratio M_{ult}/M_{el}
IPE400	2,209m	1,00
Eq. welded 400	2,209m	0,98

Restrained at 0,5*h*

Table 18 The ratio of the ultimate moment and the elastic capacity for the derived stable length, standard sections

Cross-section	Derived length $L_{r,0,5h}$	Ratio M_{ult}/M_{el}
IPE200	1,060m	1,06
IPE400	1,854m	1,04
IPE600	2,215m	1,04

Table 19 The ratio of the ultimate moment and the elastic capacity for the derived stable length, Eq. welded sections.

Cross-section	Derived length $L_{r,0,5h}$	Ratio M_{ult}/M_{el}
Eq. welded 200	1,060m	1,04
Eq. welded 400	1,854m	1,02
Eq. welded 600	2,215m	1,02

Restrained at 0,75*h*

Table 20 The ratio of the ultimate moment and the elastic capacity for the derived stable length, standard sections

Cross-section	Derived length $L_{r,0,75h}$	Ratio M_{ult}/M_{el}
IPE200	1,098m	1,05
IPE400	1,927m	1,02
IPE600	2,304m	1,03

Table 21 The ratio of the ultimate moment and the elastic capacity for the derived stable length, Eq. welded sections.

Cross-section	Derived length $L_{r,0,75h}$	Ratio M_{ult}/M_{el}
Eq. welded 200	1,098m	1,03
Eq. welded 400	1,927m	1,01
Eq. welded 600	2,304m	1,03

Appendix B

The derived stable length and the stable lengths according to Eurocode3

IPE 200

Material parameters

$E := 210GPa$

$G_1 := 81GPa$

$f_y := 235 \frac{N}{mm^2}$

Geometrical Parameters

Dimensions of the cross-section

$h := 200mm \quad b := 100mm \quad t_f := 8.5mm \quad t_w := 5.6mm$

$h_w := h - t_f \cdot 2 = 183 \cdot mm \qquad d := h - t_f = 0.192\,m$

$A := h_w \cdot t_w + b \cdot t_f \cdot 2 = 2.725 \times 10^{-3}\,m^2$

Second moment of inertia according to the software LTB

$I_z := 141.93cm^4 \quad I_w := 13013cm^6 \quad I_t := 5.0237cm^4$

Second moment of inertia about the major axis

$A_1 := b \cdot t_f = 8.5 \times 10^{-4}\,m^2$

$I_y := \frac{h_w^3 \cdot t_w}{12} + \left(\frac{h_w}{2} + \frac{t_f}{2}\right)^2 \cdot (2A_1) + \frac{2t_f^3 \cdot b}{12} = 1.846 \times 10^7 \cdot mm^4$

$w_y := \frac{I_y}{\frac{h}{2}} = 1.846 \times 10^5 \cdot mm^3$

Polar radius of gyration about the minor axis

$i_z := \sqrt{\frac{I_z}{A}} = 22.823 \cdot mm$

Plastic sectional modulus about major axis

$A_{t1} := t_f \cdot b = 8.5 \times 10^{-4}\,m^2$

$A_{t2} := \left(\frac{h_w}{2}\right) \cdot t_w = 5.124 \times 10^{-4}\,m^2$

$y_n := \frac{A_{t1} \cdot \left(\frac{t_f}{2} + \frac{h_w}{2}\right) + A_{t2} \cdot \left(\frac{h_w}{4}\right)}{\left(\frac{A}{2}\right)} = 76.945 \cdot mm \qquad w_{pl} := \left(\frac{A}{2} \cdot y_n\right) \cdot 2 = 2.097 \times 10^5 \cdot mm^3$

Cross section class

Internal compression

$c := h - 2 \cdot t_f = 0.183\,m$

$t := t_w = 5.6 \cdot mm$

$\frac{c}{t} = 32.679$ Less than 72ε, Class 1

Outstanding

$c_{out} := \frac{b - t_w}{2} = 0.047\,m$

$t_{out} := t_f = 8.5 \cdot mm$

$\frac{c_{out}}{t_{out}} = 5.553$ less than 9ε, Class 1

The derived stable length

Unrestrained

$x := 1m$

Given

$$0.4 = \sqrt{\frac{w_y \cdot f_y}{\frac{\pi^2 \cdot E \cdot I_z}{x^2}\left(\frac{I_w}{I_z} + \frac{x^2 \cdot G_1 \cdot I_t}{\pi^2 \cdot E \cdot I_z}\right)^{0.5}}}$$

$L_{unr} := Find(x)$

$L_{unr} = 1.06\,m$

Critical buckling moment for a derived stable length unrestrained

$$M_{cr.unr} := \frac{\pi^2 \cdot E \cdot I_z}{L_{unr}^2}\left(\frac{I_w}{I_z} + \frac{L_{unr}^2 \cdot G_1 \cdot I_t}{\pi^2 \cdot E \cdot I_z}\right)^{0.5} = 271.071 \cdot kN \cdot m$$

Restrained at 0.5h

$a_1 := 0.5 \cdot h = 0.1\,m$

$$L_{r.05h} := \sqrt{\frac{\pi^2 \cdot E \cdot \left(I_z \cdot a_1^2 + I_w\right)}{\left(\frac{2 \cdot a_1 \cdot w_y \cdot f_y}{0.4^2} - G_1 \cdot I_t\right)}} = 1.06\,m$$

Critical buckling moment for a derived stable length restrained at 0,5h

$$M_{cr.r05} := \frac{1}{2a_1}\cdot\left(\frac{\pi^2\cdot E\cdot I_z\cdot a_1^{\,2}}{L_{r.05h}^{\,2}} + \frac{\pi^2\cdot E\cdot I_w}{L_{r.05h}^{\,2}} + G_1\cdot I_t\right) = 271.071\cdot kN\cdot m$$

Restrained at 0.75h

$$a_2 := 0.75\cdot h = 0.15\,m$$

$$L_{r.075h} := \sqrt{\frac{\pi^2\cdot E\cdot\left(I_z\cdot a_2^{\,2} + I_w\right)}{\left(\frac{2\cdot a_2\cdot w_y\cdot f_y}{0.4^2} - G_1\cdot I_t\right)}} = 1.098\,m$$

Critical buckling moment for a derived stable length restrained at 0,75h

$$M_{cr.0.r075} := \frac{1}{2a_2}\cdot\left(\frac{\pi^2\cdot E\cdot I_z\cdot a_2^{\,2}}{L_{r.075h}^{\,2}} + \frac{\pi^2\cdot E\cdot I_w}{L_{r.075h}^{\,2}} + G_1\cdot I_t\right) = 271.071\cdot kN\cdot m$$

The stable length according to Eurocode

The plastic stable length, unrestrained

$$L_m := \frac{38 i_z}{\sqrt{\frac{1}{756}\cdot\left(\frac{w_{pl}^{\,2}}{A\cdot I_t}\right)\cdot\left(\frac{f_y}{235\,\frac{N}{mm^2}}\right)^2}} = 1.331\,m$$

The plastic stable length, restrained

$$L_k := \frac{\left(5.4 + \frac{600 f_y}{E}\right)\cdot\left(\frac{h}{t_f}\right)\cdot i_z}{\sqrt{5.4\cdot\left(\frac{f_y}{E}\right)\cdot\left(\frac{h}{t_f}\right)^2 - 1}} = 2.129\,m$$

The stable length according to the simplified method

$$f := \frac{h_w}{6} = 0.031\,m$$

$$I_{zf} := \frac{b^3 \cdot t_f}{12} + \frac{f \cdot t_w^{\,3}}{12} = 7.088 \times 10^{-7}\,m^4$$

$$A_{simp} := \left(b \cdot t_f\right) + \left(f \cdot t_w\right) = 1.021 \times 10^{-3}\,m^2$$

$$i_f := \sqrt{\frac{I_{zf}}{A_{simp}}} = 0.026\,m$$

$$L_c := i_f \cdot 93.9 \cdot 0.5 = 1.237\,m$$

IPE 400

Material parameters

$E := 210GPa$

$G_1 := 81GPa$

$f_y := 235 \frac{N}{mm^2}$

Geometrical Parameters

Dimensions of the cross-section

$h := 400mm \quad b := 180mm \quad t_f := 13.5mm \quad t_w := 8.6mm$

$h_w := h - t_f \cdot 2 = 373 \cdot mm \qquad d := h - t_f = 0.387\,m$

$A := h_w \cdot t_w + b \cdot t_f \cdot 2 = 8.068 \times 10^{-3}\,m^2$

Second moment of inertia according to the software LTB

$I_z := 13.142 \cdot 10^6 mm^4 \qquad I_w := 490.79 \cdot 10^9 mm^6 \quad I_t := 364.87 \cdot 10^3 mm^4$

Second moment of inertia about the major axis

$A_1 := b \cdot t_f = 2.43 \times 10^{-3}\,m^2$

$I_y := \frac{h_w^{\,3} \cdot t_w}{12} + \left(\frac{h_w}{2} + \frac{t_f}{2}\right)^2 \cdot (2A_1) + \frac{2t_f^{\,3} \cdot b}{12} = 2.188 \times 10^8 \cdot mm^4$

$w_y := \frac{I_y}{\frac{h}{2}} = 1.094 \times 10^6 \cdot mm^3$

Polar radius of gyration about the minor axis

$i_z := \sqrt{\frac{I_z}{A}} = 40.36 \cdot mm$

Plastic sectional modulus about major axis

$A_{t1} := t_f \cdot b = 2.43 \times 10^{-3}\,m^2$

$A_{t2} := \left(\frac{h_w}{2}\right) \cdot t_w = 1.604 \times 10^{-3}\,m^2$

$y_n := \frac{A_{t1} \cdot \left(\frac{t_f}{2} + \frac{h_w}{2}\right) + A_{t2} \cdot \left(\frac{h_w}{4}\right)}{\left(\frac{A}{2}\right)} = 153.489 \cdot mm \qquad w_{pl} := \left(\frac{A}{2} \cdot y_n\right) \cdot 2 = 1.238 \times 10^6 \cdot mm^3$

Cross section class

Internal compression

$c := h - 2 \cdot t_f = 0.373\,m$

$t := t_w = 8.6 \cdot mm$

$\frac{c}{t} = 43.372$ Less than 72ε, Class 1

Outstanding

$c_{out} := \frac{b - t_w}{2} = 0.086\,m$

$t_{out} := t_f = 13.5 \cdot mm$

$\frac{c_{out}}{t_{out}} = 6.348$ less than 9ε, Class 1

The derived stable length

Unrestrained

$x := 1m$

Given

$$0.4 = \sqrt{\frac{w_y \cdot f_y}{\frac{\pi^2 \cdot E \cdot I_z}{x^2}\left(\frac{I_w}{I_z} + \frac{x^2 \cdot G_1 \cdot I_t}{\pi^2 \cdot E \cdot I_z}\right)^{0.5}}}$$

$L_{unr} := Find(x)$

$L_{unr} = 1.854\,m$

Critical buckling moment for a derived stable length unrestrained

$$M_{cr.unr} := \frac{\pi^2 \cdot E \cdot I_z}{L_{unr}^2}\left(\frac{I_w}{I_z} + \frac{L_{unr}^2 \cdot G_1 \cdot I_t}{\pi^2 \cdot E \cdot I_z}\right)^{0.5} = 1.607 \times 10^3 \cdot kN \cdot m$$

Restrained at 0.5h

$a_1 := 0.5 \cdot h = 0.2\,m$

$$L_{r.05h} := \sqrt{\frac{\pi^2 \cdot E \cdot \left(I_z \cdot a_1^2 + I_w\right)}{\left(\frac{2 \cdot a_1 \cdot w_y \cdot f_y}{0.4^2} - G_1 \cdot I_t\right)}} = 1.854\,m$$

Critical buckling moment for a derived stable length restrained at 0,5h

$$M_{cr.r05} := \frac{1}{2a_1}\cdot\left(\frac{\pi^2\cdot E\cdot I_z\cdot a_1^{\,2}}{L_{r.05h}^{\,2}} + \frac{\pi^2\cdot E\cdot I_w}{L_{r.05h}^{\,2}} + G_1\cdot I_t\right) = 1.607\times 10^3\cdot kN\cdot m$$

Restrained at 0.75h

$$a_2 := 0.75\cdot h = 0.3\,m$$

$$L_{r.075h} := \sqrt{\frac{\pi^2\cdot E\cdot\left(I_z\cdot a_2^{\,2} + I_w\right)}{\left(\frac{2\cdot a_2\cdot w_y\cdot f_y}{0.4^2} - G_1\cdot I_t\right)}} = 1.927\,m$$

Critical buckling moment for a derived stable length restrained at 0,75h

$$M_{cr.0.r075} := \frac{1}{2a_2}\cdot\left(\frac{\pi^2\cdot E\cdot I_z\cdot a_2^{\,2}}{L_{r.075h}^{\,2}} + \frac{\pi^2\cdot E\cdot I_w}{L_{r.075h}^{\,2}} + G_1\cdot I_t\right) = 1.607\times 10^3\cdot kN\cdot m$$

The stable length according to Eurocode

The plastic stable length, unrestrained

$$L_m := \frac{38 i_z}{\sqrt{\frac{1}{756}\cdot\left(\frac{w_{pl}^{\,2}}{A\cdot I_t}\right)\cdot\left(\frac{f_y}{235\,\frac{N}{mm^2}}\right)^2}} = 1.848\,m$$

The plastic stable length, restrained

$$L_k := \frac{\left(5.4 + \frac{600 f_y}{E}\right)\cdot\left(\frac{h}{t_f}\right)\cdot i_z}{\sqrt{5.4\cdot\left(\frac{f_y}{E}\right)\cdot\left(\frac{h}{t_f}\right)^2 - 1}} = 3.499\,m$$

The stable length according to the simplified method

$$f := \frac{h_w}{6} = 0.062\,m$$

$$I_{zf} := \frac{b^3 \cdot t_f}{12} + \frac{f \cdot t_w^{\,3}}{12} = 6.564 \times 10^{-6}\,m^4$$

$$A_{simp} := \left(b \cdot t_f\right) + \left(f \cdot t_w\right) = 2.965 \times 10^{-3}\,m^2$$

$$i_f := \sqrt{\frac{I_{zf}}{A_{simp}}} = 0.047\,m$$

$$L_c := i_f \cdot 93.9 \cdot 0.5 = 2.209\,m$$

IPE 600

Material parameters

$E := 210GPa$

$G_1 := 81GPa$

$f_y := 235 \frac{N}{mm^2}$

Geometrical Parameters

Dimensions of the cross-section

$h := 600mm \quad b := 220mm \quad t_f := 19mm \quad t_w := 12mm$

$h_w := h - t_f \cdot 2 = 562 \cdot mm \qquad d := h - t_f = 0.581\,m$

$A := h_w \cdot t_w + b \cdot t_f \cdot 2 = 0.015\,m^2$

Second moment of inertia according to the software LTB

$I_z := 3380cm^4 \qquad I_w := 2.8523 \cdot 10^6 cm^6 \quad I_t := 129.22cm^4$

Second moment of inertia about the major axis

$A_1 := b \cdot t_f = 4.18 \times 10^{-3}\,m^2$

$I_y := \frac{h_w^3 \cdot t_w}{12} + \left(\frac{h_w}{2} + \frac{t_f}{2}\right)^2 \cdot (2A_1) + \frac{2t_f^3 \cdot b}{12} = 8.833 \times 10^8 \cdot mm^4$

$w_y := \frac{I_y}{\frac{h}{2}} = 2.944 \times 10^6 \cdot mm^3$

Polar radius of gyration about the minor axis

$i_z := \sqrt{\frac{I_z}{A}} = 47.306 \cdot mm$

Plastic sectional modulus about major axis

$A_{t1} := t_f \cdot b = 4.18 \times 10^{-3}\,m^2$

$A_{t2} := \left(\frac{h_w}{2}\right) \cdot t_w = 3.372 \times 10^{-3}\,m^2$

$y_n := \frac{A_{t1} \cdot \left(\frac{t_f}{2} + \frac{h_w}{2}\right) + A_{t2} \cdot \left(\frac{h_w}{4}\right)}{\left(\frac{A}{2}\right)} = 223.524 \cdot mm \qquad w_{pl} := \left(\frac{A}{2} \cdot y_n\right) \cdot 2 = 3.376 \times 10^6 \cdot mm^3$

Cross section class

Internal compression

$c := h - 2 \cdot t_f = 0.562\,m$

$t := t_w = 12 \cdot mm$

$\frac{c}{t} = 46.833$ Less than 72ε, Class 1

Outstanding

$c_{out} := \frac{b - t_w}{2} = 0.104\,m$

$t_{out} := t_f = 19 \cdot mm$

$\frac{c_{out}}{t_{out}} = 5.474$ less than 9ε, Class 1

The derived stable length

Unrestrained

$x := 1m$

Given

$$0.4 = \sqrt{\frac{w_y \cdot f_y}{\frac{\pi^2 \cdot E \cdot I_z}{x^2}\left(\frac{I_w}{I_z} + \frac{x^2 \cdot G_1 \cdot I_t}{\pi^2 \cdot E \cdot I_z}\right)^{0.5}}}$$

$L_{unr} := Find(x)$

$L_{unr} = 2.215\,m$

Critical buckling moment for a derived stable length unrestrained

$$M_{cr.unr} := \frac{\pi^2 \cdot E \cdot I_z}{L_{unr}^2}\left(\frac{I_w}{I_z} + \frac{L_{unr}^2 \cdot G_1 \cdot I_t}{\pi^2 \cdot E \cdot I_z}\right)^{0.5} = 4.324 \times 10^3 \cdot kN \cdot m$$

Restrained at 0.5h

$a_1 := 0.5 \cdot h = 0.3\,m$

$$L_{r.05h} := \sqrt{\frac{\pi^2 \cdot E \cdot \left(I_z \cdot a_1^2 + I_w\right)}{\left(\frac{2 \cdot a_1 \cdot w_y \cdot f_y}{0.4^2} - G_1 \cdot I_t\right)}} = 2.215\,m$$

Critical buckling moment for a derived stable length restrained at 0,5h

$$M_{cr.r05} := \frac{1}{2a_1}\cdot\left(\frac{\pi^2\cdot E\cdot I_z\cdot a_1^{\,2}}{L_{r.05h}^{\,2}} + \frac{\pi^2\cdot E\cdot I_w}{L_{r.05h}^{\,2}} + G_1\cdot I_t\right) = 4.324\times 10^3\cdot kN\cdot m$$

Restrained at 0.75h

$$a_2 := 0.75\cdot h = 0.45\,m$$

$$L_{r.075h} := \sqrt{\frac{\pi^2\cdot E\cdot\left(I_z\cdot a_2^{\,2} + I_w\right)}{\left(\frac{2\cdot a_2\cdot w_y\cdot f_y}{0.4^2} - G_1\cdot I_t\right)}} = 2.304\,m$$

Critical buckling moment for a derived stable length restrained at 0,75h

$$M_{cr.0.r075} := \frac{1}{2a_2}\cdot\left(\frac{\pi^2\cdot E\cdot I_z\cdot a_2^{\,2}}{L_{r.075h}^{\,2}} + \frac{\pi^2\cdot E\cdot I_w}{L_{r.075h}^{\,2}} + G_1\cdot I_t\right) = 4.324\times 10^3\cdot kN\cdot m$$

The stable length according to Eurocode

The plastic stable length, unrestrained

$$L_m := \frac{38 i_z}{\sqrt{\frac{1}{756}\cdot\left(\frac{w_{pl}^{\,2}}{A\cdot I_t}\right)\cdot\left(\frac{f_y}{235\,\frac{N}{mm^2}}\right)^2}} = 2.045\,m$$

The plastic stable length, restrained

$$L_k := \frac{\left(5.4 + \frac{600 f_y}{E}\right)\cdot\left(\frac{h}{t_f}\right)\cdot i_z}{\sqrt{5.4\cdot\left(\frac{f_y}{E}\right)\cdot\left(\frac{h}{t_f}\right)^2 - 1}} = 4.046\,m$$

The stable length according to the simplified method

$$f := \frac{h_w}{6} = 0.094\,m$$

$$I_{zf} := \frac{b^3 \cdot t_f}{12} + \frac{f \cdot t_w^{\,3}}{12} = 1.687 \times 10^{-5}\,m^4$$

$$A_{simp} := \left(b \cdot t_f\right) + \left(f \cdot t_w\right) = 5.304 \times 10^{-3}\,m^2$$

$$i_f := \sqrt{\frac{I_{zf}}{A_{simp}}} = 0.056\,m$$

$$L_c := i_f \cdot 93.9 \cdot 0.5 = 2.648\,m$$

Customized, depth 200

Material parameters

$E := 210GPa$

$G_1 := 81GPa$

$f_y := 235 \frac{N}{mm^2}$

Geometrical Parameters

Dimensions of the cross-section

$h := 200mm \quad b := 200mm \quad t_f := 10mm \quad t_w := 6mm$

$h_w := h - t_f \cdot 2 = 180 \cdot mm \qquad d := h - t_f = 0.19\,m$

$A := h_w \cdot t_w + b \cdot t_f \cdot 2 = 5.08 \times 10^{-3}\,m^2$

Second moment of inertia according to the software LTB

$I_z := 1333.7cm^4 \quad I_w := 120363cm^6 \quad I_t := 14.324cm^4$

Second moment of inertia about the major axis

$A_1 := b \cdot t_f = 2 \times 10^{-3}\,m^2$

$I_y := \frac{h_w^3 \cdot t_w}{12} + \left(\frac{h_w}{2} + \frac{t_f}{2}\right)^2 \cdot (2A_1) + \frac{2t_f^3 \cdot b}{12} = 3.905 \times 10^7 \cdot mm^4$

$w_y := \frac{I_y}{\frac{h}{2}} = 3.905 \times 10^5 \cdot mm^3$

Polar radius of gyration about the minor axis

$i_z := \sqrt{\frac{I_z}{A}} = 51.239 \cdot mm$

Plastic sectional modulus about major axis

$A_{t1} := t_f \cdot b = 2 \times 10^{-3}\,m^2$

$A_{t2} := \left(\frac{h_w}{2}\right) \cdot t_w = 5.4 \times 10^{-4}\,m^2$

$y_n := \frac{A_{t1} \cdot \left(\frac{t_f}{2} + \frac{h_w}{2}\right) + A_{t2} \cdot \left(\frac{h_w}{4}\right)}{\left(\frac{A}{2}\right)} = 84.37 \cdot mm \qquad w_{pl} := \left(\frac{A}{2} \cdot y_n\right) \cdot 2 = 4.286 \times 10^5 \cdot mm^3$

Cross section class

Internal compression

$c := h - 2 \cdot t_f = 0.18\,m$

$t := t_w = 6 \cdot mm$

$\frac{c}{t} = 30$ Less than 72ε, Class 1

Outstanding

$c_{out} := \frac{b - t_w}{2} = 0.097\,m$

$t_{out} := t_f = 10 \cdot mm$

$\frac{c_{out}}{t_{out}} = 9.7$ less than 9ε, Class 1

The derived stable length

Unrestrained

$x := 1m$

Given

$$0.4 = \sqrt{\frac{w_y \cdot f_y}{\frac{\pi^2 \cdot E \cdot I_z}{x^2}\left(\frac{I_w}{I_z} + \frac{x^2 \cdot G_1 \cdot I_t}{\pi^2 \cdot E \cdot I_z}\right)^{0.5}}}$$

$L_{unr} := Find(x)$

$L_{unr} = 2.257\,m$

Critical buckling moment for a derived stable length unrestrained

$$M_{cr.unr} := \frac{\pi^2 \cdot E \cdot I_z}{L_{unr}^2}\left(\frac{I_w}{I_z} + \frac{L_{unr}^2 \cdot G_1 \cdot I_t}{\pi^2 \cdot E \cdot I_z}\right)^{0.5} = 573.537 \cdot kN \cdot m$$

Restrained at 0.5h

$a_1 := 0.5 \cdot h = 0.1\,m$

$$L_{r.05h} := \sqrt{\frac{\pi^2 \cdot E \cdot \left(I_z \cdot a_1^2 + I_w\right)}{\left(\frac{2 \cdot a_1 \cdot w_y \cdot f_y}{0.4^2} - G_1 \cdot I_t\right)}} = 2.258\,m$$

Critical buckling moment for a derived stable length restrained at 0,5h

$$M_{cr.r05} := \frac{1}{2a_1}\cdot\left(\frac{\pi^2\cdot E\cdot I_z\cdot a_1^{\,2}}{L_{r.05h}^{\,2}} + \frac{\pi^2\cdot E\cdot I_w}{L_{r.05h}^{\,2}} + G_1\cdot I_t\right) = 573.537\cdot kN\cdot m$$

Restrained at 0.75h

$$a_2 := 0.75\cdot h = 0.15\,m$$

$$L_{r.075h} := \sqrt{\frac{\pi^2\cdot E\cdot\left(I_z\cdot a_2^{\,2} + I_w\right)}{\left(\frac{2\cdot a_2\cdot w_y\cdot f_y}{0.4^2} - G_1\cdot I_t\right)}} = 2.33\,m$$

Critical buckling moment for a derived stable length restrained at 0,75h

$$M_{cr.0.r075} := \frac{1}{2a_2}\cdot\left(\frac{\pi^2\cdot E\cdot I_z\cdot a_2^{\,2}}{L_{r.075h}^{\,2}} + \frac{\pi^2\cdot E\cdot I_w}{L_{r.075h}^{\,2}} + G_1\cdot I_t\right) = 573.537\cdot kN\cdot m$$

The stable length according to Eurocode

The plastic stable length, unrestrained

$$L_m := \frac{38 i_z}{\sqrt{\frac{1}{756}\cdot\left(\frac{w_{pl}^{\,2}}{A\cdot I_t}\right)\cdot\left(\frac{f_y}{235\,\frac{N}{mm^2}}\right)^2}} = 3.369\,m$$

The plastic stable length, restrained

$$L_k := \frac{\left(5.4 + \frac{600 f_y}{E}\right)\cdot\left(\frac{h}{t_f}\right)\cdot i_z}{\sqrt{5.4\cdot\left(\frac{f_y}{E}\right)\cdot\left(\frac{h}{t_f}\right)^2 - 1}} = 5.227\,m$$

The stable length according to the simplified method

$$f := \frac{h_w}{6} = 0.03\,m$$

$$I_{zf} := \frac{b^3 \cdot t_f}{12} + \frac{f \cdot t_w^{\,3}}{12} = 6.667 \times 10^{-6}\,m^4$$

$$A_{simp} := \left(b \cdot t_f\right) + \left(f \cdot t_w\right) = 2.18 \times 10^{-3}\,m^2$$

$$i_f := \sqrt{\frac{I_{zf}}{A_{simp}}} = 0.055\,m$$

$$L_c := i_f \cdot 93.9 \cdot 0.5 = 2.596\,m$$

Customized, depth 400

Material parameters

$E := 210GPa$

$G_1 := 81GPa$

$f_y := 235 \frac{N}{mm^2}$

Geometrical Parameters

Dimensions of the cross-section

$h := 400mm \quad b := 200mm \quad t_f := 10mm \quad t_w := 6mm$

$h_w := h - t_f \cdot 2 = 380 \cdot mm \qquad d := h - t_f = 0.39\,m$

$A := h_w \cdot t_w + b \cdot t_f \cdot 2 = 6.28 \times 10^{-3}\,m^2$

Second moment of inertia according to the software LTB

$I_z := 1334cm^4 \quad I_w := 507260cm^6 \quad I_t := 15.764cm^4$

Second moment of inertia about the major axis

$A_1 := b \cdot t_f = 2 \times 10^{-3}\,m^2$

$I_y := \frac{h_w^3 \cdot t_w}{12} + \left(\frac{h_w}{2} + \frac{t_f}{2}\right)^2 \cdot (2A_1) + \frac{2t_f^3 \cdot b}{12} = 1.796 \times 10^8 \cdot mm^4$

$w_y := \frac{I_y}{\frac{h}{2}} = 8.978 \times 10^5 \cdot mm^3$

Polar radius of gyration about the minor axis

$i_z := \sqrt{\frac{I_z}{A}} = 46.089 \cdot mm$

Plastic sectional modulus about major axis

$A_{t1} := t_f \cdot b = 2 \times 10^{-3}\,m^2$

$A_{t2} := \left(\frac{h_w}{2}\right) \cdot t_w = 1.14 \times 10^{-3}\,m^2$

$y_n := \frac{A_{t1} \cdot \left(\frac{t_f}{2} + \frac{h_w}{2}\right) + A_{t2} \cdot \left(\frac{h_w}{4}\right)}{\left(\frac{A}{2}\right)} = 158.694 \cdot mm \qquad w_{pl} := \left(\frac{A}{2} \cdot y_n\right) \cdot 2 = 9.966 \times 10^5 \cdot mm^3$

Cross section class

Internal compression

$c := h - 2 \cdot t_f = 0.38\,m$

$t := t_w = 6 \cdot mm$

$\frac{c}{t} = 63.333$ Less than 72ε, Class 1

Outstanding

$c_{out} := \frac{b - t_w}{2} = 0.097\,m$

$t_{out} := t_f = 10 \cdot mm$

$\frac{c_{out}}{t_{out}} = 9.7$ larger than 9ε, Class 2

The derived stable length

Unrestrained

$x := 1m$

Given

$$0.4 = \sqrt{\frac{w_y \cdot f_y}{\frac{\pi^2 \cdot E \cdot I_z}{x^2}\left(\frac{I_w}{I_z} + \frac{x^2 \cdot G_1 \cdot I_t}{\pi^2 \cdot E \cdot I_z}\right)^{0.5}}}$$

$L_{unr} := Find(x)$

$L_{unr} = 2.047\,m$

Critical buckling moment for a derived stable length unrestrained

$$M_{cr.unr} := \frac{\pi^2 \cdot E \cdot I_z}{L_{unr}^2}\left(\frac{I_w}{I_z} + \frac{L_{unr}^2 \cdot G_1 \cdot I_t}{\pi^2 \cdot E \cdot I_z}\right)^{0.5} = 1.319 \times 10^3 \cdot kN \cdot m$$

Restrained at 0.5h

$a_1 := 0.5 \cdot h = 0.2\,m$

$$L_{r.05h} := \sqrt{\frac{\pi^2 \cdot E \cdot \left(I_z \cdot a_1^2 + I_w\right)}{\left(\frac{2 \cdot a_1 \cdot w_y \cdot f_y}{0.4^2} - G_1 \cdot I_t\right)}} = 2.047\,m$$

Critical buckling moment for a derived stable length restrained at 0,5h

$$M_{cr.r05} := \frac{1}{2a_1}\cdot\left(\frac{\pi^2\cdot E\cdot I_z\cdot a_1^{\,2}}{L_{r.05h}^{\,2}} + \frac{\pi^2\cdot E\cdot I_w}{L_{r.05h}^{\,2}} + G_1\cdot I_t\right) = 1.319\times 10^3\cdot kN\cdot m$$

Restrained at 0.75h

$$a_2 := 0.75\cdot h = 0.3\,m$$

$$L_{r.075h} := \sqrt{\frac{\pi^2\cdot E\cdot\left(I_z\cdot a_2^{\,2} + I_w\right)}{\left(\frac{2\cdot a_2\cdot w_y\cdot f_y}{0.4^2} - G_1\cdot I_t\right)}} = 2.132\,m$$

Critical buckling moment for a derived stable length restrained at 0,75h

$$M_{cr.0.r075} := \frac{1}{2a_2}\cdot\left(\frac{\pi^2\cdot E\cdot I_z\cdot a_2^{\,2}}{L_{r.075h}^{\,2}} + \frac{\pi^2\cdot E\cdot I_w}{L_{r.075h}^{\,2}} + G_1\cdot I_t\right) = 1.319\times 10^3\cdot kN\cdot m$$

The stable length according to Eurocode

The plastic stable length, unrestrained

$$L_m := \frac{38 i_z}{\sqrt{\frac{1}{756}\cdot\left(\frac{w_{pl}^{\,2}}{A\cdot I_t}\right)\cdot\left(\frac{f_y}{235\,\frac{N}{mm^2}}\right)^2}} = 1.52\,m$$

The plastic stable length, restrained

$$L_k := \frac{\left(5.4 + \frac{600 f_y}{E}\right)\cdot\left(\frac{h}{t_f}\right)\cdot i_z}{\sqrt{5.4\cdot\left(\frac{f_y}{E}\right)\cdot\left(\frac{h}{t_f}\right)^2 - 1}} = 3.802\,m$$

The stable length according to the simplified method

$$f := \frac{h_w}{6} = 0.063\,m$$

$$I_{zf} := \frac{b^3 \cdot t_f}{12} + \frac{f \cdot t_w^{\,3}}{12} = 6.668 \times 10^{-6}\,m^4$$

$$A_{simp} := \left(b \cdot t_f\right) + \left(f \cdot t_w\right) = 2.38 \times 10^{-3}\,m^2$$

$$i_f := \sqrt{\frac{I_{zf}}{A_{simp}}} = 0.053\,m$$

$$L_c := i_f \cdot 93.9 \cdot 0.5 = 2.485\,m$$

Customized, depth 600

Material parameters

$E := 210GPa$

$G_1 := 81GPa$

$f_y := 235 \frac{N}{mm^2}$

Geometrical Parameters

Dimensions of the cross-section

$h := 600mm \quad b := 200mm \quad t_f := 10mm \quad t_w := 6mm$

$h_w := h - t_f \cdot 2 = 580 \cdot mm \qquad d := h - t_f = 0.59\,m$

$A := h_w \cdot t_w + b \cdot t_f \cdot 2 = 7.48 \times 10^{-3}\,m^2$

Second moment of inertia according to the software LTB

$I_z := 1334.6cm^4 \qquad I_w := 1.1612 \cdot 10^6 cm^6 \qquad I_t := 17.204cm^4$

Second moment of inertia about the major axis

$A_1 := b \cdot t_f = 2 \times 10^{-3}\,m^2$

$I_y := \frac{h_w^3 \cdot t_w}{12} + \left(\frac{h_w}{2} + \frac{t_f}{2}\right)^2 \cdot (2A_1) + \frac{2t_f^3 \cdot b}{12} = 4.457 \times 10^8 \cdot mm^4$

$w_y := \frac{I_y}{\frac{h}{2}} = 1.486 \times 10^6 \cdot mm^3$

Polar radius of gyration about the minor axis

$i_z := \sqrt{\frac{I_z}{A}} = 42.24 \cdot mm$

Plastic sectional modulus about major axis

$A_{t1} := t_f \cdot b = 2 \times 10^{-3}\,m^2$

$A_{t2} := \left(\frac{h_w}{2}\right) \cdot t_w = 1.74 \times 10^{-3}\,m^2$

$y_n := \frac{A_{t1} \cdot \left(\frac{t_f}{2} + \frac{h_w}{2}\right) + A_{t2} \cdot \left(\frac{h_w}{4}\right)}{\left(\frac{A}{2}\right)} = 225.214 \cdot mm \qquad w_{pl} := \left(\frac{A}{2} \cdot y_n\right) \cdot 2 = 1.685 \times 10^6 \cdot mm^3$

Cross section class

Internal compression

$c := h - 2 \cdot t_f = 0.58\,m$

$t := t_w = 6 \cdot mm$

$\frac{c}{t} = 96.667$ Less than 72ε, Class 1

Outstanding

$c_{out} := \frac{b - t_w}{2} = 0.097\,m$

$t_{out} := t_f = 10 \cdot mm$

$\frac{c_{out}}{t_{out}} = 9.7$ larger than 9ε, Class 2

The derived stable length

Unrestrained

$x := 1m$

Given

$$0.4 = \sqrt{\frac{w_y \cdot f_y}{\frac{\pi^2 \cdot E \cdot I_z}{x^2}\left(\frac{I_w}{I_z} + \frac{x^2 \cdot G_1 \cdot I_t}{\pi^2 \cdot E \cdot I_z}\right)^{0.5}}}$$

$L_{unr} := Find(x)$

$L_{unr} = 1.944\,m$

Critical buckling moment for a derived stable length unrestrained

$$M_{cr.unr} := \frac{\pi^2 \cdot E \cdot I_z}{L_{unr}^2}\left(\frac{I_w}{I_z} + \frac{L_{unr}^2 \cdot G_1 \cdot I_t}{\pi^2 \cdot E \cdot I_z}\right)^{0.5} = 2.182 \times 10^3 \cdot kN \cdot m$$

Restrained at 0.5h

$a_1 := 0.5 \cdot h = 0.3\,m$

$$L_{r.05h} := \sqrt{\frac{\pi^2 \cdot E \cdot \left(I_z \cdot a_1^2 + I_w\right)}{\left(\frac{2 \cdot a_1 \cdot w_y \cdot f_y}{0.4^2} - G_1 \cdot I_t\right)}} = 1.944\,m$$

Critical buckling moment for a derived stable length restrained at 0,5h

$$M_{cr.r05} := \frac{1}{2a_1}\cdot\left(\frac{\pi^2\cdot E\cdot I_z\cdot a_1^{\,2}}{L_{r.05h}^{\,2}} + \frac{\pi^2\cdot E\cdot I_w}{L_{r.05h}^{\,2}} + G_1\cdot I_t\right) = 2.182\times 10^3\cdot kN\cdot m$$

Restrained at 0.75h

$$a_2 := 0.75\cdot h = 0.45\,m$$

$$L_{r.075h} := \sqrt{\frac{\pi^2\cdot E\cdot\left(I_z\cdot a_2^{\,2} + I_w\right)}{\left(\frac{2\cdot a_2\cdot w_y\cdot f_y}{0.4^2} - G_1\cdot I_t\right)}} = 2.027\,m$$

Critical buckling moment for a derived stable length restrained at 0,75h

$$M_{cr.0.r075} := \frac{1}{2a_2}\cdot\left(\frac{\pi^2\cdot E\cdot I_z\cdot a_2^{\,2}}{L_{r.075h}^{\,2}} + \frac{\pi^2\cdot E\cdot I_w}{L_{r.075h}^{\,2}} + G_1\cdot I_t\right) = 2.182\times 10^3\cdot kN\cdot m$$

The stable length according to Eurocode

The plastic stable length, unrestrained

$$L_m := \frac{38 i_z}{\sqrt{\frac{1}{756}\cdot\left(\frac{w_{pl}^{\,2}}{A\cdot I_t}\right)\cdot\left(\frac{f_y}{235\,\frac{N}{mm^2}}\right)^2}} = 0.94\,m$$

The plastic stable length, restrained

$$L_k := \frac{\left(5.4 + \frac{600 f_y}{E}\right)\cdot\left(\frac{h}{t_f}\right)\cdot i_z}{\sqrt{5.4\cdot\left(\frac{f_y}{E}\right)\cdot\left(\frac{h}{t_f}\right)^2 - 1}} = 3.378\,m$$

The stable length according to the simplified method

$$f := \frac{h_w}{6} = 0.097\,m$$

$$I_{zf} := \frac{b^3 \cdot t_f}{12} + \frac{f \cdot t_w^{\,3}}{12} = 6.668 \times 10^{-6}\,m^4$$

$$A_{simp} := \left(b \cdot t_f\right) + \left(f \cdot t_w\right) = 2.58 \times 10^{-3}\,m^2$$

$$i_f := \sqrt{\frac{I_{zf}}{A_{simp}}} = 0.051\,m$$

$$L_c := i_f \cdot 93.9 \cdot 0.5 = 2.387\,m$$